STUDIES TOWARDS THE SYNTHESIS OF [10]-ANNULENES

A Thesis Submitted to the College of

Graduate and Postdoctoral Studies

In Partial Fulfillment of the Requirements

For the Degree of Master of Science

in the Department of Chemistry

University of Saskatchewan

Saskatoon, Canada

By

Christa Blaquiere

PERMISSION TO USE

In presenting this thesis/dissertation in partial fulfillment of the requirements for a postgraduate degree from the University of Saskatchewan, I agree that the Libraries of this University may make it freely available for inspection. I further agree that permission for copying of this thesis/dissertation in any manner, in whole or in part, for scholarly purposes may be granted by the professor or professors who supervised my thesis/dissertation work or, in their absence, by the Head of the Department or the Dean of the College in which my thesis work was done. It is understood that any copying or publication or use of this thesis/dissertation or parts thereof for financial gain shall not be allowed without my written permission. It is also understood that due recognition shall be given to me and to the University of Saskatchewan in any scholarly use which may be made of any material in my thesis/dissertation.

Requests for permission to copy or to make other uses of materials in this thesis/dissertation in whole or part should be addressed to:

Head of the Department of Chemistry

165-110 Science Place

University of Saskatchewan

Saskatoon, Saskatchewan S7N 5C9

Canada

ABSTRACT

This thesis begins with a historical perspective on aromaticity and benzene, including the discovery and proposed structures for benzene as well as proposed criteria for measuring aromaticity. The history of the synthesis and characterization of [10]-annulene is also discussed.

Studies towards the synthesis of an aromatic all-*cis*-[10]-annulene derivative is covered in this dissertation. Two routes that were explored in efforts to obtain a chlorinated all-*cis*-[10]-annulene derivative, **40**, are described. The primary route utilizes six chlorine atoms on the hydrocarbon skeleton (R=H) and uses a carbene [2+1] cycloaddition reaction as a key step to incorporate one of the two cyclopropane substituents (Scheme 1.0). The second cyclopropane unit is incorporated through a Diels-Alder reaction between diene **49** and tetrachlorocyclopropene **50**, which also established the 10-carbon framework. The cleavage of the central olefin in the 10-carbon skeleton **51** is discussed, as well as difficulties encountered. In attempts to obtain the planar, aromatic [10]-annulene, efforts towards the elimination and oxidation reactions which lead to the aromatization of **55** are also presented.

This thesis also discusses an alternative route that incorporates an additional chlorine atom on the carbon framework (R=Cl). The alternative route mirrors the previous pathway; one cyclopropane substituent is incorporated through a carbene [2+1] cycloaddition reaction, whereas the second unit is established *via* a Diels-Alder reaction (Scheme 1.0). Efforts towards cleaving the olefin in **51** to obtain the carbon skeleton **40** are also discussed.

This work concludes with a general discussion and proposal for future directions, with an emphasis on alternative synthetic pathways. This study demonstrates the Diels-Alder reactions and

ozonolysis of **51** is a viable strategy to form the functionalized skeleton required for [10]-annulene derivative **40**.

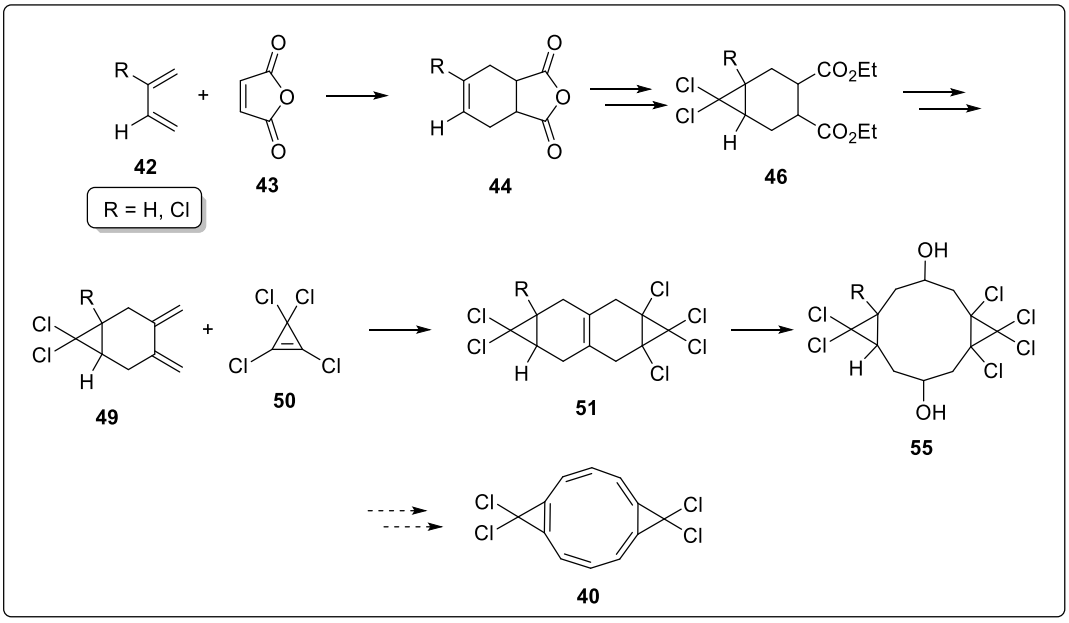

Scheme 1.0 Synthetic route.

ACKNOWLEDGEMENTS

I would like to sincerely thank my supervisor, Dr. Michel Gravel, for taking me on as a graduate student. Thanks to Dr. Gravel for all the guidance, support, and patience in the past three years, especially during the thesis writing process. Thank you, Dr. Gravel for making the graduate school experience a positive one.

Secondly, I would like to express my extreme gratitude to my parents, Barb and Gil, for their endless encouragement and emotional and financial support throughout my undergraduate and graduate studies. Thanks to my siblings, Brett and Shanae, and my grandparents for the encouragement and interest in what I have been doing. Finally, thank you to Matthew Hougham for the support and encouragement throughout my studies. The chauffeur services to and from the university and many meals are much appreciated.

I am grateful for the previous and current Gravel group members. I would like to thank Steven and Pouyan for their guidance in the laboratory and for answering all my questions, as well as Karn for his suggestions with the ozonolysis and for the help with the 2D NMR analysis. Thank you to Venkata, Mehran and Myron for informative and interesting discussions. Graduate school would have been a completely different (and less fun) experience without these people.

Thank you to the chemistry staff for their expertise: Dr. Keith Brown and Dr. Jianfeng (Peter) Zhu in the Saskatchewan Structural Sciences Center (SSSC) and Ms. Leah Hildebrandt for being an information source and for keeping me sane during my graduate program.

Lastly, I would like to thank the faculty at Augsburg University, especially Dr. Michael Wentzel and Dr. Z. Vivian Feng, for the undergraduate research opportunities and for encouraging me to pursue graduate studies.

TABLE OF CONTENTS

LIST OF TABLES

LIST OF FIGURES

LIST OF SCHEMES

LIST OF ABBREVIATIONS

abs	absolute
ASE	aromatic stabilization energy
aq	aqueous
Bn	benzyl
calcd	calculated
COSY	correlation spectroscopy
d	day(s), doublet (spectral)
DBU	1,8-diazabicyclo[5.4.0]undec-7-ene
DEAD	diethyl azodicarboxylate
δ	chemical shift (in parts per million)
DDQ	2,3-dichloro-5,6-dicyano-*p*-benzoquinone
DMAP	4-dimethylaminopyridine
DMDO	dimethyldioxirane
DMF	*N*,*N*-dimethyl formamide
DME	dimethoxy ethane
DMS	dimethyl sulfide
DMSO	dimethyl sulfoxide
dr	diastereomeric ratio
equiv.	equivalent(s)
ESI	electrospray ionization
Et	ethyl
expt	experiment

FCC	flash column chromatography
h	hour(s)
HMBC	heteronuclear multiple bond correlation
HRMS	high resolution mass spectrometry
HSQC	heteronuclear single quantum coherence
Hz	hertz
J	coupling constant (spectral)
kcal	kilocalories
m	multiplet (spectral)
m-CPBA	*meta*-chloroperoxybenzoic acid
MAE	mean absolute error
min	minute(s)
mmol	millimole(s)
MsCl	methanesulfonyl chloride
m/z	mass-to-charge ratio
NaHMDS	sodium hexamethyldisilazane
NaTCA	sodium trichloroacetate
NICS	nucleus-independent chemical shifts
NMR	nuclear magnetic resonance
p-TSA	*para*-toluenesulfonic acid
pm	picometers
PTLC	preparatory thin layer chromatography
ppm	parts per million

pyr	pyridine
q	quartet (spectral)
rt	room temperature
s	singlet (spectral)
t	triplet (spectral)
t-BuOK	potassium *tert*-butoxide
TEBA	triethylbenzyl ammonium chloride
THF	tetrahydrofuran
TsCl	toluenesulfonyl chloride
TLC	thin layer chromatography

CHAPTER 1: INTRODUCTION

1.1 Historical Background on Aromaticity

Aromaticity has intrigued chemists since the discovery of benzene almost two hundred years ago.[1] At the time of its discovery, "aromatic" referred to compounds with an aroma, however it is now known that not all aromatic compounds possess an odor.[2] Benzene is the most well-known aromatic compound and was discovered in 1825 by Michael Faraday, who isolated it from lamp oil. He determined its empirical formula to be C_1H_1. Later investigations revealed the chemical formula of benzene to be C_6H_6.[3] This information implied that the molecule was unsaturated, however many viable structures fit this criteria. The closest suggestion to the now known structure of benzene was proposed by Loschmidt in 1861, **1**,[4] four years before Kekulé's proposal, **2**[5] (Figure 1.1).

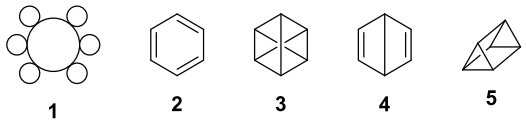

Figure 1.1 Suggested structures of benzene.

Kekulé's cyclohexatriene structure, **2**, was met with criticism as the structure was expected to behave like an alkene, which was contrary to observation. For example, benzene did not undergo electrophilic addition reactions as an alkene would, but instead underwent substitution reactions.[2] The value found for the heat released from hydrogenation of benzene also presented a problem with Kekulé's proposed structure. The expected value for triene **2** is 86.0 kcal/mol, however, benzene was found to release 50.2 kcal/mol of energy when hydrogenated, 35.9 kcal/mol less than predicted.[2] This surprising stability is now known as aromatic stabilization energy, or the energy gained from delocalization of multiple bonds in a ring system. The aforementioned anomalies led

to other proposals for the structure of benzene, including the 1867 proposals of Claus **3** and Dewar **4**,[6] as well as Ladenburg's prismane proposal **5** in 1869.[7]

Kekulé's benzene structure gained popularity as the field of chemistry developed and as more was discovered about aromaticity. Major breakthroughs include Pascal's 1910 discovery of the higher diamagnetic susceptibility of aromatic compounds[2] and Armit and Robinson's 1925 proposal of an aromatic sextet.[8] This proposal states that the six π electrons in benzene form a group resistant to disruption, explaining benzene's difficulty with addition reactions.[8] Schrödinger's development of wave mechanics in 1926 led to molecular orbital theory, which guided Hückel in establishing π orbitals and the $4n+2$ rule.[9] Hückel also developed other guidelines in determining if a compound is aromatic: an aromatic molecule must be cyclic and planar, have a *p* orbital on each atom in the ring contributing to delocalization, and have $4n+2$ π electrons. Extension of these guidelines from benzene predict several aromatic molecules, including the all-*cis*-[10]-annulene (**6**), [14]-annulene (**7**), and [18]-annulene (**8**) (Figure 1.2). The [18]-annulene isomer (**8**) is aromatic, and was the first higher aromatic annulene synthesized.[10,11] The [14]-annulene isomer (**7**) was determined to be an aromatic compound, although unstable to light and air.[12] Bridged [14]-annulenes such as **9** have also been prepared and are more stable than the unbridged molecules.[13] Aromaticity can also be found in polycyclic molecules like naphthalene **10**, heterocycles such as pyridine **11**, kekulene structures **12**,[14] and metalla-aromatic structures **13**.[15,16]

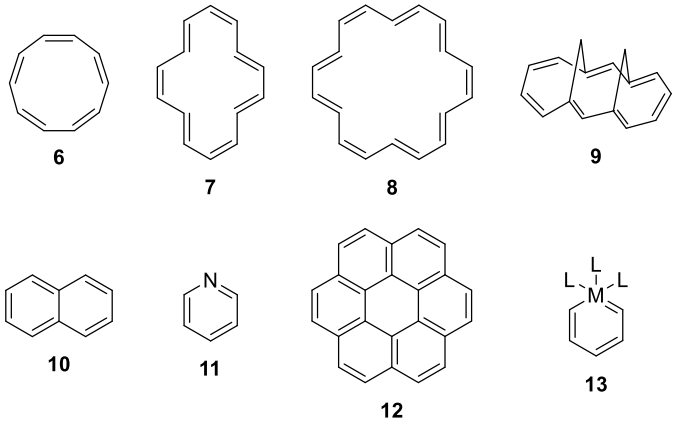

Figure 1.2 Expected aromatic molecules.

1.2 Measuring Aromaticity

Although Hückel's rules establish guidelines for determining aromaticity, there is still much debate about the definition of aromaticity and how to measure it. It was initially suggested that aromaticity be classified through reactivity. It was proposed that all olefinic molecules that undergo substitution reactions instead of addition reactions should be classified as aromatic. This simple method, first suggested by Erlenmeyer, proved to be problematic as aromatic compounds like phenanthrene **14** and anthracene **15** unexpectedly undergo addition reactions with bromine (Figure 1.3).[2,3] It was therefore suggested that the heats of hydrogenation would be a more suitable way to measure aromaticity. This method was also problematic as errors in calculations lead benzene to be assigned a stabilization energy between 9.6 and 28.7 kcal/mol,[2] making it difficult to determine how much stabilization energy is necessary to make a compound aromatic.

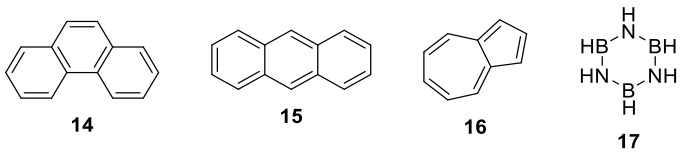

Figure 1.3 Some aromatic compounds and non-aromatic borazine.

A third criteria was proposed based on benzene's unique bond lengths, 139 pm, which is between the length of a typical carbon-carbon single bond, 154 pm, and a carbon-carbon double bond, 134 pm.[17] This proposal by Albert in 1959 states that molecules possessing the same bond lengths as benzene were to be considered aromatic.[18] The criteria were expanded to include a range of bond lengths as most aromatic molecules were excluded with a set value.[2] This modification again failed to encompass all aromatic molecules. For example, aromatic azulene **16** has longer bond lengths than expected, while the non-aromatic compound borazine **17** has equal bond lengths (Figure 1.3).[2]

A modern criteria of measuring aromaticity utilizes the aromatic ring current.[2] The induced ring current in an aromatic molecule occurs when a magnetic field is applied perpendicular to the plane of the aromatic system. The magnetic field is increased outside the ring because it is in the same direction as the applied field, resulting in the deshielding effect observed for aromatic compounds in nuclear magnetic resonance (Figure 1.4). Aromatic protons are found in the range of δ = 7-8 ppm and not the olefinic range of δ = 5-6 ppm. Proton anisotropy, however, can be an unreliable tool for measuring aromaticity, as seen by the resonance of the protons in [16]-annulene **18**, a non-aromatic compound. All protons in [16]-annulene isomer **18** resonate as one signal at δ = 6.73 ppm, suggesting an aromatic molecule (Figure 1.5). This cannot be true, as [16]-annulene is known to be non-aromatic because it does not follow Hückel's 4*n*+2 rule and it is non-planar.

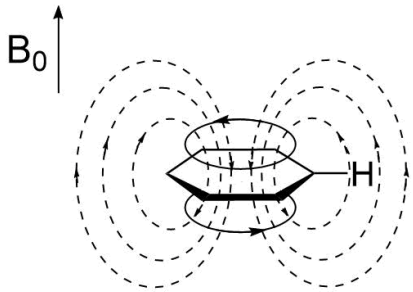

Figure 1.4 Induced magnetic current in benzene. Image adapted from ref. 19.

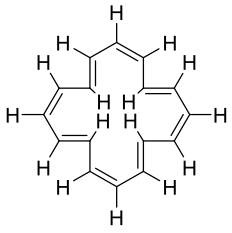

18

Figure 1.5 Non-aromatic [16]-annulene.

Nucleus-independent chemical shifts (NICS) was more recently proposed as a probe of aromaticity by Schleyer and coworkers.[20] This method was suggested due to the observation that bridging protons and inner protons on an aromatic molecule are significantly shielded because of ring current. For example, the outer protons of [18]-annulene isomer **8** has a shift of $\delta = 9.28$ ppm, while the inner protons have a chemical shift of $\delta = -3.0$ ppm (Figure 1.2). Therefore, it was hypothesized that computationally placing atoms, such as a lithium cation, in the center of a presumed aromatic ring would give insight into its aromaticity. Later computational methods utilized a dummy atom, or a point in space, in the center of the ring and in the same plane of the ring. This method is known as NICS(0). A negative value indicates anisotropic shielding, as would be expected in the case of an aromatic ring. The disadvantage to this method is the difficulty in producing experimentally equivalent results.[21] NICS(0) also gives non-zero values for non-aromatic, saturated, and unsaturated hydrocarbon rings due to the CH and CC σ framework.[21,22]

Further development of the NICS method led to a refined process of determining the aromaticity of a molecule. NICS(1) differs from NICS(0) by placing a dummy atom 1 Å above the plane of the ring. This adjustment minimizes the influence of the σ framework as the π orbitals have their maximum density at this point.[23,24] NICS(1) shows the π electron delocalization rather than the shielding effect only. A further adjustment to the NICS method, $NICS_{zz}$, determines the

shielding effect as a function of the distance away from the plane of the ring. This calculation is a more accurate characterization of the π structure of the ring.[25,26]

The suggested criteria for determining aromaticity are incomplete and, at times, inaccurate as there are always exceptions to the rule. This leads to debates amongst chemists as to what the definition of an aromatic compound is and the best way to determine the degree of aromaticity of a molecule. The most reasonable suggestion has been to measure the ring current; however, it leaves many questions about what the threshold for aromaticity should be.

1.3 [10]-Annulene

1.3.1 Synthesis of [10]-Annulenes

Hückel's 4*n*+2 rule predicts that [10]-annulene is a prototypical aromatic hydrocarbon. Of all the possible combinations of *cis*/*trans* isomers, only three are geometrically possible, the all-*cis* **20**, the mono-*trans* **21**, and the naphthalene-like di-*trans* annulene **19** (Figure 1.6). All isomers meet most of Hückel's criteria; each atom in the molecule has a *p* orbital, the molecules are conjugated and cyclic, and there are ten π electrons; an accepted value for the 4*n*+2 rule. It was unknown, however, if any [10]-annulene isomers are planar; the final criteria that needs to be met to be considered aromatic.

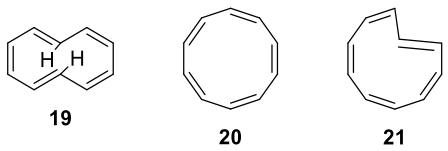

Figure 1.6 [10]-Annulene isomers.

The naphthalene-like di-*trans* annulene **19** has not been synthesized. The inner hydrogen atoms are predicted to be in close proximity, causing the molecule to distort from planarity,[27,28]

thus making it non-aromatic. The problem has been addressed through bridging these positions with a methylene **22**,[29] oxygen **23**,[30] or nitrogen atom **24**[31] (Figure 1.7). Characterization of these derivatives indicates that each molecule is aromatic. Dicupra-[10]-annulene derivatives **25** were also found to be aromatic.[32]

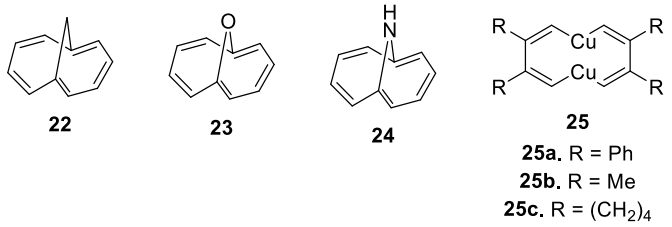

22 **23** **24** **25**

25a. R = Ph
25b. R = Me
25c. R = $(CH_2)_4$

Figure 1.7 Di-*trans* [10]-annulene derivatives.

It was not until 1967 that van Tamelen and coworkers reported the first synthesis of [10]-annulene (Scheme 1.1).[33] The authors began the synthesis with *trans*-dione **26** which was reduced using lithium aluminum hydride to obtain diol **27**. An Appel-like reaction was used to substitute bromides for the hydroxyl substituents providing dibromide **28**. This intermediate was then reacted with *N*-bromosuccinimde to obtain tetrabromide **29**. Dehalogenation using lithium amalgam furnished *trans*-9,10-dihydronaphthalene **30**. Photolysis of **30** led to an array of products, including [10]-annulenes **20** and **21**. Upon warming the reaction mixture to room temperature, *cis*-9,10-dihydroxynaphthalene **31** was also formed. This result indicates that [10]-annulene **20** or **21** could be present at low temperatures, but it is unstable at relatively high temperatures. Low temperature diimide reduction of the cold photolysis mixture produced cyclodecane in about 40% yield, implying a [10]-annulene precursor. The authors were unable to isolate and characterize the annulene due to the instability of the molecule. The aromatic character of [10]-annulene, therefore, was not determined.

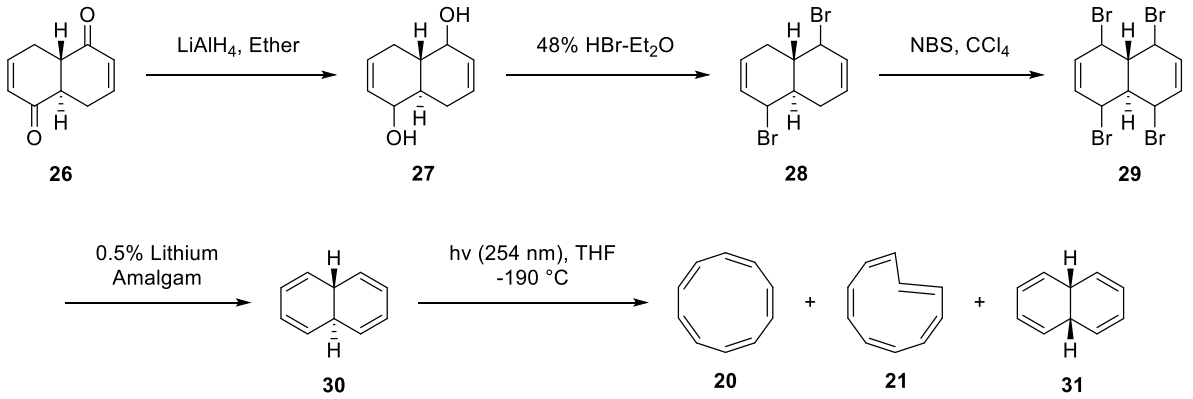

Scheme 1.1 van Tamelen's synthesis of [10]-annulene.

Masamune attempted to reproduce van Tamelen's [10]-annulene procedure starting from stereoisomer **30**, but found that [10]-annulene isomers **20** or **21** were not obtained.[34] Photolysis of the *cis* isomer **31** showed the formation of two new signals; a temperature dependent signal A at τ 4.16 (δ = 5.84 ppm) and a temperature independent signal B at τ 4.34 (δ = 5.66 ppm). Signal A broadened at lower temperatures and the intensity of the signal diminished as the temperature increased, giving rise to *trans*-9,10-dihydronaphthalene **30** signals. As the temperature was further increased, the intensity of the *cis*-9,10-dihydronaphthalene **31** signals increased at the expense of signal B. It was therefore concluded that the molecules responsible for signals A and B are stable at low temperatures.

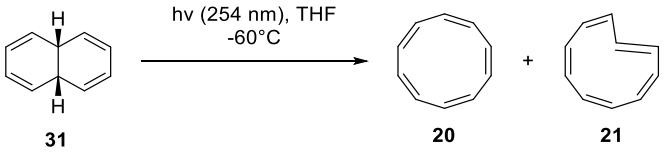

Scheme 1.2 Masamune's synthesis of [10]-annulene.

Hydrogenation of the mixture of compounds responsible for signals A and B was conducted to confirm the identity of the unknowns.[34] Cyclodecane was produced at low temperatures and was recovered in more than 80% yield based on calculated amounts of signals A and B. Hydrogenation

of **30** and **31** failed to produce cyclodecane, indicating that these molecules are not transformed into cyclodecane under these conditions. It therefore became reasonable to suggest that **20** and **21** are responsible for the signals B and A, respectively (Scheme 1.2). Thus, mono-*trans*-[10]-annulene **21** is isomerized to **30**, while the all-*cis* configuration isomerizes to **31** (Scheme 1.3).

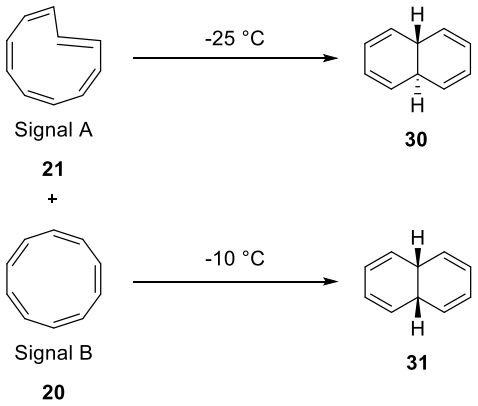

Scheme 1.3 Isomerization of [10]-annulenes.

Masamune and coworkers later report the first characterization of isolated [10]-annulenes produced from photolysis of *cis*-9,10-dihydronaphthalene.[35] The removal of tetracyclo[4.4.0.0^{2,10}.0^{5,7}]deca-3,8-diene **32** was achieved *via* crystallization at -80 °C (Figure 1.8). The [10]-annulene enriched mixture was chromatographed on alumina with *n*-pentane:CH_2Cl_2 gradient column at -80 °C.[36] The proton spectrum of the assumed all-*cis*-[10]-annulene (**20**) showed a temperature independent singlet at τ 4.33 (δ = 5.67 ppm), while the ^{13}C NMR showed a signal at τ 130.4. The single proton and carbon signals suggest that the all-*cis*-[10]-annulene isomer is either planar and highly symmetrical so all protons are chemically equivalent or it is non-planar but flexible, allowing for non-equivalent protons to give rise to a single time-averaged signal. The UV spectrum suggests that [10]-annulene **20** is not aromatic as it has a dissimilar spectrum to its aromatic analogue **22 (**Figure 1.7).[35] It is therefore inferred that the all-*cis* derivative is not planar, which is also indicated by the olefinic proton chemical shift rather than the more deshielded aromatic shift.

32

Figure 1.8 Tetracyclo[4.4.0.0^{2,10}.0^{5,7}]deca-3,8-diene.

The second isolated molecule, presumably the *trans*-[10]-annulene **21**, showed temperature dependent signals.[34] Monitoring the transformation of this molecule to **30** showed that **21** was frozen in its conformation below -100 °C. As the temperature increases, however, the proton signal splits into an apparent doublet. A singlet is again observed at -40 °C, indicating the protons in the molecule achieve chemical equivalence at higher temperatures. The ^{13}C NMR signals are temperature dependent as well; at -100 °C five carbon signals are observed, while only one signal is observed at -40 °C.[35] It is therefore suggested that the *trans* double bond can move around the ring, creating atom equivalence. Based on the proton and carbon NMR spectra, it can be concluded that *trans*-[10]-annulene **21** is not aromatic either.

Neither [10]-annulene configurations are aromatic because the molecules do not meet the planar requirement. It is expected that the all-*cis*-[10]-annulene (**20**) isomer is not planar, as geometry dictates that each angle in a decagon must be 144°, much larger than the preferred 120° angle for sp^2 hybridized carbon atoms. It was therefore suggested that **20** adopts a tub-like conformation, **20a**, to relieve angle strain present in a planar [10]-annulene (Figure 1.9).[35]

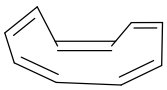

20a

Figure 1.9 Tub-like conformation of all-cis-[10]-annulene.

Although [10]-annulene cannot be classified as an aromatic molecule, there are other ten-electron systems that have been identified as aromatic. Some examples include **22** – **25**, as well as

the dianionic cyclooctatetraene **33**, anionic cyclononatetraenyl **34**,[37] and heteroannulene **35**[28] (Figure 1.10).

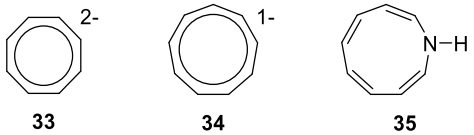

Figure 1.10 Other 10-electron aromatic systems.

1.3.2 Computational Studies on [10]-Annulene

Several computational studies on [10]-annulenes have been published investigating aromaticity[38] and the measurement of aromatic stabilization energy of the compounds.[39] Computational investigations by the groups of Schaefer III and Schleyer concluded that the tub-like *cis* conformation **20a** and *trans* **21** configuration were lower in energy than the planar structures of delocalized molecule **36** and localized polyene **20** (Figure 1.11).[40] These results validate Masamune's conclusions on the identity and conformation of the [10]-annulenes previously described.[35] Further computational studies examined several [10]-annulene configurations and conformations.[41] This enquiry reports the delocalized structure **36** is slightly lower in energy than localized polyene **20** using the MP2 theory level. It also finds that the twisted mono-*trans* conformer **21a** is the global minimum, while the naphthalene-like di-*trans* structure **19** is the second lowest energy configuration at the MP2 theory level. Calculations at the MP2 level on the all-*cis*, planar conformer **20** predicts the heats of formation to be 157.17 kcal/mol higher in energy than di-*trans* [10]-annulene **19** and mono-*trans* **21**, whereas the tub-like conformation is predicted to be a transition state as it is 6.1 kcal/mol above the global minimum **21a**.

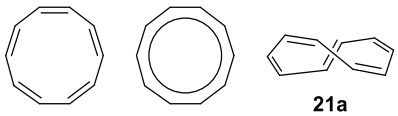

Figure 1.11 Localized polyene, aromatic [10]-annulene and the mono-trans twisted conformation of [10]-annulene.

Computational studies completed in 1995 again confirmed that Masamune was correct in assigning the all-*cis* configuration **20** to one of the isolated products**.**[42] The study finds that di-*trans* configuration **19** is not experimentally observed due to the steric strain between the internal hydrogen atoms. It is likely that this molecule would quickly cyclize to *cis*-9,10-dihydronaphthalene **31** to relieve the steric strain.

It was also realized that the mono-*trans* conformation **21b** is nearly planar, indicating it may be aromatic (Figure 1.12). Computations on the physicochemical properties of this conformer show that it is indeed aromatic; it has bond lengths similar to that of benzene (1.378 – 1.423 Å and it has an ASE of 18 kcal/mol.[42] The predicted ^{1}H NMR spectrum shows downfield chemical shifts in the δ 7.9 – 8.6 ppm range, whereas the inner proton has a chemical shift of δ -6.2 ppm, further confirming **21b** is aromatic.

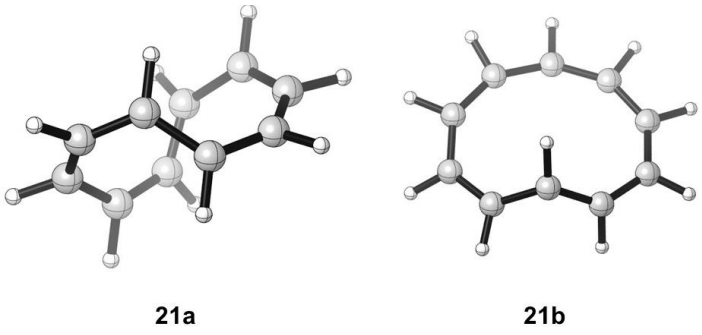

Figure 1.12 Non-aromatic, mono-*trans* [10]-annulene conformation **21a** and planar, aromatic mono-*trans* conformation **21b**. Images adapted from ref. 42.

Schleyer and coworkers were also interested in identifying if Masamune isolated this nearly planar, aromatic [10]-annulene **21b**. ^{13}C NMR chemical shift predictions show that six signals should be observed for **21b** due to a plane of symmetry, however Masamune's experiments showed five signals at low temperatures. Additionally, comparison of the predicted chemical shifts to the observed chemical shifts showed a mismatch between predicted aromatic **21b** and Masamune's isolated product.[35,42] The computed ^{13}C NMR chemical shifts of non-aromatic conformation **21a**, however, showed a close match to Masamune's mono-*trans* product. These computations verify Masamune's conclusion that the isolate mono-*trans* [10]-annulene was non-aromatic.

Additional computational studies were completed on all-*cis* [10]-annulene derivatives to investigate if the non-planarity problem can be overcome (Figure 1.13).[43] It was hypothesized that additional strain in the molecule could force the all-*cis* [10]-annulene to adopt a planar conformation. Fused cyclopropene and cyclobutene rings were chosen due to the similarity of angles to those present in a hypothetical planar [10]-annulene. Indeed, the H-C=C angles are similar to the angles a carbon atom would experience in a planar [10]-annulene. It was reasoned that these comparable angles would alleviate the strain experienced by the 10-membered ring and would thus allow it to adopt a planar conformation. Computations completed on **37**, **38**, and **39** show that angle strain is indeed reduced in the annulenes, signifying these analogues prefer to be planar, and thus aromatic.

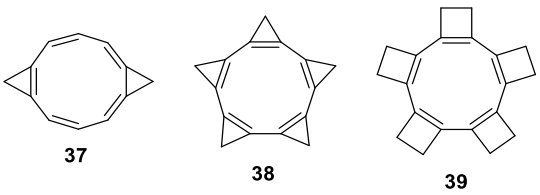

Figure 1.13 All-cis-[10]-annulene derivatives.

Aromatic characteristics such as bond lengths, total magnetic susceptibilities, anisotropies, NICS, and the aromatic stabilization energies of each derivative was examined. The bond lengths of each derivative were comparable to that of benzene, indicating the delocalization of the π electrons (Table 1.1).[43] The aromatic stabilization energy (ASE) was calculated using MP2(fc)/DZd geometry, and it was found that each molecule possessed some ASE, with **38** having the lowest predicted aromatic stabilization energy, and **39** having a higher stabilization energy than that of benzene. The ring current was also probed using the NICS method; placing a dummy atom in the center of each [10]-annulene derivative. The chemical shift of the dummy atom was calculated and found to be significantly upfield, which is indicative of an aromatic molecule.

It is interesting to note that two different ASE are reported in Schleyer's [10]-annulene papers.[42,43] An uncorrected ASE does not account for the strain in a molecule, whereas the corrected ASE accommodates this destabilizing effect. For example, Schleyer and coworkers predict planar [10]-annulene **20** to have an uncorrected ASE of -50 kcal/mol. When the strain is taken into consideration, however, the corrected aromatic stabilization energy of **20** becomes +26.14 kcal/mol. The corrected ASE of [10]-annulene derivative **37** was calculated to be 13.9 kcal/mol, which is 7.8 kcal/mol lower in stabilization energy than benzene. The optimized structures of the [10]-annulene derivatives are shown in Figure 1.14.

Table 1.1 Aromatic character of [10]-annulene derivatives.

Compound	Bond Lengths (Å)	ASE (kcal/mol)	NICS(0) (ppm)
Benzene	1.40	21.7	-11.5
37	1.378 - 1.410	13.9	-14.9
38	1.358 & 1.379	18.5	-10.8
39	1.389 & 1.423	23.0	-15.0

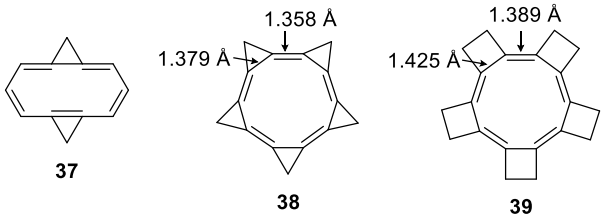

Figure 1.14 Schleyer's optimized [10]-annulene derivatives. Image adapted from ref. 43.

1.4 Research Objectives

As discussed above, it was concluded that the all-*cis*-[10]-annulene derivatives **37**, **38**, and **39** overcome the reported non-planarity problem observed by Masamune and can be considered aromatic. It is suggested, however that **37** is the most attractive candidate for synthesis as it allows investigation of aromatic substitution reactions.[43] Compound **40**, a derivative of aromatic **37**, is an interesting target structure for several reasons. First, the synthesis of an aromatic [10]-annulene derivative would validate Schleyer's computational predictions. Second, investigations into the reactivity of [10]-annulene would give insight into its usefulness in synthesis. Third, investigations into the physicochemical properties of the aromatic molecule would determine if the conjugated π system can be useful in photovoltaic cells, as these cells use π systems to donate and accept electrons. Finally, the synthesis of an aromatic [10]-annulene will probe the concept of aromaticity, which still intrigues chemists and provokes debate about its definition and measurement. The primary objective is thus to explore synthetic routes toward [10]-annulene **40** and derivative **41** (Figure 1.15). The reason for the chlorine atoms will be made clear in the next chapter.

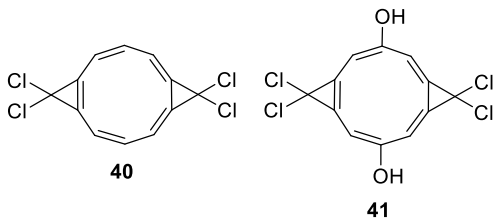

Figure 1.15 Target [10]-annulene structures.

[10]-Annulene derivative **41** is an interesting target compound due to derivation possibilities. As a way to explore potential usefulness in optoelectronic devices, it would be useful to access a derivative that is easy to derivatize to extended π systems. As such, derivative **41** is a good candidate as transition metal catalyzed cross-coupling reactions of the corresponding ditriflate can be explored.

CHAPTER 2: RESULTS AND DISCUSSION

2.1 Proposed Routes

A general route was proposed to reach the framework of the target [10]-annulenes based on an initial sequence of reported reactions (Scheme 2.1). The route begins with a Diels-Alder reaction between diene **42** and maleic anhydride (**43**) to produce anhydride **44**.[44] Ethanolysis of **44** results in diester **45**,[45] which can then undergo a key [2+1] cycloaddition reaction with dichlorocarbene.[46] This cycloaddition installs one of the desired cyclopropane units on substrate **45** to give bicyclic diester **46**. Reduction of the diester and subsequent activation of the resulting diol with methanesulfonyl chloride yields dimesylate **48**, which prepares the molecule for double elimination. Elimination of the mesylates using potassium *tert*-butoxide would result in diene **49**, ending the reported sequence of reactions. It was proposed that a Diels-Alder reaction between diene **49** and tetrachlorocyclopropene (**50**) would occur as a similar reaction has been reported with 1-bromo-2-chlorocyclopropene.[47] Tetrachlorocyclopropene was chosen as the dienophile because it was readily available and would provide symmetry to the subsequent synthetic intermediates that would make NMR spectra easy to analyze. It also had the advantage of placing two additional chlorine atoms directly on the polycyclic structure **51**, which could later be used as synthetic handles for possible derivations. The resulting Diels-Alder adduct **51** is an essential intermediate to access as it establishes the hydrocarbon skeleton and incorporates the second cyclopropane unit. The adduct also has an olefin in the center of the molecule, which is imperative to obtain the cyclodecane skeleton. It was therefore hypothesized that alkene **51** can be cleaved through ozonolysis to yield dione **52**.

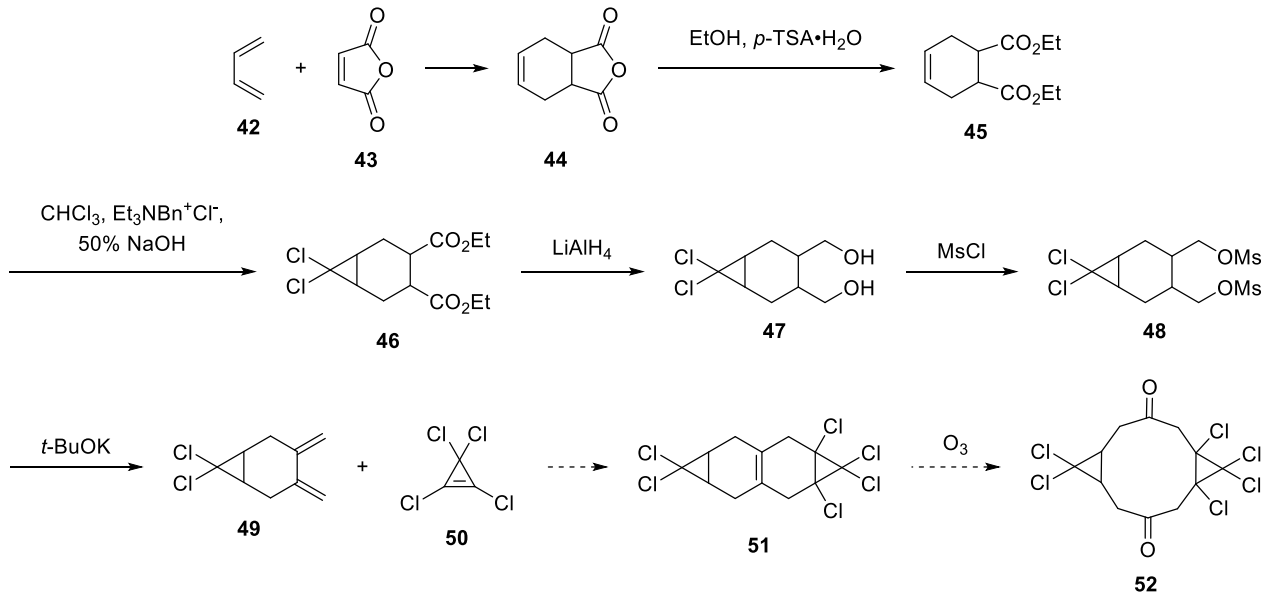

Scheme 2.1 Proposed route to reach dione **52**.

From dione **52** it was thought that two alternative routes were possible to obtain an aromatic [10]-annulene product (Scheme 2.2). Route A uses an elimination reaction to eliminate the two chlorine substituents located on the 10-membered ring to give diene **53** (Scheme 2.2a). It was postulated that oxidation of diene **53** followed by keto-enol tautomerism would establish the remaining olefins, resulting in target [10]-annulene **41**. Route B, however, uses a reduction reaction to reduce dione **52** to diol **55**, which could be activated with methanesulfonyl chloride or toluenesulfonyl chloride to give compound **56** (Scheme 2.2b). A four-fold elimination of the sulfonates and the chlorine substituents on the cyclodecane framework would produce tetraene **57**. It was presumed that an oxidation would be possible to achieve aromatic annulene **40**. Additionally, this [10]-annulene could undergo a hydrodechlorination step using Zn/AcOH to provide the parent [10]-annulene **37** modelled by Schleyer and coworkers.

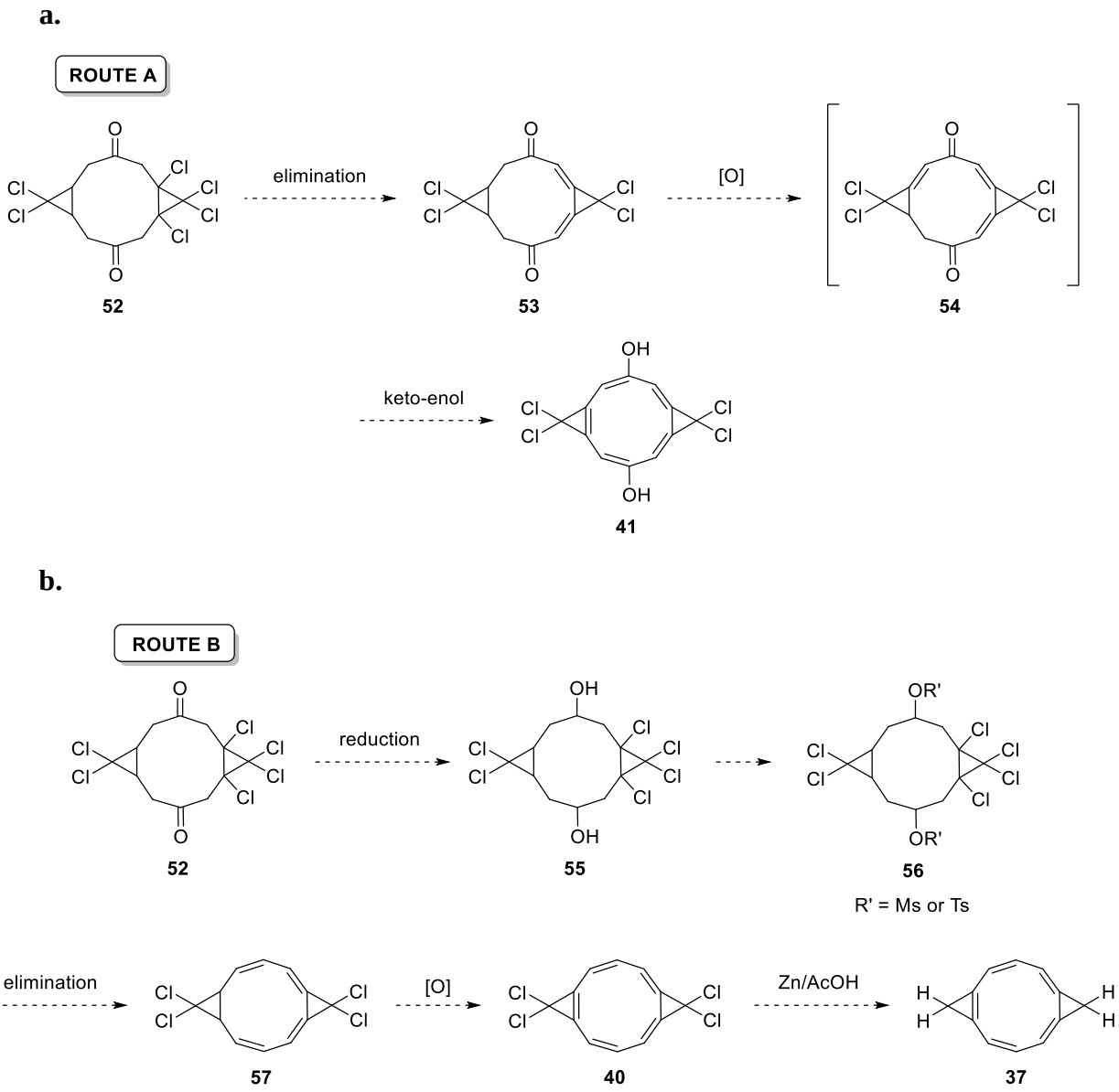

Scheme 2.2 Proposed completion of the route to obtain [10]-annulene derivatives **37**, **40** and **41**.

Compound **41** is synthetically more versatile because of the possible derivatization of the molecule that can be accomplished with the hydroxyl handles (Scheme 2.2). Target **40** is also an interesting candidate as its reactivity could be explored, like electrophilic aromatic substitution. Both **40** and **41** greatly resemble Schleyer's predicted aromatic [10]-annulene derivative **37**.

This overall strategy is based on known reactions and utilizes two different Diels-Alder reactions (Scheme 2.1). The route would use butadiene sulfone as the diene precursor for the first Diels-Alder reaction. Precedents for the ozonolysis of **51** and elimination of halides on related compounds will guide the remaining transformations.[48] Elimination of the chlorine substituents must be carried out carefully, as the resulting polyene has the possibility to dimerize.[48] This route provides the hydrocarbon framework with the incorrect oxidation state as the elimination of the chlorine and hydroxyl substituents would not result in the final product. This is a potential problem at a late stage in the synthesis, possibly making it difficult to obtain the aromatic target **37**, **40** or **41**.

A solution to the potential oxidation state problem is to incorporate an additional leaving group in the original diene, therefore eliminating the need for a final oxidation. Five-fold elimination may therefore be plausible for route B, leading directly to the aromatic product **40** (Scheme 2.3). It was also postulated that route A could lead to annulene **41** through elimination of the three leaving groups followed by keto-enol tautomerism.

A chlorine atom was chosen as a suitable substituent for the synthesis of [10]-annulene **40**, as it was assumed the corresponding intermediates would be stable to various reaction conditions and it could be eliminated with the other chlorine substituents. It appeared synthetically simpler to incorporate the additional substituent at the beginning of the synthesis rather than near the end. This would be most easily accomplished through using 2-chlorobutadiene in the first step.[49]

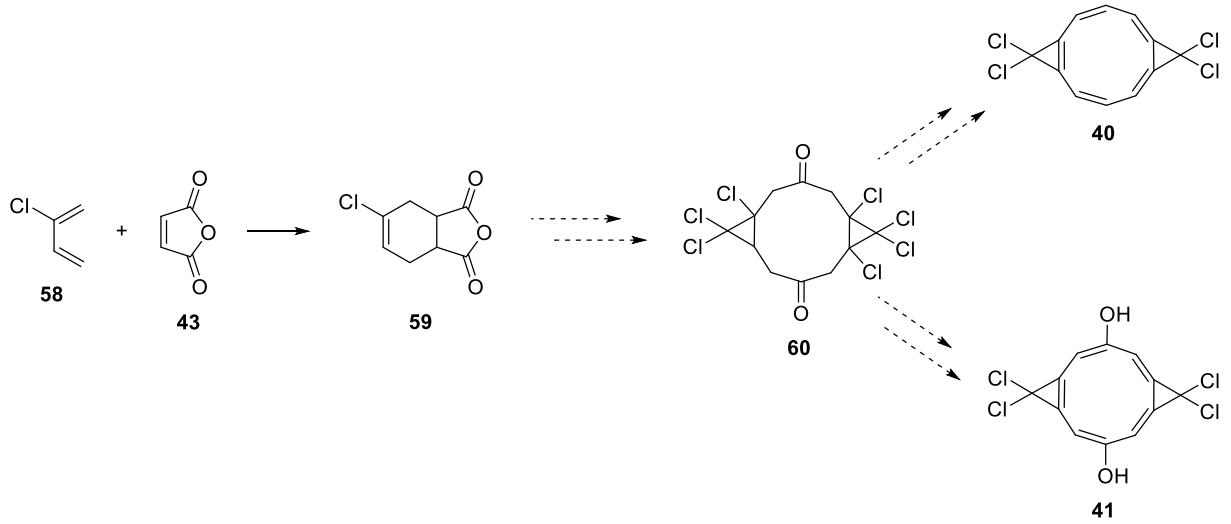

Scheme 2.3 Proposed chloroprene route to reach [10]-annulene targets **40** and **41**.

2.2 Butadiene Route

The butadiene route was chosen as the primary route to obtain an all-*cis* [10]-annulene because it featured many known reactions. The synthesis began with heating the butadiene precursor, butadiene sulfone (**61**), in the presence of maleic anhydride (**43**) to produce cycloadduct **44**,[44] placing an olefin in the ring for later cyclopropanation. Acid-catalyzed ethanolysis of anhydride **44** produced diester **45** in good yield.[45]

Cyclopropanation was achieved through modification of Müller's carbene phase transfer procedure.[46] Initial attempts used ethanol-free chloroform, a chilled solution of 50% $NaOH_{(aq)}$, triethylbenzylammonium chloride as the phase transfer catalyst, and a reaction temperature of 50 °C (Scheme 2.4). These reported conditions did not give a measurable amount of bicyclic diester **46**. Completing the reaction under an inert atmosphere did not alter the results. Sealing the reaction vessel, however, resulted in a good conversion to the desired product, suggesting that chloroform evaporation hinders this reaction. Vessel shape proved to be significant as well, as reactions carried out in a round bottom flask were lower yielding than a reaction carried out in a vial. This

observation can be rationalized by a more efficient mixing of the biphasic mixture, leading to more effective dichlorocarbene formation.

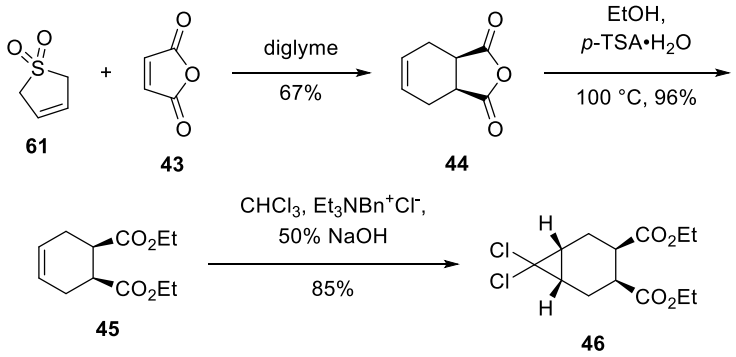

Scheme 2.4 Diels-Alder reaction of **61** with maleic anhydride, and subsequent ethanolysis and carbene [2+1] cycloaddition reactions to reach bicyclic diester **46**.

Other difficulties and safety considerations were encountered as more biphasic cyclopropanation reactions were performed. A combination of the exothermic nature of the reaction and the sealed vessel resulted in two explosions. The procedure was therefore modified to include a condenser open to air to prevent future explosions as well as the evaporation of chloroform. It was also noted that obtaining the mass spectrum of the bicyclic compound **46** was difficult. The mass spectrometer parameters were changed (see chapter 3) and the ESI ionization method was utilized to account for this difficulty.

Large scale carbene [2+1] cycloaddition reactions (88.5 mmol) were performed without external heat, as the exotherm quickly heated the solution. The vessel was placed in a cold bath when refluxing became too rapid and was removed when the solution had cooled. An addition of four more equivalents of chloroform to the ten already present resulted in another exotherm. The vessel was again cooled when refluxing became rapid. The reaction vessel was then monitored by TLC at room temperature. It is presumed that the additional chloroform allows for further carbene generation, aiding in the increase in yield from the reported 50% up to 85%.[46] Scale up of the

reaction and the addition of a condenser minimized chloroform evaporation, evidenced by the higher yields obtained by this method.

Finally, it was found that using ACS grade chloroform had no effect on the yield of **46**, therefore ethanol-free chloroform was no longer used. Following these modifications to the reported conditions, large quantities of **46** could be secured and the synthetic route could be pursued.

Reduction of bicyclic diester **46** with lithium aluminum hydride yielded diol **47**, which was then activated with methanesulfonyl chloride (Scheme 2.5).[46] Elimination of the dimesylate using potassium *tert*-butoxide gave diene **49** in low yield. It was discovered that the presence of water in the dimesylate sample led to the production of tetrahydrofuran **62** as a side product. It also became apparent that an increase in water in samples of **48** led to a higher yield of ether **62**, therefore prompting recrystallization of **48** to obtain higher yields of diene **49**.

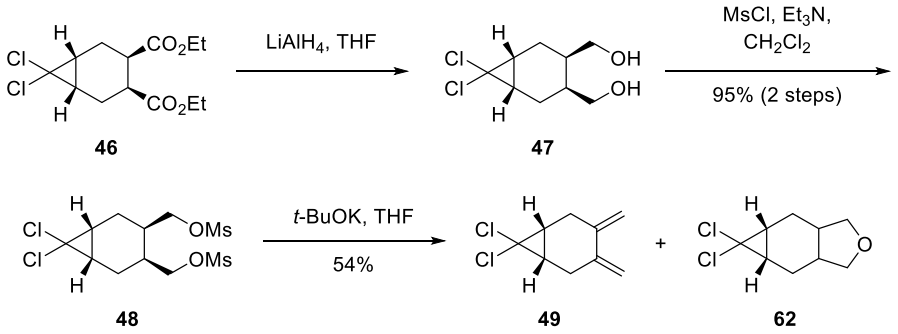

Scheme 2.5 Reduction of **46**, mesylation of the resulting diol **47** and elimination of **48** to obtain diene **49**.

Despite these precautions, elimination of the dimesylate **48** to diene **49** were inconsistent and low yielding, typically between 20% and 30% instead of the reported 50%.[46] Higher yields were more consistently obtained through a two step elimination process (Scheme 2.6).[50] The dimesylates were substituted for iodides, followed by a DBU-mediated elimination. It was noted

that the diiodide compound is volatile, therefore it should be concentrated under reduced pressure without heat. Diene **49** cannot be vacuum dried or stored for longer than a day as it is susceptible to polymerization.[51]

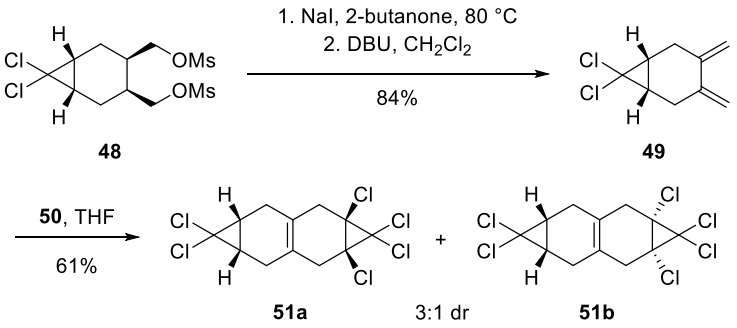

Scheme 2.6 Elimination of dimesylate **48** and Diels-Alder reactions between diene **49** and tetrachlorocyclopropene (**50**).

Diene **49** was reacted with tetrachlorocyclopropene to yield adducts **51a** and **51b** in a 3:1 ratio (Scheme 2.6). The identity of the diastereomers were determined using ^{1}H NMR chemical shift predictions completed at the B3LYP/6-311+G(2d,p)//M062X/6-31+G(d,p) level of theory. The computed and experimental shifts were compared and a mean absolute error (MAE) was calculated to indicate how closely the spectra match. Mean absolute error values less than or equal to 0.11 ppm for ^{1}H NMR indicates that the proposed structure is consistent with the observed chemical shifts. ^{13}C NMR chemical shift predictions are completed at the same level of theory as the ^{1}H NMR chemical shift predictions, with MAE values less than or equal to 2.5 ppm considered possible matches.

The computed shifts for cis adduct **51a** were compared to the observed shifts for the major and minor adducts.* The *cis* adduct had an MAE of 0.03 ppm when compared to the major experimental product, whereas comparison to the minor product gave an MAE of 0.10 ppm (Figure

* Calculations performed by Dr. Michel Gravel

2.1). The *trans* diastereomer **51b**, however, had an MAE of 0.05 ppm when compared to the major experimental product and MAE of 0.04 ppm when compared to the minor experimental product. These results indicate that both the *cis* and *trans* adducts are consistent with the observed shifts, however the *cis* adduct is a closer match to the major product than the *trans* stereoisomer. The *cis* diastereomer **51a** was therefore tentatively identified as the major product, as had previously been reported for similar reactions.[52] ^{13}C NMR chemical shift comparisons were not calculated due to the mismatch of the *cis* diastereomer with the minor predicted spectrum. This assignment was later confirmed through X-ray crystallography (*vide infra*).

A sample of diastereoenriched cycloadduct (**51a**/**51b** = 6:1) was subjected to ozonolysis conditions with a DMS quench, likely yielding the *cis* dione **52a** (Scheme 2.6). Attempts at purifying the compound were unsuccessful as it was found to decompose on silica, a behaviour observed on a similar substrate.[53] Recrystallization afforded dione **52** in 84% yield. This molecule, which was later confirmed as the *cis* dione **52a**, forms stable crystals that can be stored at room temperature for months. Larger scale reactions (>12 mg) did not go to completion as the Diels-Alder adducts **51a** and **51b** were recovered after the reaction.

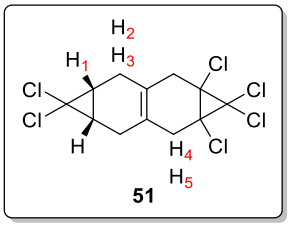

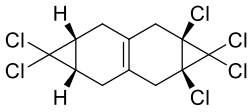

51a

MAE (ppm)
^{1}H NMR (major) = 0.03
^{1}H NMR (minor) = 0.10

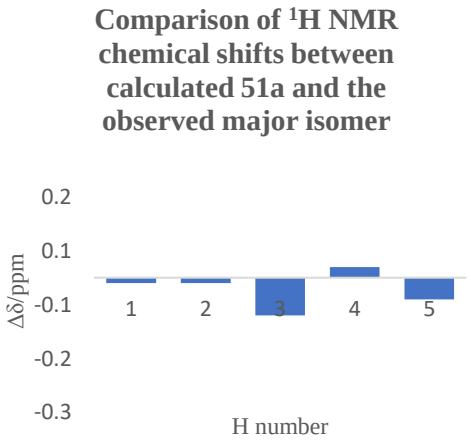

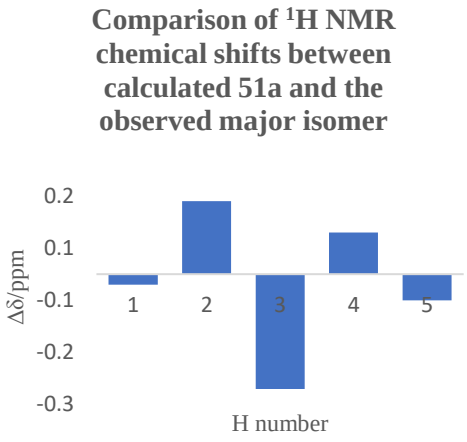

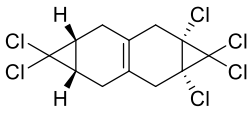

51b

MAE (ppm)
^{1}H NMR (major) = 0.05
^{1}H NMR (minor) = 0.04

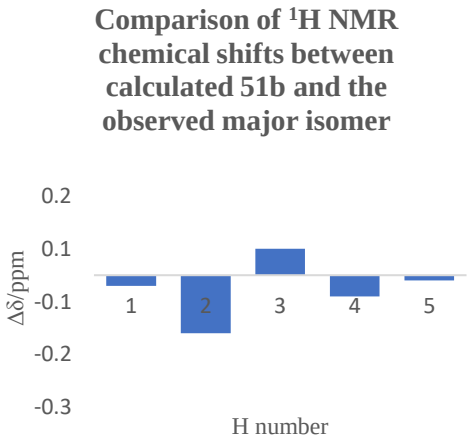

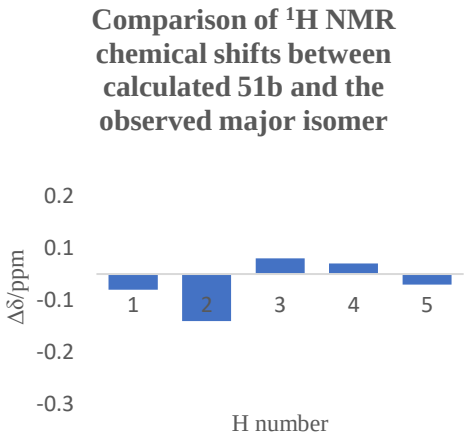

Figure 2.1 ^{1}H NMR chemical shifts comparison of Diels-Alder adducts **51a** and **51b** to the observed major isomer.

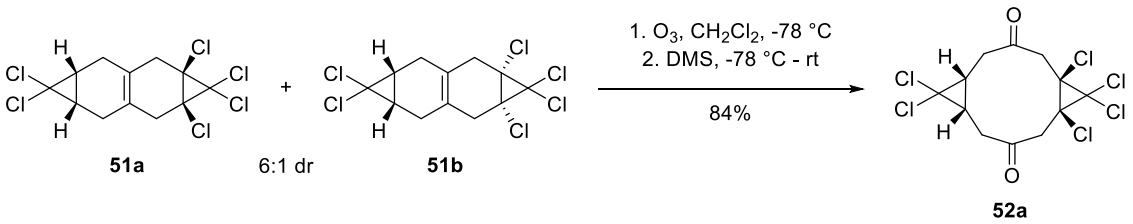

Scheme 2.7 Ozonolysis of Diels-Alder adducts with a DMS quench.

Calculations were undertaken to confirm the identity of the major dione diastereomer (Figure 2.2).* Both ^{1}H and ^{13}C NMR chemical shift predictions were utilized to determine the identity of the stereoisomers. Carbon atoms bonded to the chlorine atoms were excluded from the MAE calculations due to the heavy atom effect.[54] This effect systematically overestimates the chemical shift of carbon atoms bonded to elements in the third row or below in the periodic table.

It was assumed that the *cis* dione **52a** would be the major diastereomer as the *cis* Diels-Alder adduct was assigned as the major product. To further support this assumption, the ^{1}H NMR of the crude ozonolysis product showed the major diastereomer **51a** was mostly consumed in the reaction whereas the *trans* product **51b** was not. The predicted shifts for the *cis* dione **52a** had an MAE of 0.08 ppm when compared to the observed ^{1}H NMR spectrum for the major product. Comparison of the experimental and predicted ^{13}C NMR chemical shifts resulted in an MAE of 1.6 ppm. The MAE calculation excluded the carbon atoms bonded to chlorine atoms due to the heavy atom effect. The comparison of the predicted and observed ^{1}H NMR and ^{13}C NMR chemical shifts of *trans* dione **52b** resulted in mean absolute errors of 0.14 ppm and 1.7 ppm, respectively, indicating a likely mismatch for the *trans* diastereomer. Based on this information, the tentative assignment of the Diels-Alder diastereomers **51a** and **51b** was further supported.

* Calculations performed by Dr. Michel Gravel

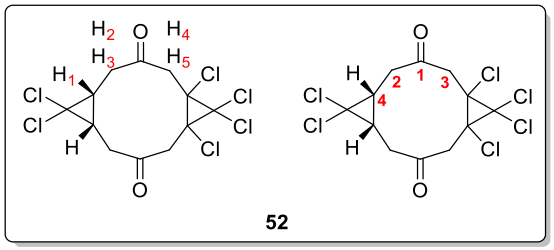

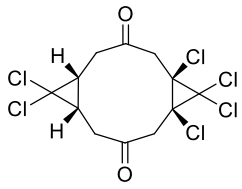

MAE (ppm)
^{1}H NMR = 0.08
^{13}C NMR = 2.1

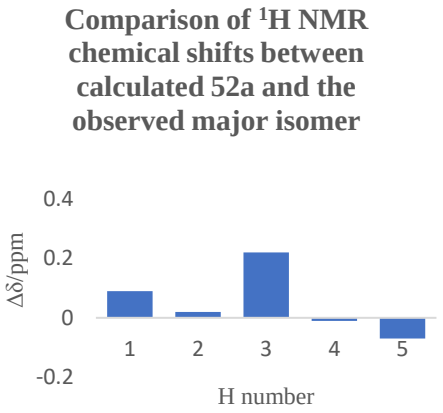

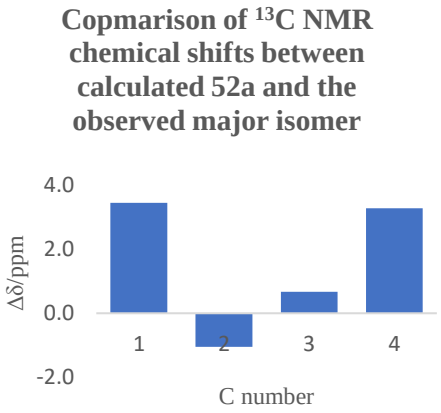

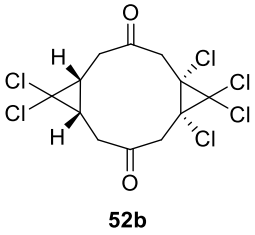

MAE (ppm)
^{1}H NMR = 0.14
^{13}C NMR = 2.6

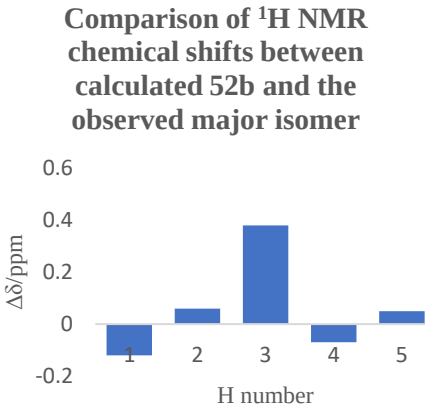

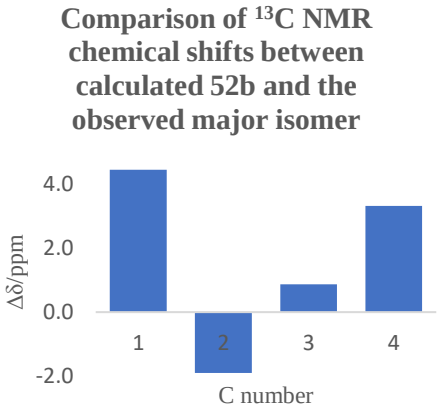

Figure 2.2 ^{1}H NMR and ^{13}C NMR chemical shifts comparison of diones **52a** and **52b** to the observed major isomer.

A crystal of dione **52a** (containing 17% unreacted minor Diels-Alder adduct **51b**) was subjected to X-ray diffraction to confirm the relative configuration of the dione and therefore the configuration of the major product in the Diels-Alder reaction (Figure 2.3). The crystal structure

confirmed the *cis* configuration of the major dione **52**, as predicted by chemical shift calculations. The fact that the *trans* Diels-Alder adduct **51b** is observed in the crystal with major dione **52a** validates the observation that the minor diastereomer **51b**, now confirmed to have the *trans* configuration, reacts more slowly than the major *cis* adduct **51a** in the ozonolysis reaction.

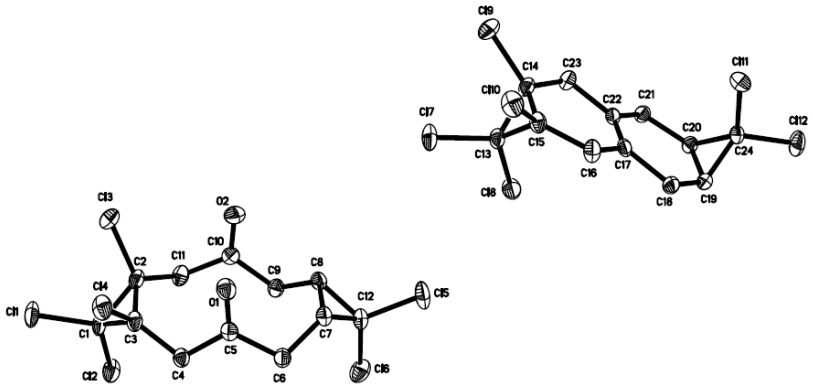

Figure 2.3 Structure of dione **52a** and Diels-Alder adduct **51b** obtained from X-ray diffraction. Thermal ellipsoids are at 50% probability.

Attempts to scale up the reaction utilized the 3:1 mixture of adducts **51a** and **51b**. A different concentration (91.5 mM vs 8.2 mM) was used and resulted in an opaque solution after the addition of DMS and removal of the vessel from the bath. After stirring the reaction overnight at room temperature, a white solid was observed that was later discovered to be insoluble in dichloromethane and $CDCl_3$. These observations were uncharacteristic of the dione previously isolated. The ^1H NMR spectrum showed that another substrate had formed in this reaction, which was assumed to be an aldol product **63** formed from a transannular aldol reaction (Figure 2.4). Further attempts at large scale reactions provided more of the undesirable side product.

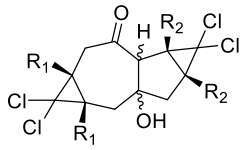

63

63a. R_1 = H, R_2 = Cl
63b. R_1 = Cl, R_2 = H

Figure 2.4 Proposed transannular aldol side product from the ozonolysis reaction.

It was postulated that the DMS quench was responsible for the formation of the aldol side product **63**. DMS requires the reaction solution to warm to room temperature over a few hours to completely quench the ozonide, allowing ample time for the transannular aldol reaction to occur. If this is true, altering the quench to include triphenylphosphine should avoid formation of **63** as it can be performed at -78 °C and requires less time to react with the ozonide. This alternative method, however, was unsuccessful in avoiding the formation of the side product.

It became necessary to elucidate the structure of the unknown ozonolysis side product to understand the various pathways the transformation could proceed through. Precedent led to speculation that the aldol transformation favours pathway A due to the position of the methylene protons (Figure 2.5).[48] These methylene protons are postulated to be more acidic as they are adjacent to an electron withdrawing chlorine substituent.

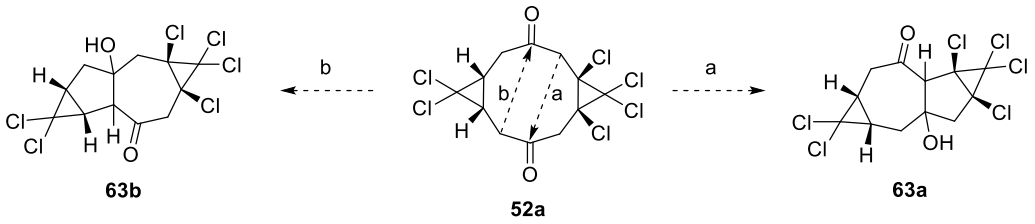

63b **52a** **63a**

Figure 2.5 Possible transannular aldol reaction pathways. Image adapted from ref. 48.

Mass spectrometry showed the isolated side product had a mass of 395.8820 amu and a molecular formula of $C_{12}H_{10}O_2Cl_6$, consistent with aldol product **63**. Two-dimensional NMR

experiments were necessary in determining which constitutional isomer was formed, **63a** or **63b**. The COSY NMR spectrum showed that signal A, assumed to be due to a hydroxyl proton because it was a broad singlet, did not show coupling correspondence to any other proton (Figure 2.6). Singlet B, with an integration of 1, also did not show a coupling correspondence to other protons. This suggests that the proton may be in the bridging position of the aldol product. If this assumption is true, then the bridging proton must be between the carbonyl and a quaternary carbon atom, suggesting isomer **63a**. Signal D did not couple to any protons in the spectrum, implying that these two protons are either between the hydroxyl and quaternary carbon atoms in **63a** and **63b** or between the carbonyl and quaternary carbon atoms in **63b**. Signal C must be near the protons responsible for signals E, E' and F, whereas signals E and E' couple to H_C, H_F and H_G. H_F and $H_{F'}$ are near the protons responsible for signals C, E and G, whereas H_G must be near the protons responsible for signals E or E' and F. It can therefore be concluded from the COSY NMR spectrum that the protons accountable for signals C, E, E', F, F' and G are in close proximity.

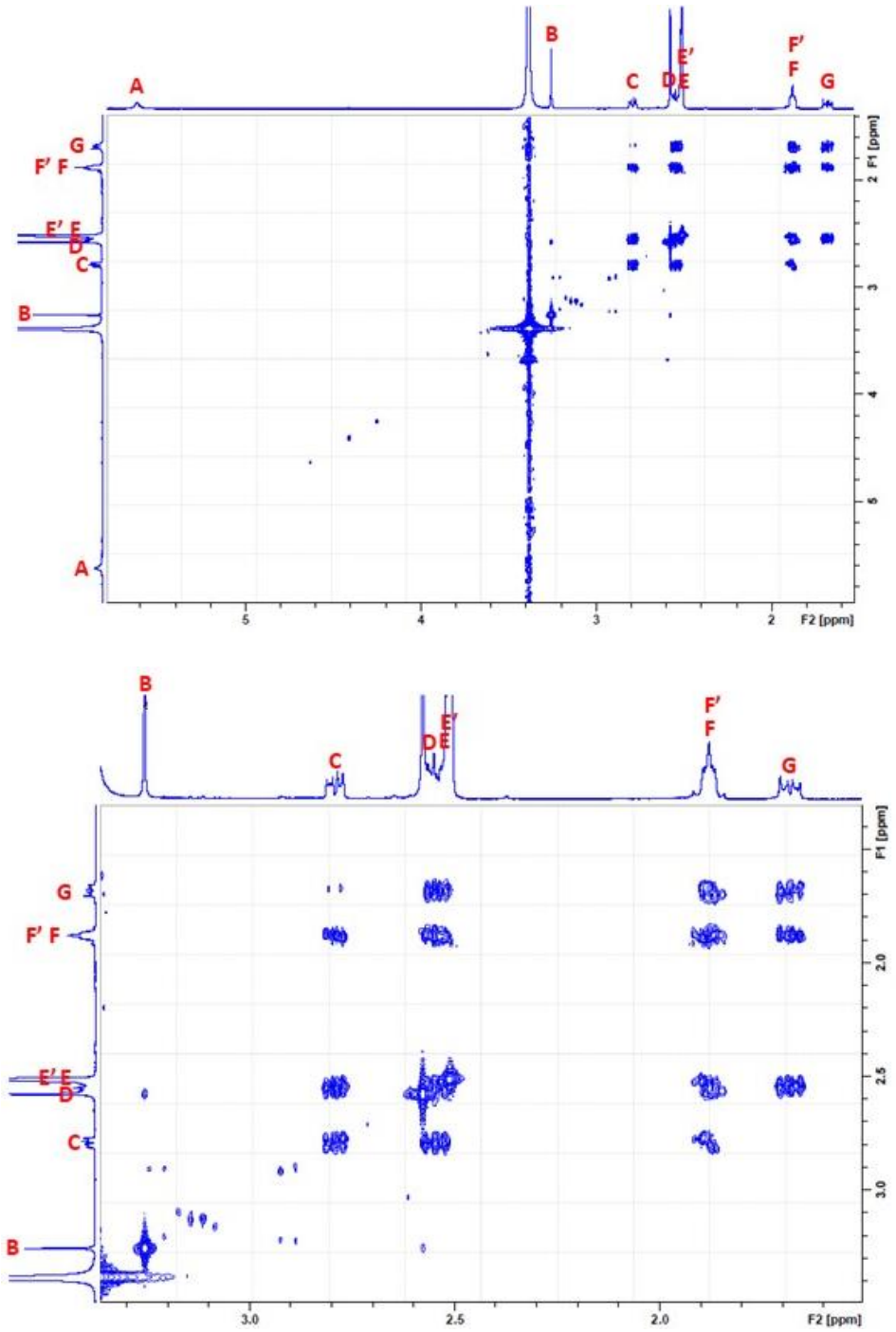

Figure 2.6 COSY NMR spectrum of aldol product **63**. The first image shows all signals in the COSY NMR spectrum, whereas the second image is an expansion of the spectrum to show the coupling correlations.

The HSQC NMR spectrum showed that carbons 1–4, 6 and 7 were quaternary carbon atoms, whereas carbons 5, 11 and 12 were methine carbon atoms (Figure 2.7). Carbon atoms 8, 9 and 10 were assigned as methylene carbon atoms. Signal A did not couple to a carbon atom, confirming it to be the hydroxyl proton in side product **63**. C_1 was assigned as the carbonyl carbon due to its chemical shift in the ^{13}C NMR spectrum (δ = 196 ppm), whereas C_2 was confirmed as the carbon bonded to the hydroxyl due to its downfield chemical shift (δ = 85 ppm). The remaining quaternary carbon atoms were bonded to the chlorine atoms. It was presumed that carbon 3 was bonded to 2 chlorine atoms and was part of the tetrachlorinated cyclopropane substituent due to its downfield chemical shift (δ = 77.5 ppm). Carbon 4 was also presumed to be CCl_2 due to its more downfield chemical shift (δ = 66.7 ppm). Both C_6 (δ = 60.0 ppm) and C_7 (δ = 59.4 ppm) represent the CCl moieties.

The HMBC NMR spectrum showed that signal A did not correlate to a carbon atom in the structure, again confirming it as the hydroxyl proton (Figure 2.8). Signal B, however, showed coupling with carbons 2, 3, 6 and 7. This correlation shows that the bridging proton is adjacent to the tetrachlorinated cyclopropane substituent as carbons 3, 6 and 7 are bonded to chlorine atoms. Due to these correlations, it can be said that a diastereomer of **63a** was formed as the side product in the ozonolysis of **52**. The remaining carbon and proton coupling correlations were analyzed to confirm the identity of **63** as **63a**.

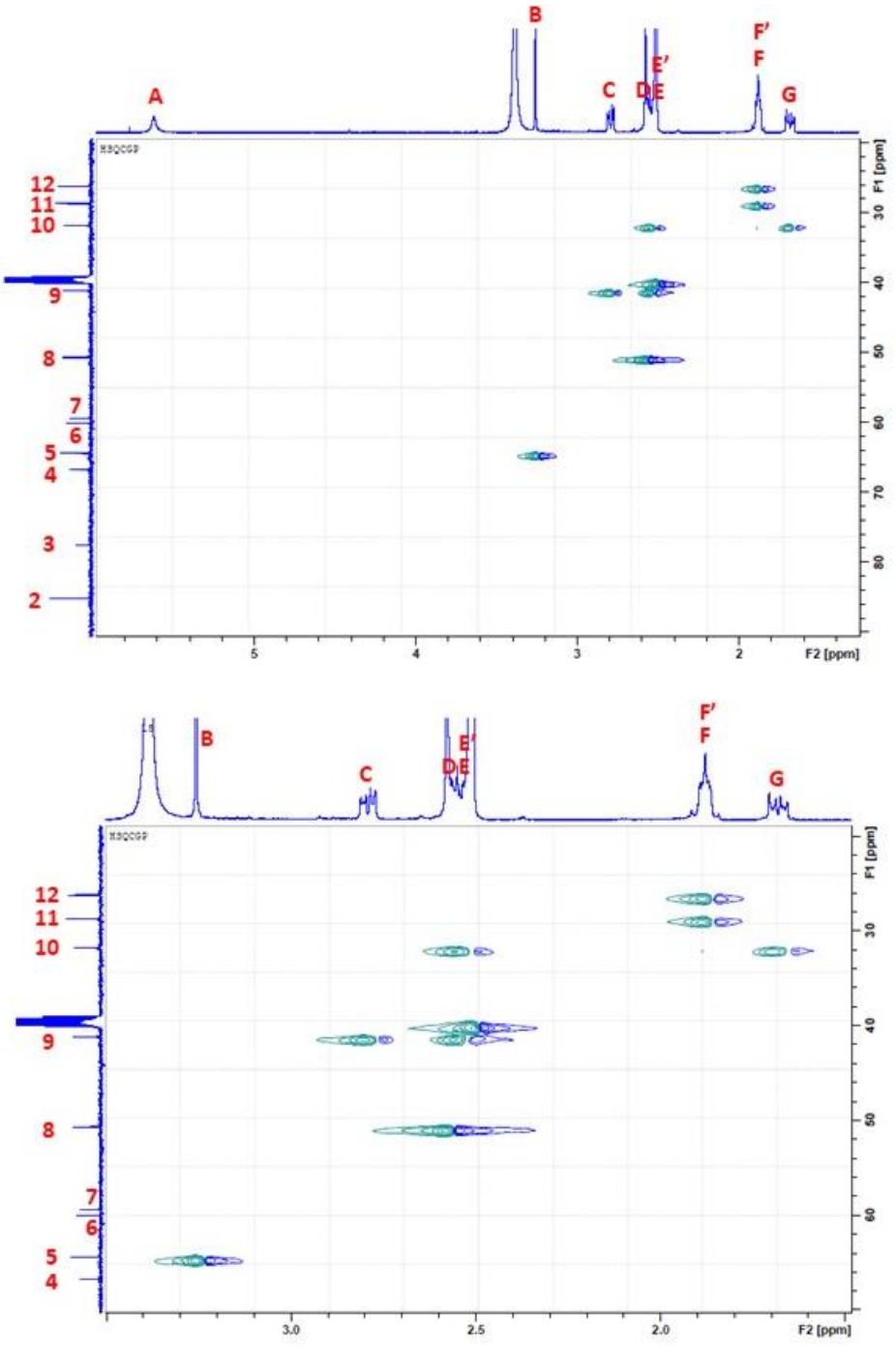

Figure 2.7 HSQC NMR spectrum of aldol product **63**. The first image shows all signals in the HSQC NMR spectrum, whereas the second image is an expansion of the spectrum to show the coupling correlations. The carbonyl carbon signal 1 (δ = 196.7 ppm) was omitted from the figure as it did not show coupling to any proton signals.

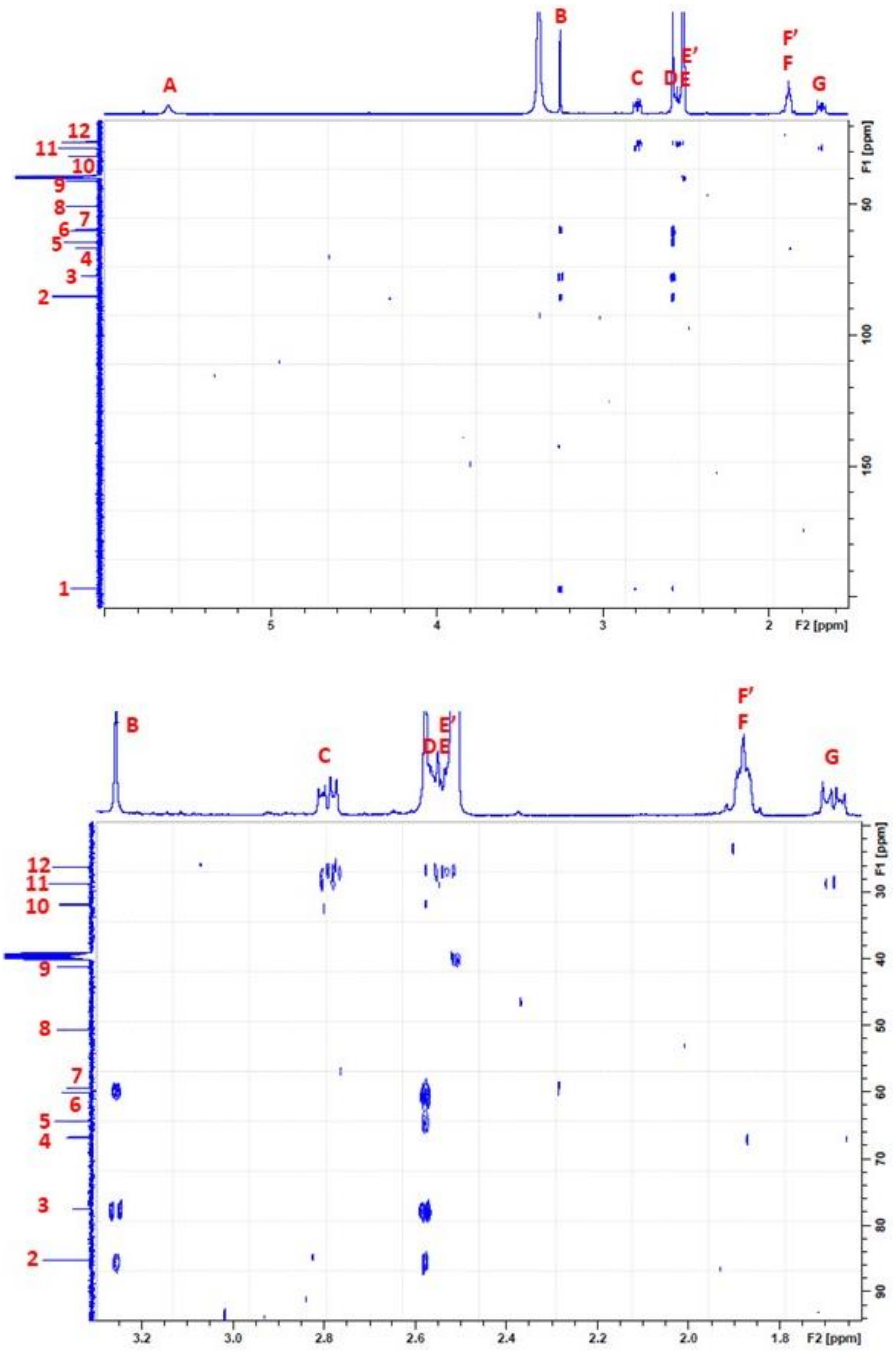

Figure 2.8 HMBC NMR spectrum of the aldol product **63**. The first image shows all signals in the HMBC NMR spectrum, whereas the second image is an expansion of the spectrum to show the coupling correlations.

Having identified the transannular aldol side product formed in the ozonolysis reaction of **51a** and **51b**, ^{1}H and ^{13}C NMR chemical shift calculations were utilized to determine its relative configuration. The ^{1}H NMR chemical shift predictions were performed using the PCM solvation models with parameters for $CHCl_3$, whereas the ^{13}C NMR predictions were performed using DMSO parameters (Figure 2.9).[55] This was done because d_6-DMSO was required to solubilize the product to get a high signal to noise ratio for the ^{13}C NMR spectrum. Again, the ^{13}C NMR chemical shift MAE calculations exclude carbon atoms bonded to chlorine substituents due to the heavy atom effect.[54] Compounds **63aa**, **63ab**, **63ac**, and **63ad** were found to have mean absolute errors of 0.11 ppm, 0.19 ppm, 0.21 ppm, and 0.34 ppm, respectively, for the ^{1}H NMR chemical shift comparison. These results indicated that diastereomer **63aa** was the likely stereoisomer of the aldol product **63**. ^{13}C NMR chemical shift predictions resulted in mean absolute errors of 3.4 ppm, 5.1 ppm, 6.2 ppm and 6.8 ppm for isomers **63aa**, **63ab**, **63ac** and **63ad**, respectively. The mean absolute error value of 3.4 ppm between calculated chemical shifts of **63aa** and the experimental chemical shifts of **63a** was the closest match of all the diastereomers modelled, verifying the relative configuration as that of isomer **63aa.**

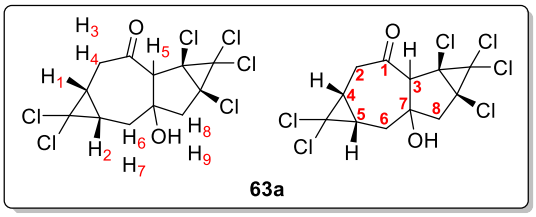

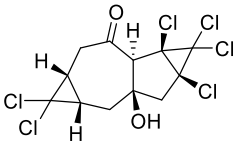

MAE (ppm):
^{1}H NMR = 0.11
^{13}C NMR = 3.4

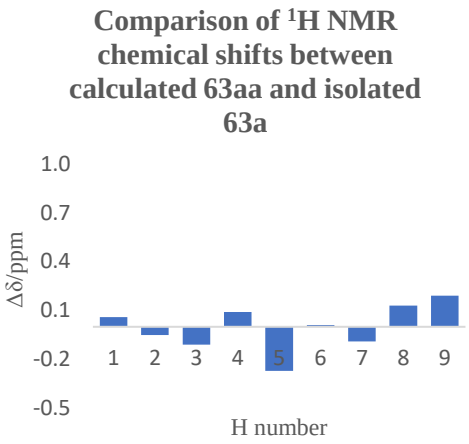

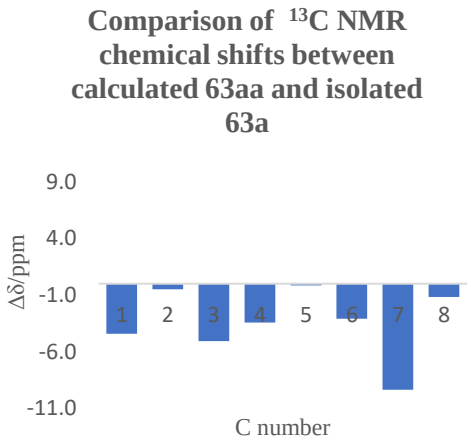

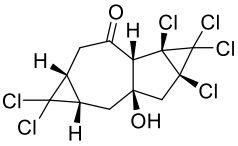

MAE (ppm):
^{1}H NMR = 0.19
^{13}C NMR = 5.1

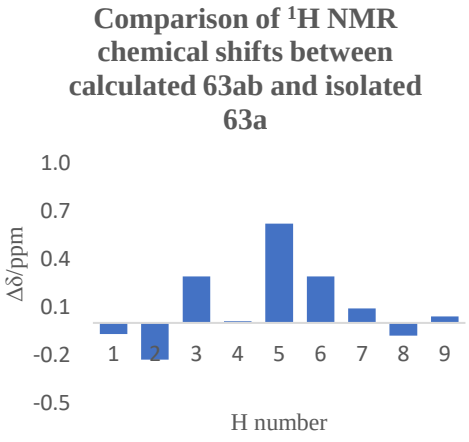

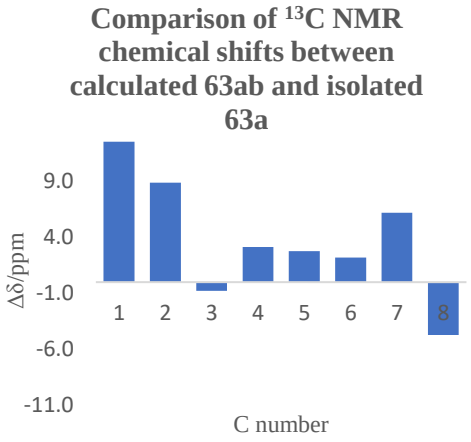

(Figure continued on next page)

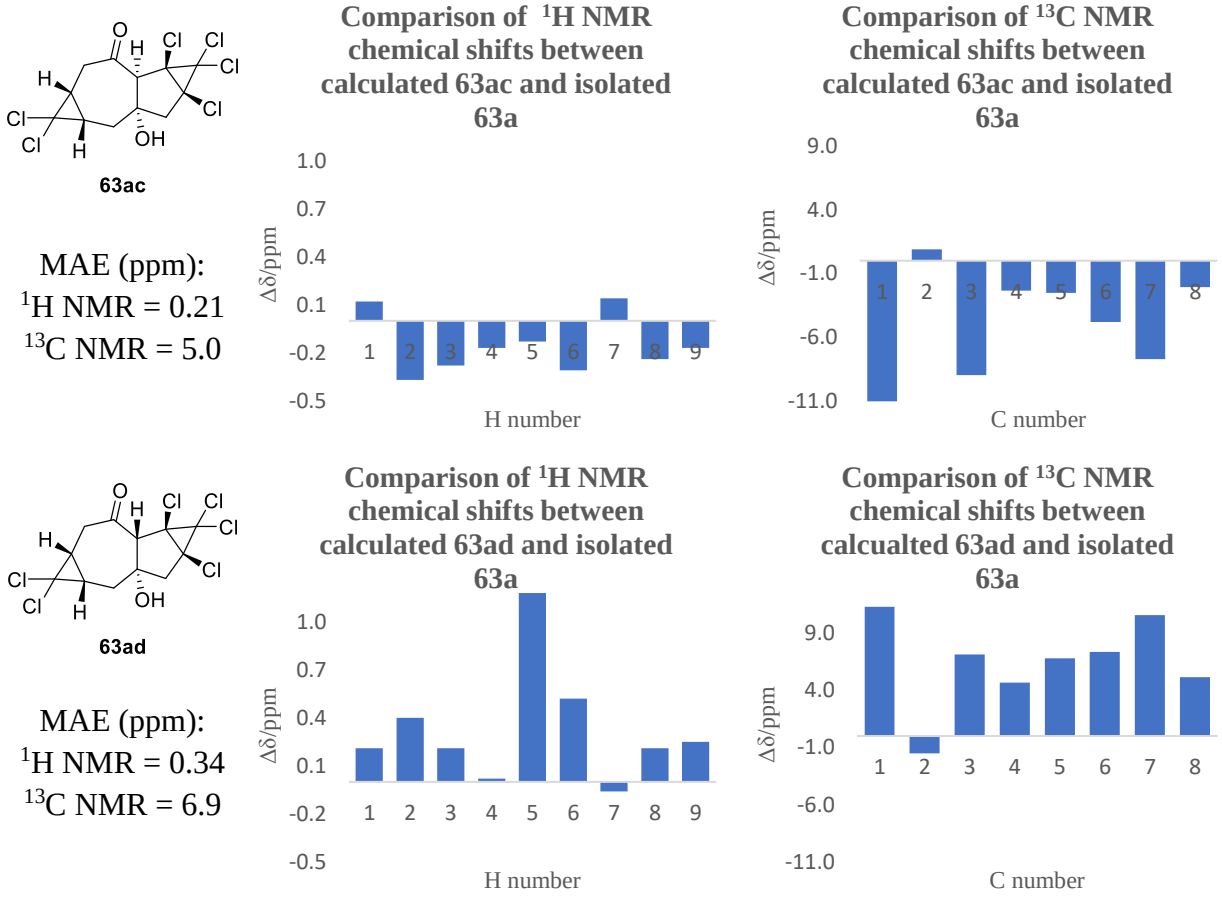

Figure 2.9 ^{1}H NMR ($CHCl_3$) and ^{13}C NMR (DMSO) chemical shifts comparison of aldol products **63aa**, **63ab**, **63ac** and **63ad** to isolated **63a**.

Alternative ozonolysis methods were investigated in an attempt to produce dione **52** more reliably as well as to avoid the formation of aldol side product **63aa** (Scheme 2.8). Two methods were found that used a dichloromethane:methanol solvent system and thiourea as the reducing agent.[48,53] One method, however, used sodium bicarbonate as an additive in the reaction vessel. It was found that the reaction using sodium bicarbonate gave a higher yield of dione **52** (89%) than the one without it (52%), therefore this method was adopted for use.

The results using the new reductive workup procedure were more reproducible than the previous DMS method. Unsurprisingly, the major product was dione **52a** and only a minor amount

of aldol product **63aa** was observed in all cases in which the reaction was performed on <410 mg scale (Scheme 2.8). Unfortunately, the amount of **63aa** increased as the reaction was scaled to four grams, as **63aa** was isolated in 49% yield. Dione **52** was inseparable from adducts **51a** and **51b** in this experiment, however the dione was calculated to have a 49% yield *via* ^{1}H NMR analysis.

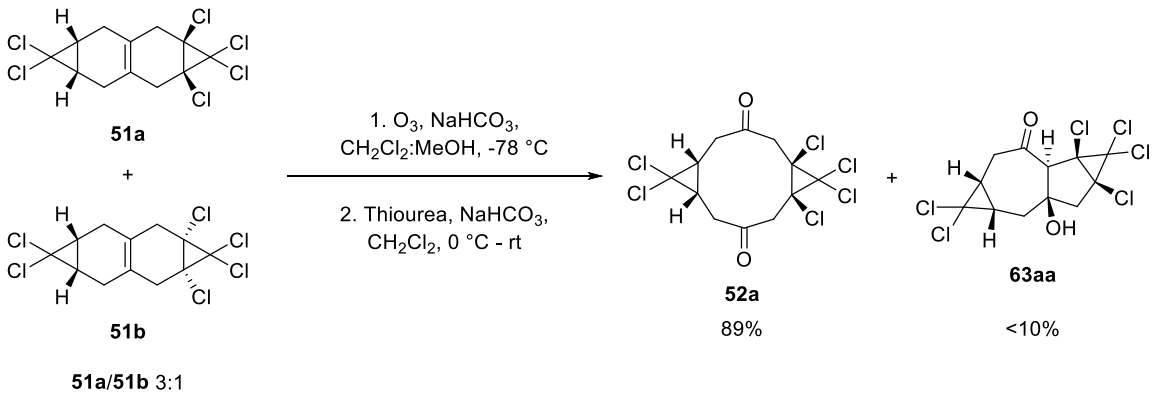

Scheme 2.8 Ozonolysis of Diels-Alder adducts **51a** and **51b** (**51a**/**51b** 3:1), on a 45-mg scale.

None of the ozonolysis reactions went to completion as both the *trans* and *cis* Diels-Alder adducts, **51a** and **51b**, were recovered. The *trans* Diels-Alder adduct **51b** was consistently recovered in higher yield than the *cis* adduct **51a** even though it was the minor isomer in the starting mixture. Additionally, the *cis* dione **52a** was identified as the lone dione product. It is postulated that *trans* **51b** is slower to react than its *cis* isomer **51a**.

Calculations support this observation as it was determined that the transition state for the ozonolysis reaction using the *trans* substrate **51b** is 2.8 kcal/mol higher in energy than that of the *cis* **51a**.[*] This is a seemingly small energy difference assuming that the ozonolysis with the *cis* adduct **51a** is instantaneous. This assumption is false, however, as **51a** has been recovered after some ozonolysis reactions. Therefore, isomer **51b** would require more time to react with the available ozone than initially thought.

[*] Calculations performed by Dr. Michel Gravel

Two hypotheses have been suggested to explain this observation. The first states that steric hindrance affects the reactivity of the Diels-Alder adducts (Figure 2.10). The *trans* diastereomer has chlorine atoms that block both faces of the olefin, resulting in a slower reaction. The *cis* diastereomer **51a**, however, has one sterically unhindered face, allowing the ozonolysis reaction to proceed more quickly. The second hypothesis states that there is an electrostatic repulsion between the electronegative chlorine atoms and the incoming ozone molecule in the *trans* stereoisomer **51b**, leading to a slower reaction.

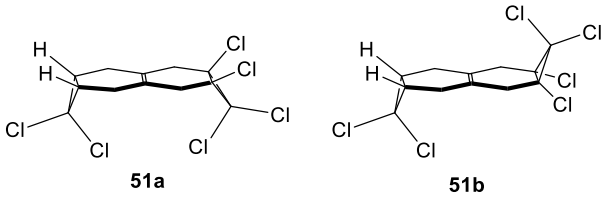

51a **51b**

Figure 2.10 *Cis* and *trans* Diels-Alder adduct diastereomers.

Dihydroxylation was attempted using osmium tetroxide in efforts to avoid the formation of aldol product **63aa** (Scheme 2.9).[56] It was postulated that the resulting diol could be cleaved using $NaIO_4$ to obtain dione **52**. The reaction conditions failed to produce diol **64**, as the *cis* starting material **51a** was recovered after two days of reaction time. An alternative dihydroxylation method was attempted that included tetrabutylammonium bromide, potassium ferricyanide, and potassium carbonate in THF and water, however this also failed to produce diol **64**.[48]

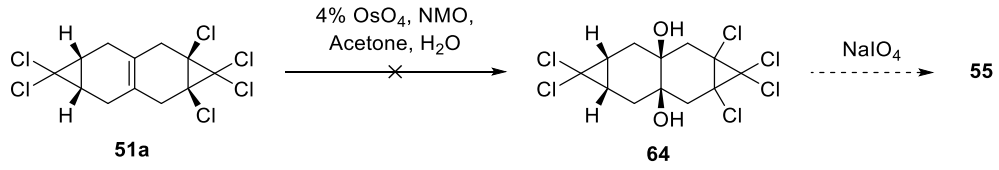

51a **64**

Scheme 2.9 Attempted dihydroxylation on Diels-Alder adduct **51a.**

Calculations were undertaken to guide the synthetic route for the final steps. The viability of the proposed keto-enol route (cf. route A, scheme 2.2) was examined through calculating the energies of the species **66** and **67** (Scheme 2.10). Trienedione **66** could potentially be obtained from a double elimination followed by an oxidation or by reversing these steps.

Calculations performed at the B3LYP/6-31G*//HF/3-21G level of theory predicted planar tautomer **67** to be 13.2 kcal/mol higher in energy than triene **66**. This was unexpected as the resulting diol **67** was shown to be planar and should therefore be aromatic. Presumably, the increased angle strain combined with the unfavourable change in bond enthalpies are more important factors than the energy gained in aromatic stabilization. The proposed keto-enol route was therefore predicted to be an invalid approach to obtain an aromatic [10]-annulene. It is hypothesized, however, that dione **66** may be useful by trapping the corresponding dienolate as the ditriflate **68**. This compound could be useful for derivatization and optoelectronic applications through transition metal catalyzed cross couplings. In view of the predicted unfavourable keto-enol equilibrium and of the difficulty in obtaining dione **52** on scale, route B (cf. Scheme 2.2) was prioritized with the hope that it would be more amenable to synthesis on a gram scale.

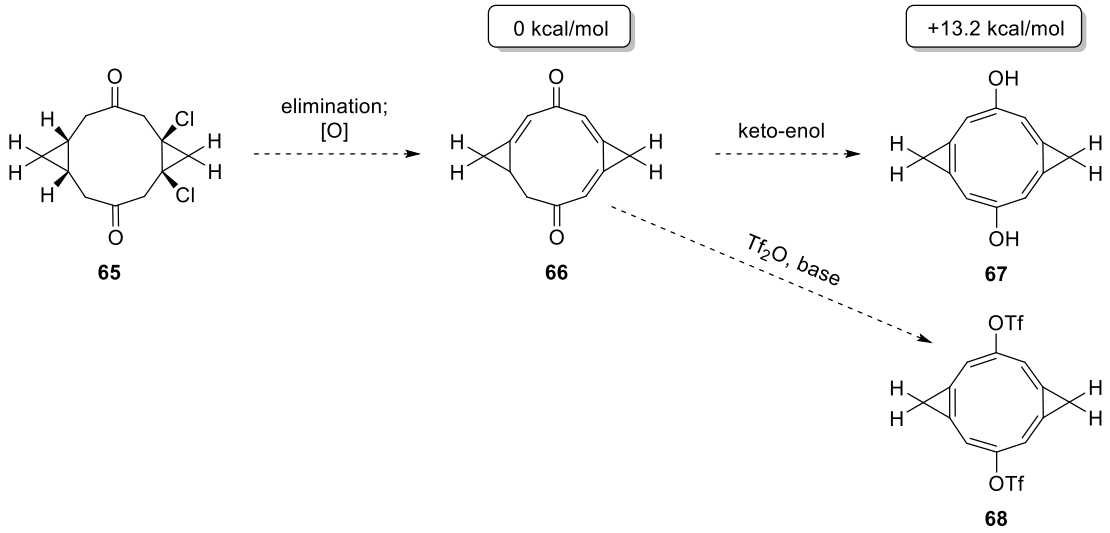

Scheme 2.10 Keto-enol route to aromatic [10]-annulenes **67** and **68**.

The approach to reach the target compound **67** therefore includes reducing dione **52a** and subsequently activating it with mesyl chloride or tosyl chloride (Scheme 2.11). A four-fold elimination of the leaving groups in **56** would result in tetraene **57**. Calculations show that the final olefin may be installed through oxidation with DDQ, as this reaction is predicted to be exergonic by 30.1 kcal/mol.*

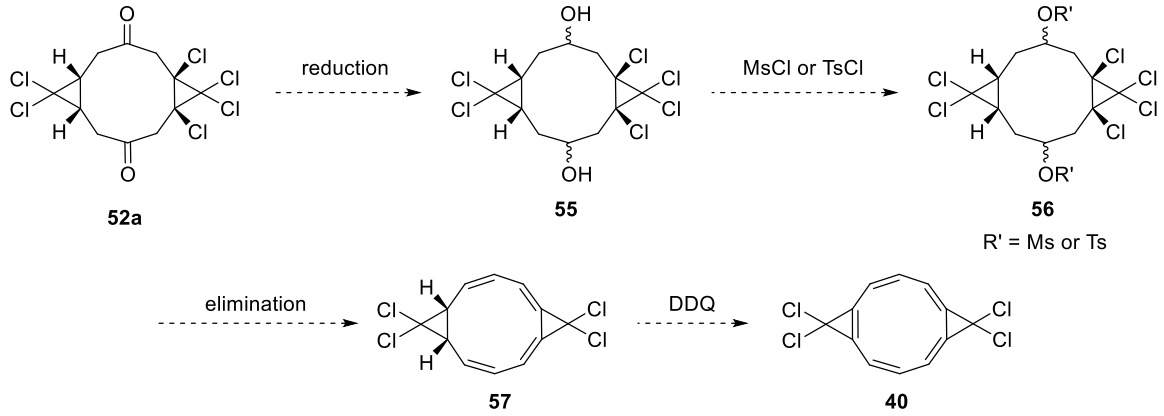

52a **55** **56** **57** **40**

Scheme 2.11 The final steps in the synthesis of aromatic [10]-annulene **40** *via* route B.

Reduction of dione **52a** occurred with sodium borohydride or lithium aluminum hydride (Scheme 2.12). The reaction was ineffective as only a small amount of diol **55** was isolated, as well as a side product. Optimization of the reaction included increasing the temperature, altering the solvent and increasing the reaction time. These changes failed to yield significant quantities of the diol, nor was the formation undesirable side product avoided.

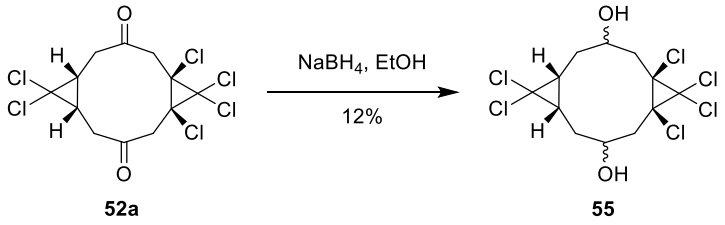

52a **55**

Scheme 2.12 Reduction of *cis* dione **52a**.

* Computations performed by Dr. Michel Gravel

^{1}H NMR chemical shift calculations were undertaken using chloroform parameters to identify the diol diastereomer produced (Figure 2.11). Seven proton signals were observed in the ^{1}H NMR spectrum, therefore excluding isomer **55c** from consideration as it is expected to have fourteen ^{1}H signals due to its lack of symmetry. The ^{1}H NMR chemical shift predictions were therefore completed on meso diols **55a** and **55b** (Figure 2.12). The MAE of these diols were 0.11 ppm and 0.16 ppm, respectively, suggesting dione **52a** is reduced to diol **55a**. ^{13}C NMR chemical shifts were predicted using DMSO parameters to validate the identity of diol **55**.[55] The MAE values of 2.2 ppm for **55a** and 3.6 ppm for **55b** further verify the configuration of diol **55** to be the all-*cis* **55a**.

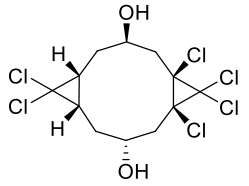

55c

Figure 2.11 Unsymmetrical diol **55c**.

The reduction side product was assumed to be hemiacetal **69** or mono-reduced **70** (Figure 2.13). Attempts at cleaving the hemiacetal with lithium aluminum hydride failed to yield diol **55**, suggesting the product was not a hemiacetal (Scheme 2.13).[57] ^{1}H NMR chemical shift calculations confirmed the side product was not hemiacetal **69** as diastereomers **69a**, **69b**, **69c**, and **69d** were calculated to have mean absolute errors of 0.44, 0.22, 0.39, and 0.44 ppm, respectively (Figure 2.14).

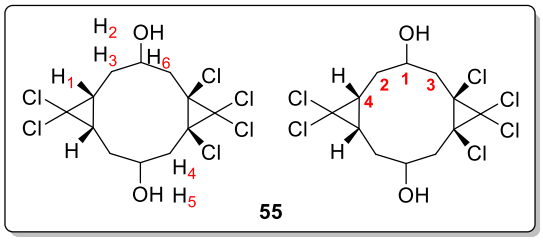

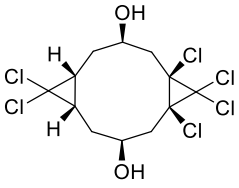

55a

MAE (ppm)
^{1}H NMR = 0.11
^{13}C NMR = 2.2

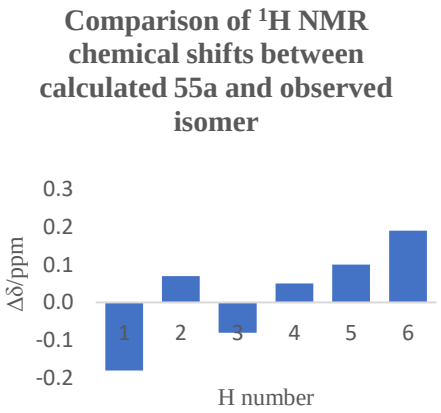

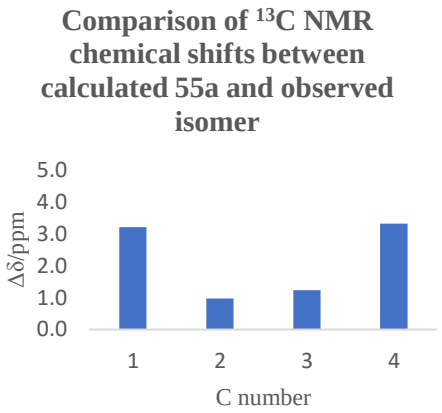

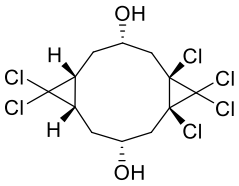

55b

MAE (ppm)
^{1}H NMR = 0.16
^{13}C NMR = 3.6

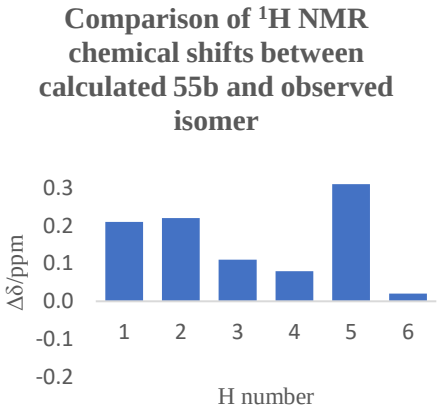

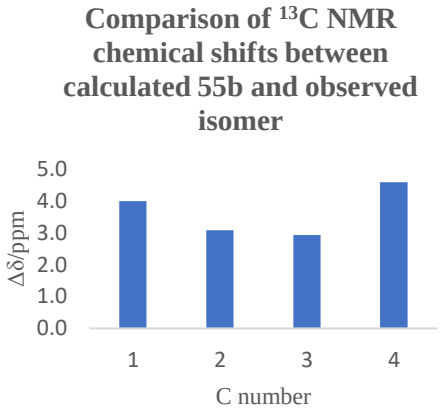

Figure 2.12 ^{1}H ($CHCl_3$) and ^{13}C NMR (DMSO) chemical shifts comparison of meso diols **55a** and **55b** to observed isomer.

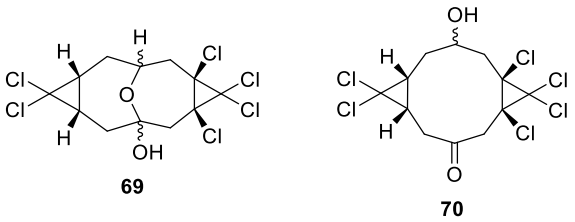

Figure 2.13 Proposed reduction side products.

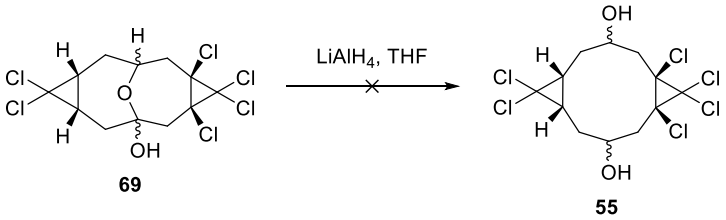

Scheme 2.13 Attempted reduction of proposed hemiacetal side product.

^{1}H NMR chemical shift calculations were also completed on monoreduced stereoisomers **70a** and **70b** in an attempt to identify the reduction side product (Figure 2.15). The MAE values for the all-*cis* **70a** and *trans* **70b** were calculated to be 0.36 ppm and 0.30 ppm, respectively. These values show that the proposed monoreduced molecules **70a** and **70b** are not the side product either.

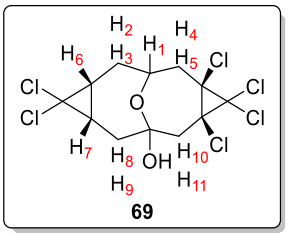

69

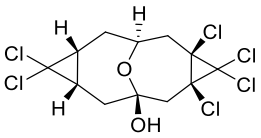

69a

MAE (ppm)
^{1}H NMR = 0.44

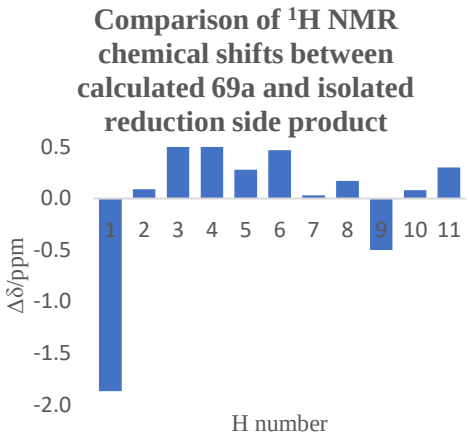

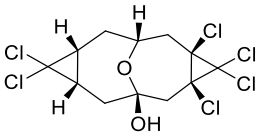

69b

MAE (ppm)
^{1}H NMR = 0.22

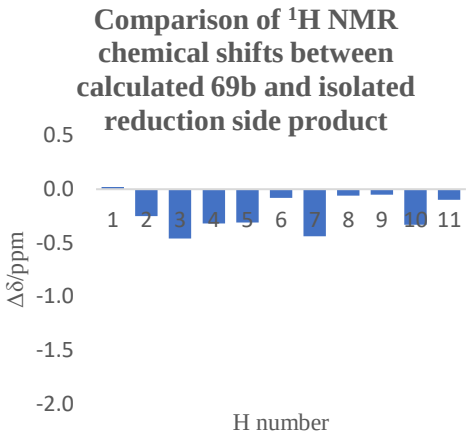

(Figure continued on next page)

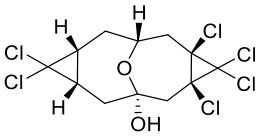

69c

MAE (ppm)

^{1}H NMR = 0.40

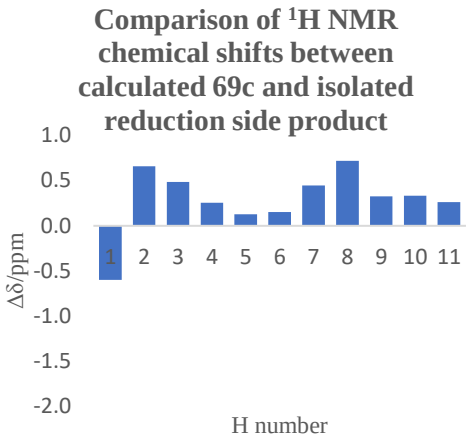

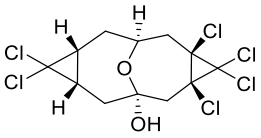

69d

MAE (ppm)

^{1}H NMR = 0.46

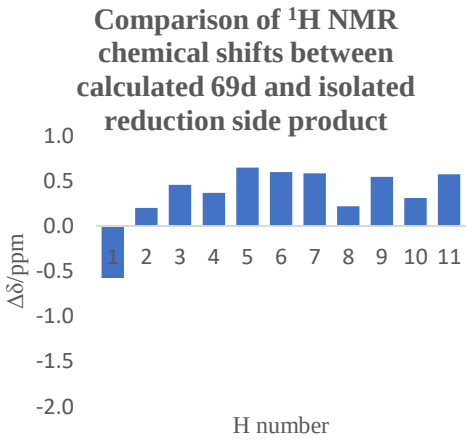

Figure 2.14 ^{1}H NMR chemical shifts comparison of hemiacetals **69a**, **69b**, **69c**, and **69d** to the isolated reduction side product.

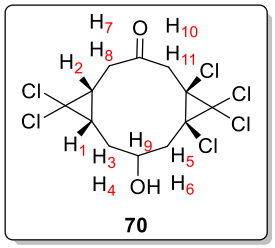

70

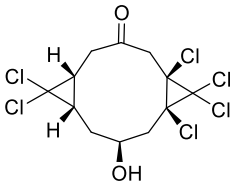

70a

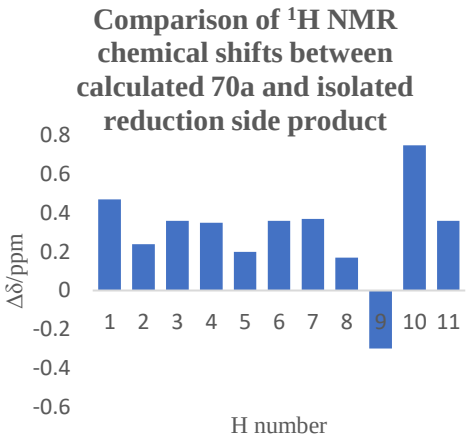

MAE (ppm)
^{1}H NMR = 0.36

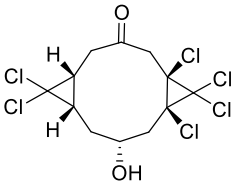

70b

MAE (ppm)
^{1}H NMR = 0.30

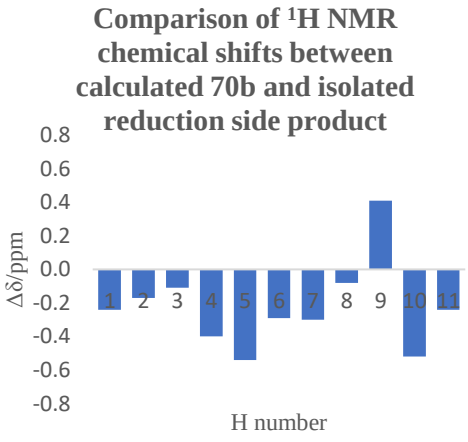

Figure 2.15 ^{1}H NMR chemical shifts comparison of mono-reduced **70a** and **70b** to the isolated reduction side product.

Further characterization of the unknown side product showed it to be two mass units larger than the dione starting material, suggesting a single reduction had occurred (Scheme 2.14). At this

point, it was hypothesized that the sensitive dione may undergo a transannular aldol reaction followed by a monoreduction. To test this hypothesis, previously isolated aldol product **63aa** was reduced with lithium aluminum hydride. The resulting ^{1}H NMR spectrum was identical to that of the unknown reduction side product and produced only one stereoisomer out of a possible two, **71a** and **71b**. Comparison of the experimental ^{1}H NMR spectrum to the predicted spectrum gave MAE values of 0.09 ppm and 0.17 ppm for **71a** and **71b** respectively, therefore identifying isomer **71a** as the side product in the reduction of dione **52** (Figure 2.16).

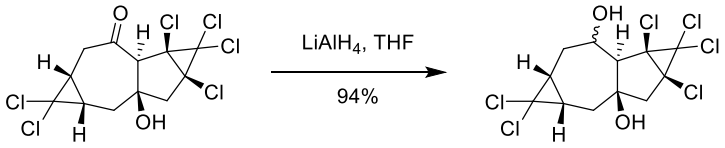

Scheme 2.14 Reduction of the aldol product **63aa**.

The complete diastereoselectivity of the reduction of **63aa** can be rationalized by simple inspection of molecular models (Figure 2.17). The favoured conformer of the relatively rigid aldol product **63aa** has its carbonyl group completely shielded by the bicyclic framework from attack on one face, leaving the other face open for a hydride addition.

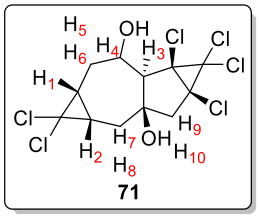

71

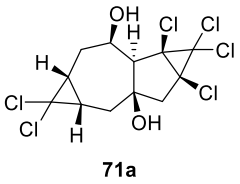

71a

MAE (ppm)
^{1}H NMR = 0.09

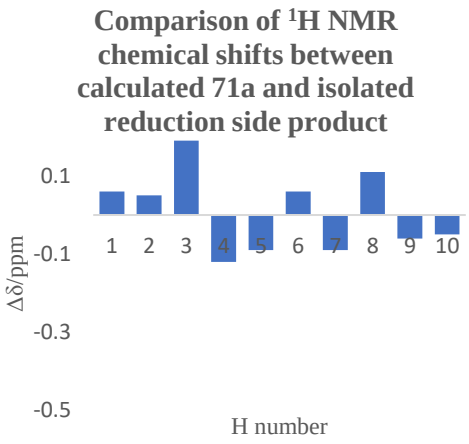

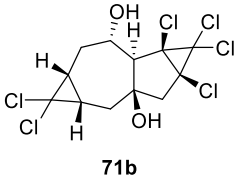

71b

MAE (ppm)
^{1}H NMR = 0.17

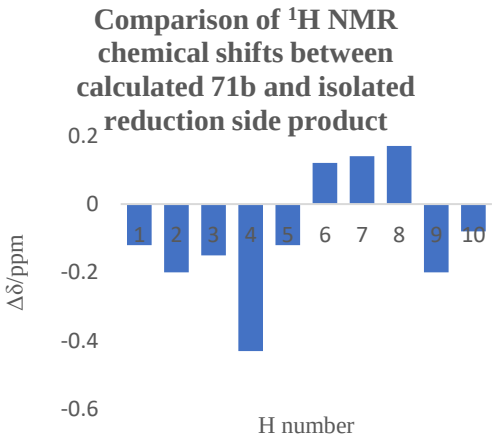

Figure 2.16 ^{1}H NMR chemical shifts comparison of reduced aldol products **71a** and **71b** to the isolated reduction side product.

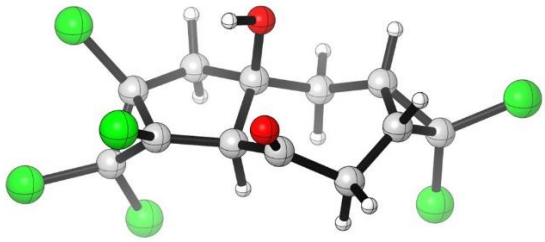

63aa

Figure 2.17 Favoured conformer of aldol product **63aa**.

The formation of a reduced aldol product is interesting, as it indicates that dione **52** undergoes a transannular aldol reaction under reducing conditions as well as ozonolysis conditions. The formation of the aldol side product and reduced aldol product is problematic because it competes with the formation of dione **52** or diol **55** in both steps. The instability of dione **52** made it necessary to access diol **55** directly from adduct **51** using a reductive workup in the ozonolysis step.*

The ozonolysis method was altered to include a stronger reductant in the workup of the ozonide, sodium borohydride, to directly access diol **55a** (Scheme 2.15).[58] This adjustment produced a single isomer of diol **55** in 56% yield, while completely avoiding formation of the aldol side product **63aa** or its reduced counterpart **71a**. It was initially unclear which diastereomer was produced, as the isolated solid appeared to be slightly soluble in solvents like dichloromethane and chloroform, unlike the *cis* diol **55a** that was isolated through reduction of dione **52a**. The identity of the diol was confirmed by ^{1}H NMR, however it is postulated that this diol is a different isomorph than the one previously observed.

* Suggested by Karnjit Parmar

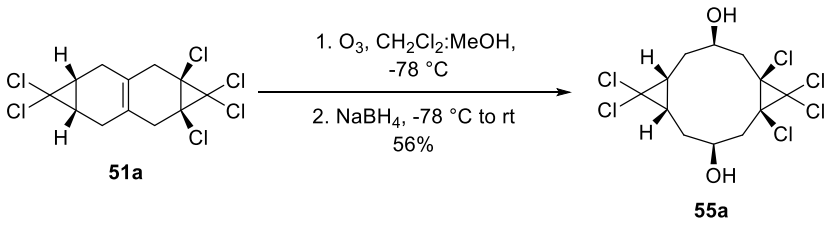

Scheme 2.15 Ozonolysis of **51** with reductive workup.

An ozonolysis reaction with the reductive workup was also attempted on a diastereoenriched sample (3:1 *trans*:*cis*) of the *trans* cycloadduct **51b** (Scheme 2.16). As observed in previous ozonolyses, the *trans* material **51b** was largely recovered after the reaction. Small amounts of a new diol diastereomer **55d** were obtained, however it was inseparable from the *cis* diol **55a**.

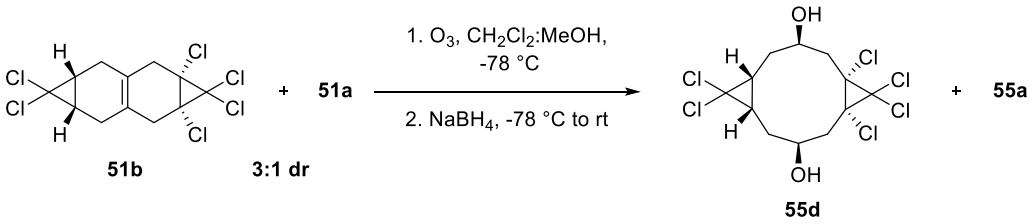

Scheme 2.16 Ozonolysis of diastereoenriched **51b** (**51b**/**51a** = 3:1) Diels-Alder adducts.

Despite the new reductive workup of the ozonolysis reaction, varying amounts of substrates **51a** and **51b** were again recovered after ozonolysis. Purification of the diol product **55a** from the starting materials **51a** and **51b** proved to be non-trivial. Diol **55a** is most soluble in acetone and slightly soluble in dichloromethane and ethyl acetate, while the adducts are completely soluble in the latter solvents. It was assumed that diol **55a** could be separated from alkenes **51a** and **51b** through filtration, however minimal separation occurred. All three compounds crystallized from a hexanes/ethyl acetate solvent system when recrystallization was attempted. Finally, purification *via* FCC with an acetone/hexanes solvent system provided some separation of the materials. The diol was loaded on the column as a solid due to its poor solubility in the solvent system, requiring

a significant amount of solvent. The large volume of solvent used resulted in co-elution of **55a** with **51** so further purification was necessary for mixed fractions.

With a somewhat satisfactory procedure to obtain diol **55a**, the mesylation and tosylation of compound **55a** was investigated (Scheme 2.17). Both mesylation and tosylation proved to be unsuccessful with the procedure previously employed on diol **47**,[46] as the reactions required several days and produced little material. An alternative method was adopted that utilized pyridine and DMAP instead of dichloromethane and triethylamine.[59] It appeared that tosylate **56a** was produced according to the ^{1}H NMR spectrum. Purification by PTLC, however, was unsuccessful as the product appeared to have decomposed on silica so this intermediate was not pursued further. Conversely, the mesylation reaction produced dimesylate **56a** in up to 98% yield under these new conditions, a vast improvement over the previous mesylation method.

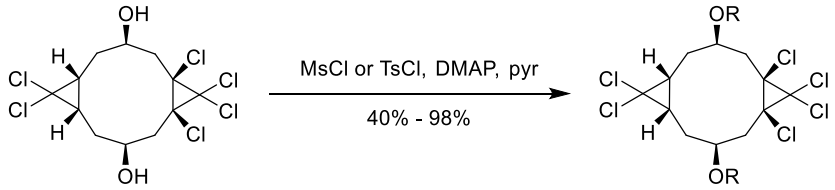

55a

56a: R = Ms
56b: R = Ts

Scheme 2.17 Activation of diol **55a** with methanesulfonyl chloride or toluenesulfonyl chloride.

Several bases were investigated for the subsequent elimination reaction including potassium hydroxide,[60] DBU,[61] potassium *tert*-butoxide,[61] and NaHMDS (Scheme 2.18). Unfortunately, the use of potassium hydroxide and NaHMDS caused the decomposition of the starting dimesylate, whereas reaction with DBU did not provide a transformation. Potassium *tert*-butoxide showed promise as it appeared to have some effect on the substrate.

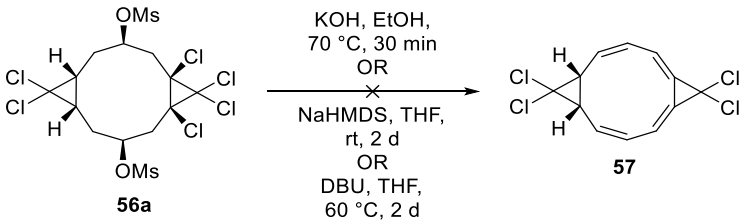

Scheme 2.18 Attempted four-fold elimination of dimesylate **56a** with KOH or NaHMDS or DBU.

The elimination reactions with potassium *tert*-butoxide initially used THF as the solvent at elevated temperatures, however it appeared that no desired tetraene product was formed (Table 2.1, entry 1). Additional reactions performed under these conditions showed a presumed mono-eliminated product, **72a** or **72b**, was produced (Scheme 2.19). It was postulated that increasing the temperature would increase the reaction rate, so DMSO was explored as a solvent in the elimination reaction.[62] d_6-DMSO was chosen as the solvent as the reactions were completed on a small scale (0.018 mmol). This alteration gave the same results as the THF elimination reaction, as a presumed mono-eliminated product, **72a** or **72b**, was produced (entry 2).

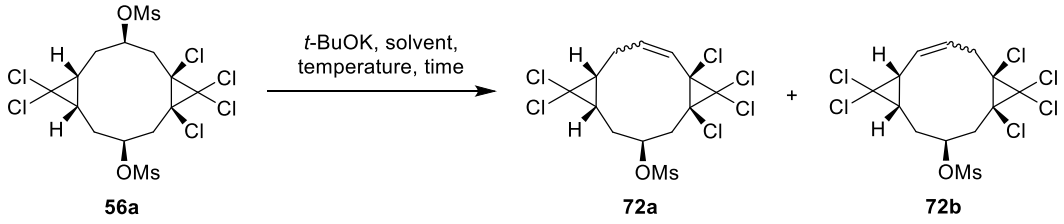

Scheme 2.19 Elimination reaction of dimesylate **56a** using *t*-BuOK and various solvents.

Table 2.1 t-BuOK elimination conditions of **56a** with various solvents.

Entry	Base	Solvent	Temp (°C)	Time (h)	Result
1	*t*-BuOK	THF	75	4.5	**72aa**
2	*t*-BuOK	d_6-DMSO	120	2	**72aa**
3	*t*-BuOK[1]	d_6-DMSO	100-120	47	Decomposition
4	*t*-BuOK[1]	MeCN	100-120	47	Decomposition
5	*t*-BuOK[1]	DMF	100-120	47	Decomposition

1) The reaction was stirred at 100 °C until an additional 1 equiv. of *t*-BuOK was added to the reaction after 29.5 hours. The mixture was then heated to 120 °C for an additional 17.5 hours.

Further elimination experiments explored other solvents, such as acetonitrile and DMF, and added an additional equivalent of potassium *tert*-butoxide (entries 4 and 5).[63,64] This method was tested with d_6-DMSO as well (entry 3). The mixture was initially heated to 100 °C for 29.5 hours before the additional equivalent was added. The temperature was increased to 120 °C at this time. This method was unsuccessful, as neither the mono-eliminated product nor the di-eliminated product were observed. In fact, a decomposition product was observed after more *t*-BuOK was added. Additionally, subjecting dimesylate **56a** to reaction conditions for ten days also resulted in a decomposition product and a trace amount of the presumed mono-eliminated product **72**.

The optimization of the elimination conditions shows that d_6-DMSO is the preferred solvent due to its higher boiling point than THF. The elimination reaction using d_6-DMSO afforded a 16% yield of mono-eliminated product **72aa** in 2.5 hours. Longer reaction times did not increase the yield of **72aa**. In fact, longer reaction times (2 days) resulted in no observed mono-eliminated product and trace amounts of an unidentified substance. The workup was altered to include distilled diethyl ether to solve impurity and emulsion problems.

^{1}H NMR chemical shift predictions were completed to identify the location and configuration of the olefin (Figure 2.18). Isomer **72aa** was the best match to the predicted spectra

as it had an MAE of 0.10 ppm, while isomers **72ab**, **72ba**, and **72bb** had mean absolute errors of 0.17 ppm, 0.16 ppm, and 0.21 ppm, respectively. ^{13}C NMR chemical shift predictions were performed to further confirm the identity of the mono-eliminated product **72**. Again, isomer **72aa** was considered the closest match to the predicted spectrum as it had an MAE of 1.9 ppm, whereas isomers **72ab**, **72ba** and **72bb** had mean absolute errors of 4.7 ppm, 3.7 ppm and 6.7 ppm, respectively. The selectivity of the elimination can be rationalized by the increased acidity of the methylene protons located adjacent to the electron-withdrawing chlorine atoms.

It was postulated that replacing the mesylate substituents with iodine *via* a substitution reaction would allow for an elimination to occur (Scheme 2.20). However the desired diiodide was not observed.[50] It is believed that the reaction was unsuccessful due to steric hindrance.

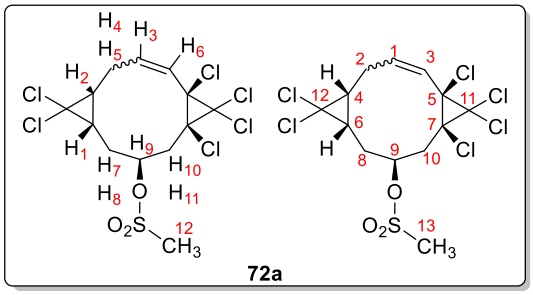

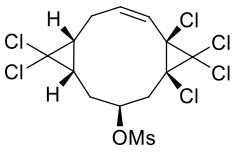

MAE (ppm)
^{1}H NMR = 0.10
^{13}C NMR = 1.9

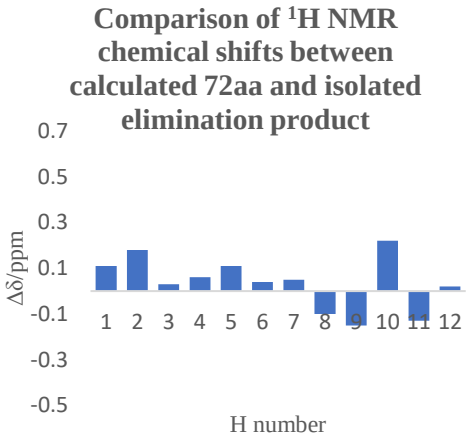

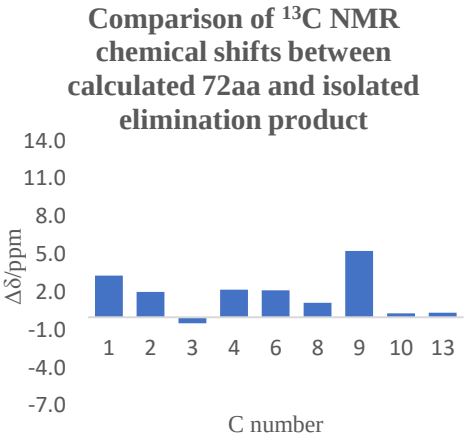

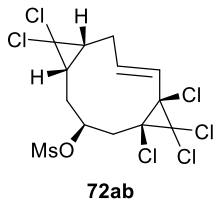

MAE (ppm)
^{1}H NMR = 0.17
^{13}C NMR = 4.7

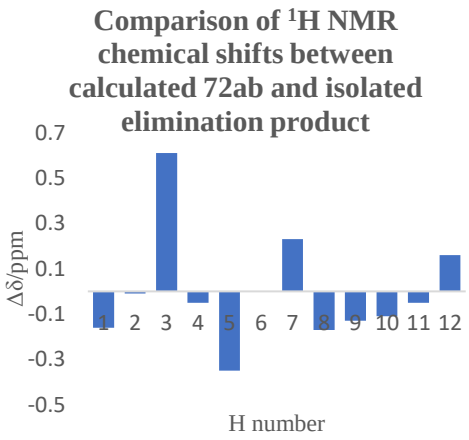

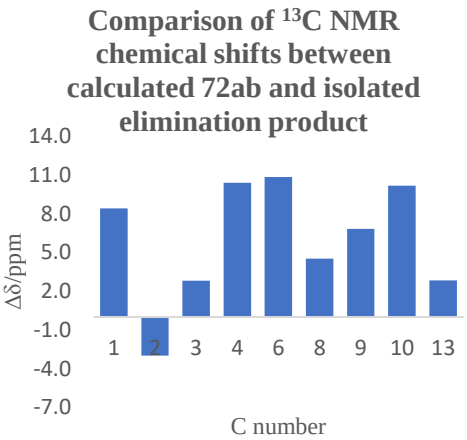

(Figure continued on next page)

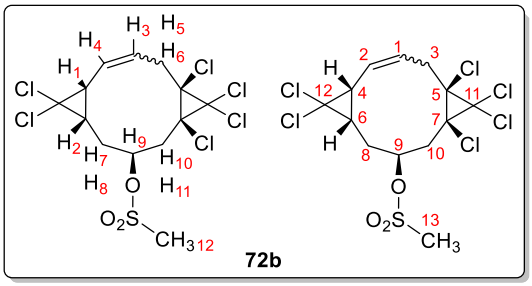

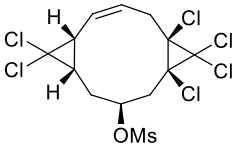

MAE (ppm)
^{1}H NMR = 0.16
^{13}C NMR = 3.7

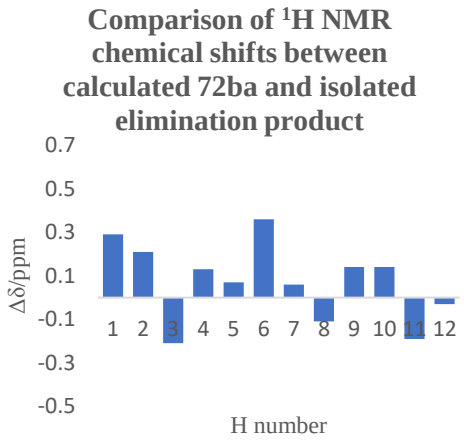

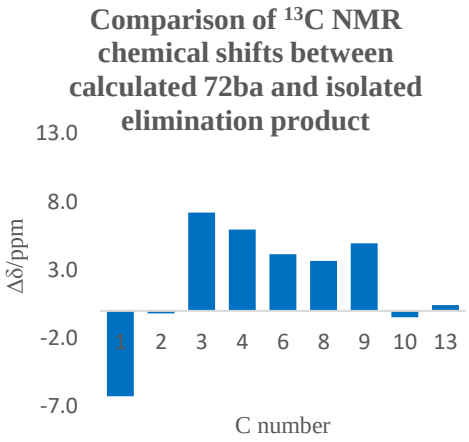

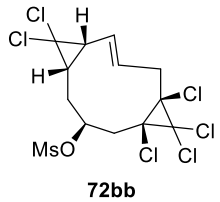

MAE (ppm)
^{1}H NMR = 0.21
^{13}C NMR = 6.7

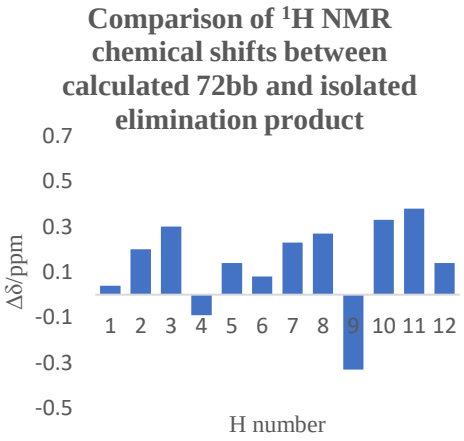

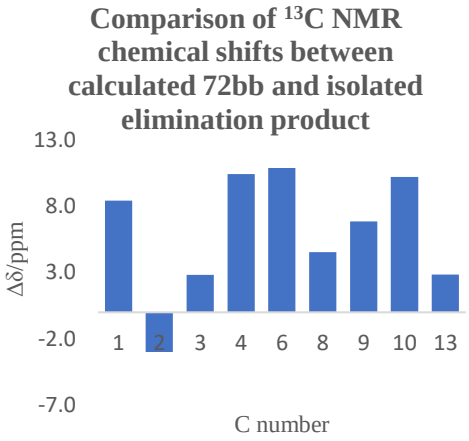

Figure 2.18 ^{1}H NMR and ^{13}C NMR chemical shifts comparison of monoeliminated products **72aa**, **72ab**, **72ba**, **72bb** to the isolated elimination product.

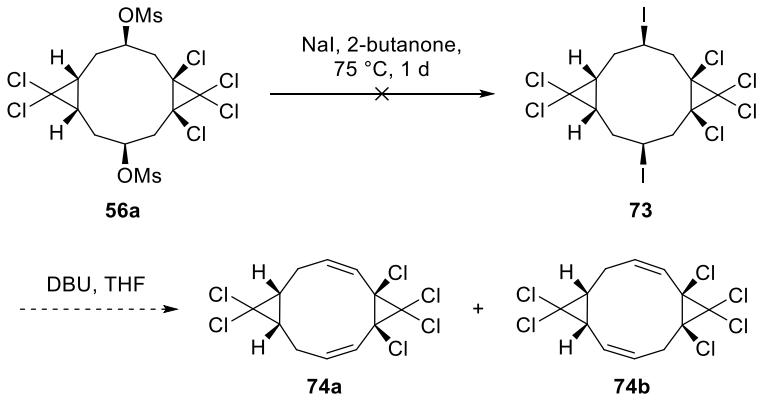

Scheme 2.20 Attempted substitution reaction with sodium iodide.

2.3 Chloroprene Route

A route using a substituted butadiene derivative was examined as an alternative due to the problems encountered in the late stage elimination (*vide supra*). Such a route is potentially advantageous over the butadiene route as an additional leaving group could be introduced in the carbon framework from the outset, obviating the need for a final oxidation of a tetraene to the desired annulene. Electronic and conformational differences from the butadiene route may also facilitate the troublesome elimination. To this end, 2-chlorobutadiene (chloroprene) was chosen as the substrate for the initial Diels-Alder reaction.

The chloroprene route began with the synthesis of chloroprene (**58**) from 3,4-dichlorobut-1-ene, (**75**) (Scheme 2.21).[49] Chloroprene was then reacted with maleic anhydride (**43**) to yield bicyclic anhydride **59** in 99% yield.[65] This Diels-Alder reaction was conducted at 50 °C in a sealed pressure vessel to avoid chloroprene evaporation. Reactions performed on a gram scale typically formed a beige solid around four hours into the reaction. On a larger scale, however, the reaction was heated and stirred overnight. Removing the solution from the heat source permitted the solid to form if it had not solidified overnight.

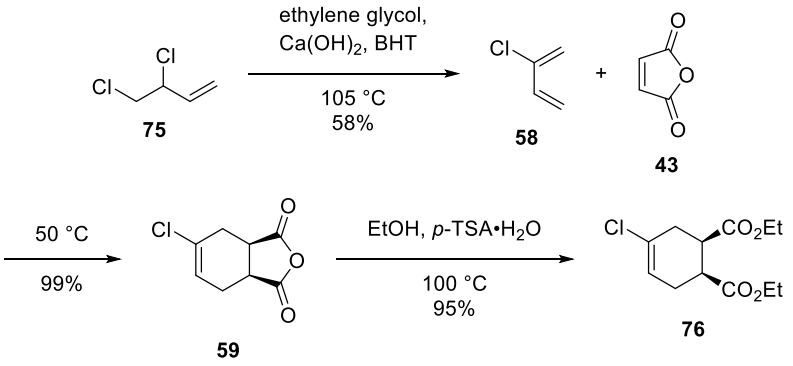

Scheme 2.21 Synthesis of cyclohexene **76**.

Ethanolysis of anhydride **59** provided diester **76** in high yield.[45] Cyclopropanation *via* a carbene [2+1] cycloaddition was attempted using the previous biphasic phase transfer catalysis method.[46] These conditions failed to yield any of the bicyclic compound **78**, however, and optimizations of the reaction conditions proved to be unsuccessful. It was thought that perhaps a longer reaction time would increase the yield since it is known that 1-chlorocyclohexene reacts more slowly than cyclohexene under similar conditions.[66] Unfortunately, an increase in the reaction time was also unsuccessful in producing a significant amount of **78**.

An alternative cyclopropanation procedure was employed that used sodium trichloroacetate as the carbene precursor rather than chloroform.[67] Initial reactions were promising, as small amounts of **78** were produced, however optimizations were necessary to attain a higher yield of the **78**.

Optimization included increasing the amount of sodium trichloroacetate from 1.1 to 2.2, 5, or 10 equivalents (Table 2.2). It was observed that the conversion increased as the amount of sodium trichloroacetate increased, presumably due to an increase in carbene production in solution. The most successful reaction occurred when 10 equivalents of sodium trichloroacetate was added to the reaction, giving a 25% conversion of starting material **76**. The addition of more sodium

trichloroacetate was considered impractical as the solution became saturated with the reagent when 10 equivalents were added.

Table 2.2 Optimization of carbene [2+1] cycloaddition onto cyclohexene **76**.

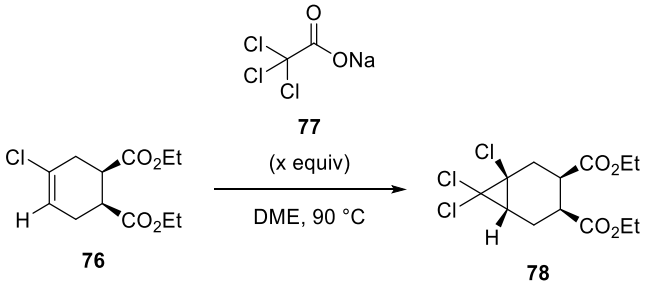

entry	# equiv. (x)	time (h)	conversion [a] (%)
1	1.1	16	5%
2	2.2	16	7%
3	5	18	12%
4	10	18	25%

a) Conversion determined by measuring the relative amounts of **76** and **78** using ^{1}H NMR spectroscopy.

To account for the low conversion observed in the presence of even a large excess of sodium trichloroacetate, it was postulated that the dichlorocarbene was lost by evaporation or dimerization. Various attempts to overcome this problem by adding the reagent in portions did not lead to a significant improvement in yield.

Due to the poor results of the sodium trichloroacetate carbene reactions, a biphasic procedure using chloroform was revisited.[66] A modified procedure by Baird called for a smaller excess of chloroform than Müller's procedure (5.2 equivalents instead of 10 equivalents), as well as much smaller amounts of the phase transfer catalyst, triethyl benzyl ammonium chloride (0.006 equivalents instead of 0.44 equivalents). These adjustments to Müller's procedure produced cyclopropanated product **78** in much improved conversions (Scheme 2.22). Purification was achieved through flash column chromatography, however compounds **76** and **78** co-elute due to

their similar polarity. This results in a low yield (28%) of the pure product, along with mixed fractions containing most of **78** formed in the cyclopropanation.

Pure **78** was reduced with lithium aluminum hydride, resulting in a 32% yield of diol **79** after purification with flash column chromatography.[46] When the crude bicyclic product **78** was directly carried forward to the reduction step, an improved yield of 62% was obtained for diol **79**. This product was separated from the side product **80** through filtration with dichloromethane, as **79** was only slightly soluble in CH_2Cl_2, whereas olefin **80** was completely soluble in the solvent.

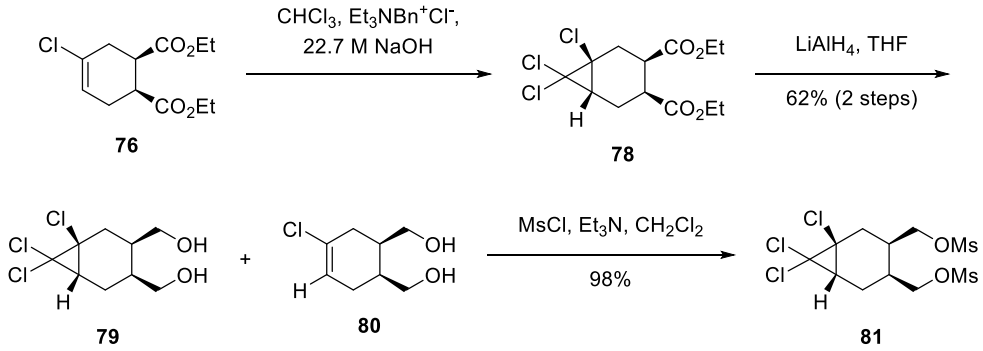

Scheme 2.22 Cycloaddition reaction and preparation of dimesylate **81**.

The purified diol **79** was then transformed into dimesylate **81** in excellent yield.[46] Various conditions were tested for the elimination, with the two-step procedure used previously in the butadiene route proving successful again (Scheme 2.23). A Diels-Alder reaction between diene **82** and tetrachlorocyclopropene (**50**) successfully produced cycloadduct **83** in 61% yield.

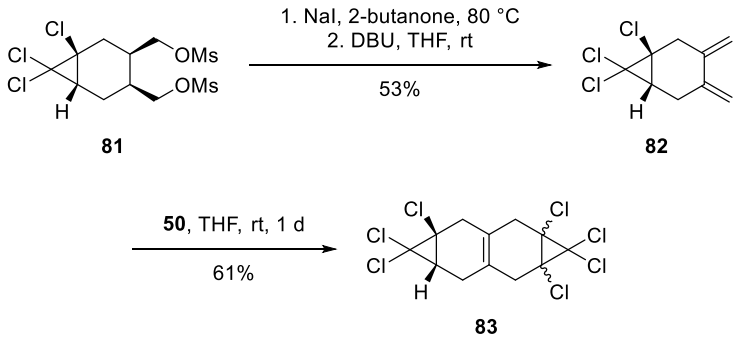

Scheme 2.23 Elimination of dimesylate **81** and a subsequent Diels-Alder reaction between the resulting diene **82** and tetrachlorocyclopropene (**50**).

A single diastereomer was observed in the Diels-Alder reaction between **82** and tetrachlorocyclopropene. ^{1}H NMR chemical shift calculations were used in an attempt to identify which diastereomer was formed (Figure 2.19). The ^{1}H NMR chemical shift results were inconclusive as both the *cis* **83a** and *trans* **83b** isomers were possible matches with MAE values of 0.04 ppm for both isomers. ^{13}C NMR chemical shift predictions were also used to determine the favoured stereoisomer, with the MAE calculations excluding carbon atoms bonded to chlorine substituents due to the heavy atom effect.[54] The *cis* stereoisomer **83a** had an MAE of 1.0 ppm, whereas the *trans* isomer **83b** had an MAE value of 1.4 ppm. The predicted chemical shifts for the *cis* diastereomer are a closer match to those of the isolated cycloadduct, however the results are again inconclusive as both values are possible matches.

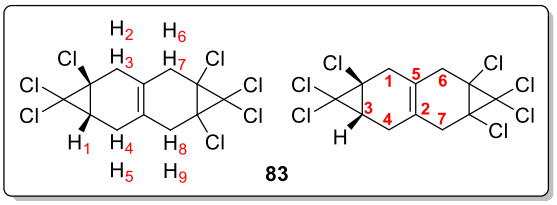

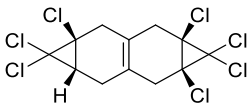

MAE (ppm)
^{1}H NMR = 0.04
^{13}C NMR = 1.0

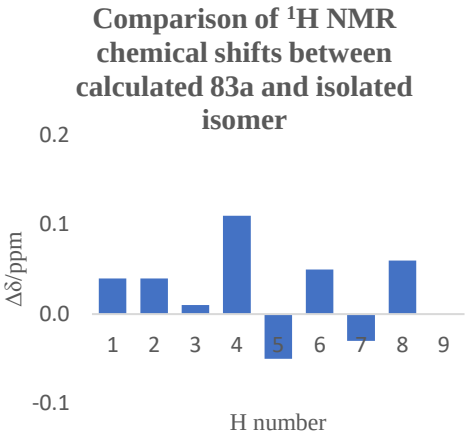

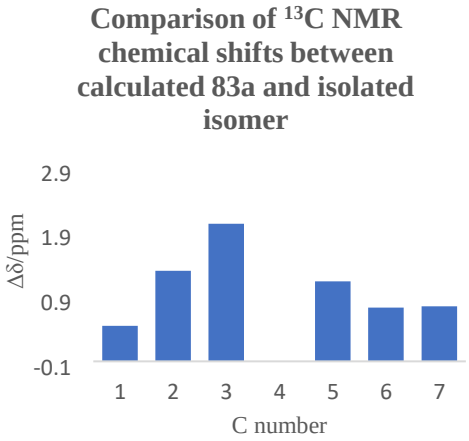

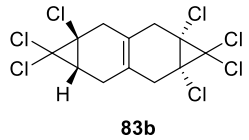

MAE (ppm)
^{1}H NMR = 0.04
^{13}C NMR = 1.4

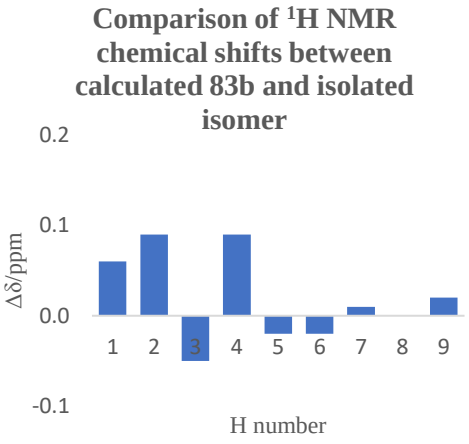

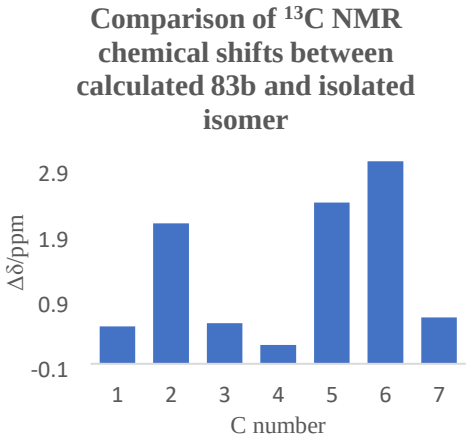

Figure 2.19 ^{1}H and ^{13}C NMR chemical shift comparison of Diels-Alder adducts **83a** and **83b** to the isolated isomer.

Initial ozonolysis attempts on olefin **83** used dimethylsulfide as the quenching agent (Scheme 2.24). No reaction was observed, perhaps due to the poor solubility of substrate **83** in cold dichloromethane. Lowering of the concentration with the aim of increasing the amount of solubilized material did not affect the outcome. The ozonolysis procedure used in the previous route, which used a 5:1 dichloromethane:methanol solvent system and a thiourea quench, was also

explored.[48] This method failed to convert adduct **83** into dione **60** as well, as only olefin **83** was recovered.

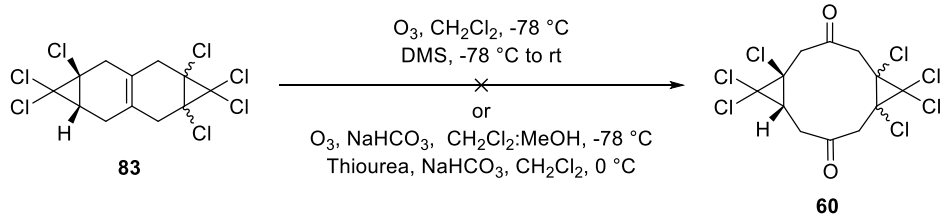

Scheme 2.24 Olefin cleavage attempts of **83** under ozonolysis reaction conditions

Other olefin cleavage methods were investigated despite the reluctance of **83** to react with even the small and very reactive ozone. Alkene **83** was subjected to osmium tetroxide dihydroxylation conditions for up to six days, however a transformation was not observed and only starting material was recovered (Scheme 2.25).[48,56] Epoxidation was also explored in an attempt to cleave olefin **83**. In any event, the use of *m*-CPBA[68] or DMDO[69] also failed to convert any starting material to epoxide **85** (Scheme 2.26).

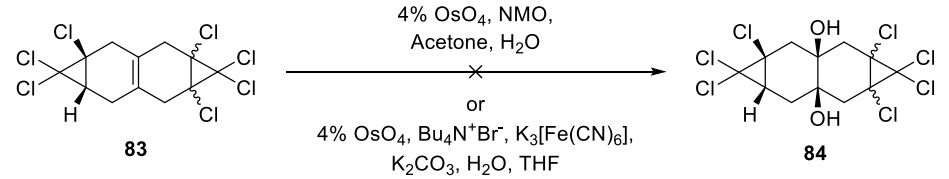

Scheme 2.25 Olefin cleavage attempts of **83** using osmium tetroxide dihydroxylation.

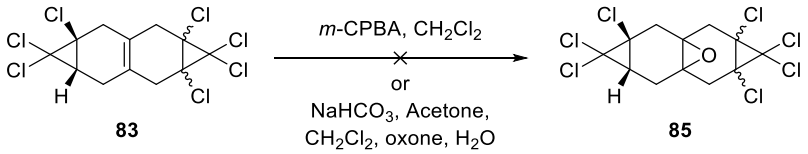

Scheme 2.26 Olefin cleavage attempts of **83** *via* epoxidation with *m*-CPBA and DMDO.

Three hypotheses have been proposed to account for the inertness of olefin **83**. The first states that the reaction between tetrachlorocyclopropene (**50**) and diene **82** yields the *trans* Diels-Alder adduct **83b** as the major product (Figure 2.20). It was noted in the butadiene route that the *trans* cycloadduct **51b** reacted more slowly with ozone than the *cis* stereoisomer, which may be occurring with substrate **83**. It is therefore presumed that much longer reaction times or higher temperatures are needed for the ozonolysis of **83** or other cleavage reactions to transform **83** to any of the desired products.

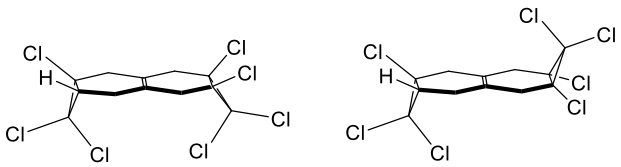

83a **83b**

Figure 2.20 Chloroprene route *cis* and *trans* Diels-Alder adducts.

The second hypothesis postulates that there is an electrostatic repulsion between the electronegative chlorine atoms and the incoming ozone molecule. Finally, an alternative hypothesis states the olefin in molecule **83** is too electron-poor to act as a nucelophile due to the many electron withdrawing chlorine atoms located on the perimeter of the framework. This rationale would explain why **83** is not transformed in the presence of ozone, osmium tetroxide and epoxidizing agents. Further work needs to be completed to understand the inertness of adduct **83**.

2.4 Conclusions

2.4.1 Butadiene Route

Significant progress has been made in the butadiene route, including a considerable yield increase in the dichlorocarbene [2+1] cycloaddition reaction reported by Müller and coworkers. It was discovered that this reaction has a risk of runaway and therefore needs to be completed in an open flask to prevent explosions. A condenser was also deemed necessary to prevent the evaporation of chloroform from the reaction vessel, however the use of ethanol-free chloroform was found to be unnecessary.

The elimination of dimesylate **48** to diene **49** using potassium *tert*-butoxide was found to be inefficient and was therefore replaced by an alternative method. This procedure substituted the mesylates for iodides followed by DBU elimination to produce diene **49** in reproducible yields.

A reliable method for ozonolysis to access dione **52** was found, which includes the use of sodium bicarbonate, as well as a thiourea quench. The *trans* Diels-Alder adduct **51b** reacts with ozone at a much slower rate than its *cis* counterpart **51a**, possibly due to steric hindrance or electrostatic repulsion between the incoming ozone molecule and the chlorine atoms. The dione is stable in crystalline form and can be stored for months at room temperature but decomposes readily under slightly acidic conditions.

A reductive workup of the ozonide using sodium borohydride was ultimately adopted to directly access diol **55** and to avoid the formation of the aldol product **63aa**. The resulting diol can be reproducibly mesylated using DMAP and pyridine.

Subjecting dimesylate **56a** to various elimination conditions reliably produces a single mono-eliminated product, **72aa**. Other mono-eliminated isomers **72ab**, **72ba** and **72bb** were not observed, nor was a di-eliminated product. It is speculated that **72aa** is the favoured product due

to the acidity of the methylene protons adjacent to the electron withdrawing chlorine atoms. The work completed in the butadiene route shows that this is a viable route to reach the functionalized skeleton of [10]-annulene.

2.4.2 Chloroprene Route

An alternative route has been developed as well that incorporates an additional chlorine atom to give the penultimate intermediate the correct oxidation state, poised for a five-fold elimination. The dichlorocarbene [2+1] cycloaddition reaction proved difficult, and several procedures were attempted to transform olefin **76** to **78**. Using sodium trichloroacetate as the carbene source afforded a minor amount of the desired bicyclic compound, however attempts to optimize this reaction failed to increase the conversion by any significant amount. A biphasic procedure, similar to that used in the butadiene route, was found to afford compound **78** in good yield. This compound can be reduced to diol **79** with lithium aluminum hydride.

Elimination of the dimesylate **81** to the diene **82** was found to be possible only by reaction with sodium iodide and subsequent elimination with DBU. A single diastereomer was produced in the Diels-Alder reaction between **82** and tetrachlorocyclopropene (**50**). Attempts at establishing the relative configuration included ^{1}H and ^{13}C NMR chemical shift predictions and comparison to the experimental spectrum, however the results were inconclusive.

Attempts at cleaving the central olefin in **83** included ozonolysis, dihydroxylation and epoxidation reactions. All reaction conditions failed to transform any starting material to the desired ten-carbon framework needed to reach [10]-annulene. It is currently speculated that the *trans* diastereomer is the major product of the Diels-Alder reaction, as it was shown to react more slowly with ozone than the *cis* diastereomer in the butadiene route. It is also possible that the

additional chlorine substituent may diminish the dipolarophilicity of the olefin through electron withdrawing effects or due to its steric bulk. The chloroprene route may also be a viable strategy in reaching aromatic [10]-annulene targets **40** or **41**.

2.5 Future Work

2.5.1 Butadiene Route

Synthesis of an annulene *via t*he butadiene route is almost complete, although several variations may still be attempted on the route. The first to be tried is the elimination of the mesylate and chlorine substituents located directly on the hydrocarbon framework. Elimination of both mesylates would result in dienes **74a** or **74b** (Scheme 2.27). If these molecules can be accessed, other elimination conditions will be tested so that the chlorine atoms may be eliminated to give tetraene **57**. To this end, either diene intermediate could potentially be subjected to further elimination, *via* E1, E2, or E2' pathways.

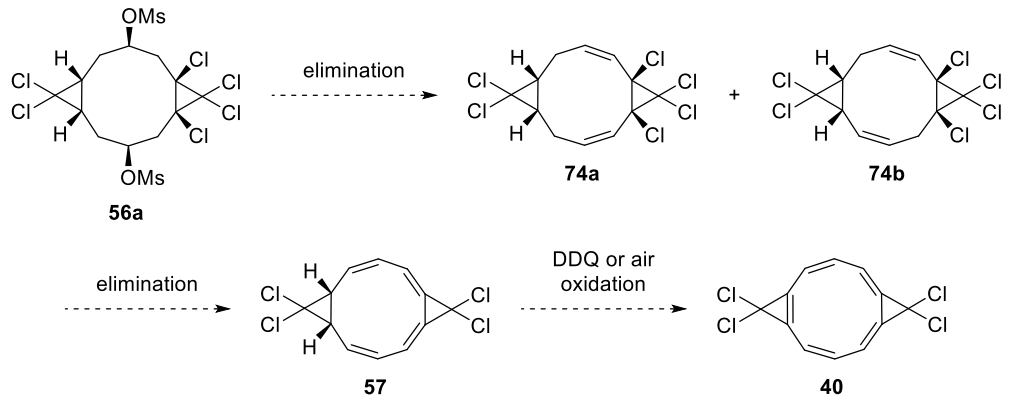

Scheme 2.27 Eliminations and oxidation of dimesylate **56a**.

Having established that keto-enol tautomerism is unlikely to occur (Scheme 2.13), it was hypothesized that a dienolate may be trapped through the use of triflic anhydride. It was thought that the elimination of the chlorine substituents would result in diene **86**, which could then be

oxidized to dione **87** (Scheme 2.28). Further oxidation to reach triene **54** would allow for enolate formation through the reaction of **54** with base and triflic anhydride to produce ditriflate **88**. This compound is synthetically interesting because the triflate functionality can be used in cross coupling reactions, allowing coupling between electron-rich or poor conjugated systems.

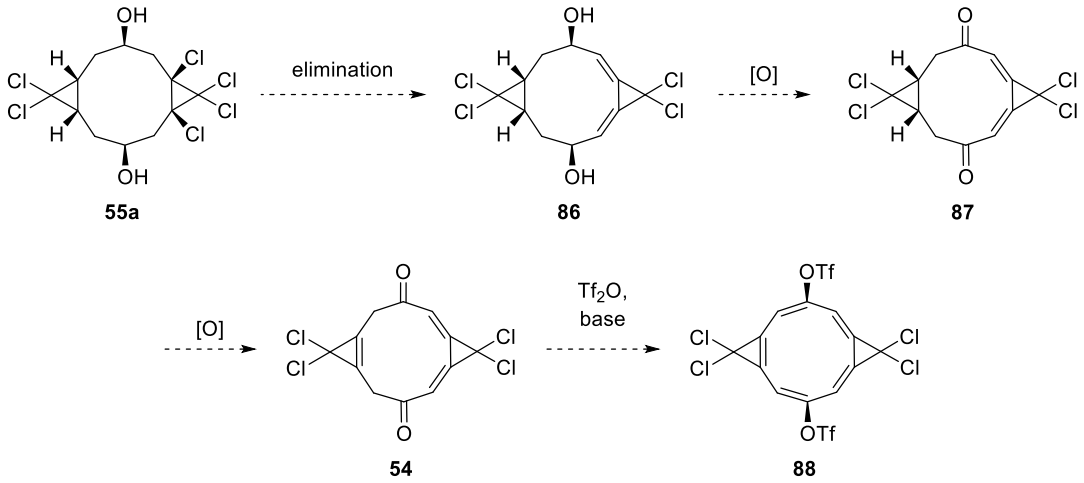

Scheme 2.28 Dienolate formation of [10]-annulene **88**.

Investigations into the reactivity of the *trans* isomer **51b** will give insight into its usefulness in the synthesis (Scheme 2.29). It is possible that elimination of the substituents in the *trans* dimesylate **56ab** may occur more readily than in the *cis* diastereomer due to the different conformations potentially available.

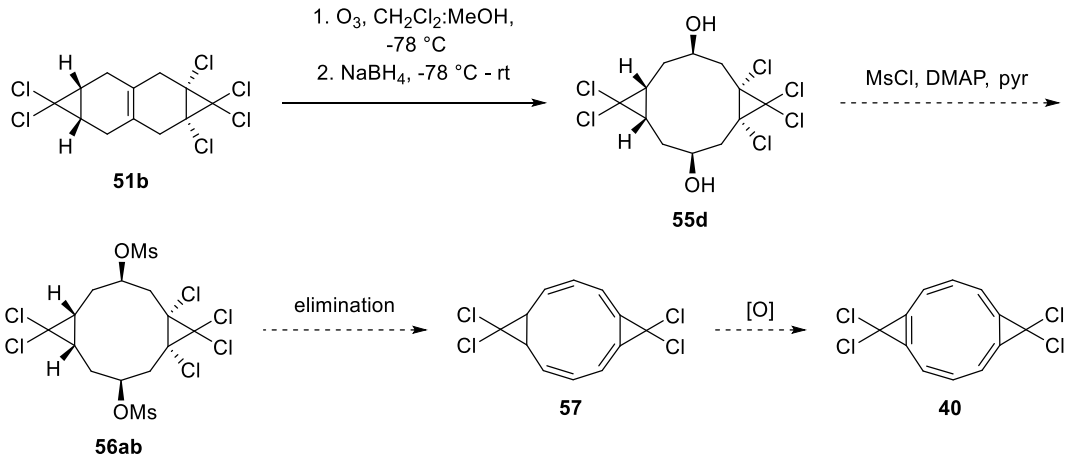

Scheme 2.29 Quadruple elimination using the *trans* stereoisomer **51b**.

It is hypothesized that the other meso diastereomer of diol **55** may be more useful for elimination than the all-*cis* stereoisomer **55b**. Diastereomer **55b** can be accessed from **55a** through a double Mitsunobu reaction to obtain diester **94**, followed by hydrolysis (Scheme 2.30). Subjecting **55b** to mesylating conditions would result in dimesylate **56c**. The dimesylate can then be eliminated to obtain diene **74a** or **74b** It may also be possible to do the desired quadruple elimination to reach [10]-annulene precursor **57**.

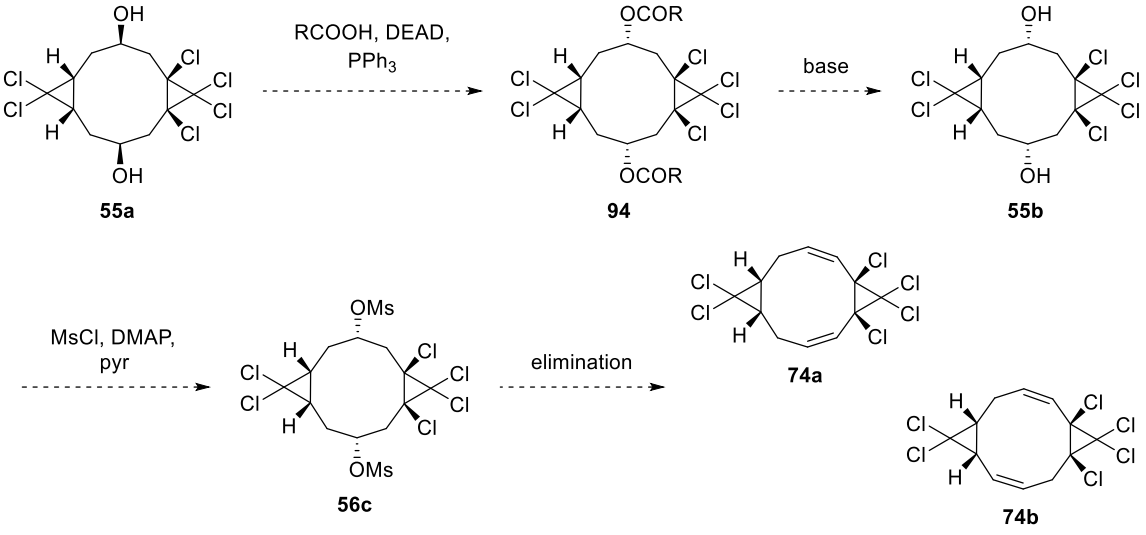

Scheme 2.30 Accessing diol **55b** through a double Mitsunobu inversion.

It was postulated that using a dienophile containing bromine atoms, such as molecule **89**, would be advantageous for later elimination (Scheme 2.31). Bromine atoms are typically easier to eliminate than chlorine atoms, which may result in a four-fold elimination to yield tetraene **92**. The compound would then only be one oxidation away from a [10]-annulene compound **93**, a derivative of target **40**.

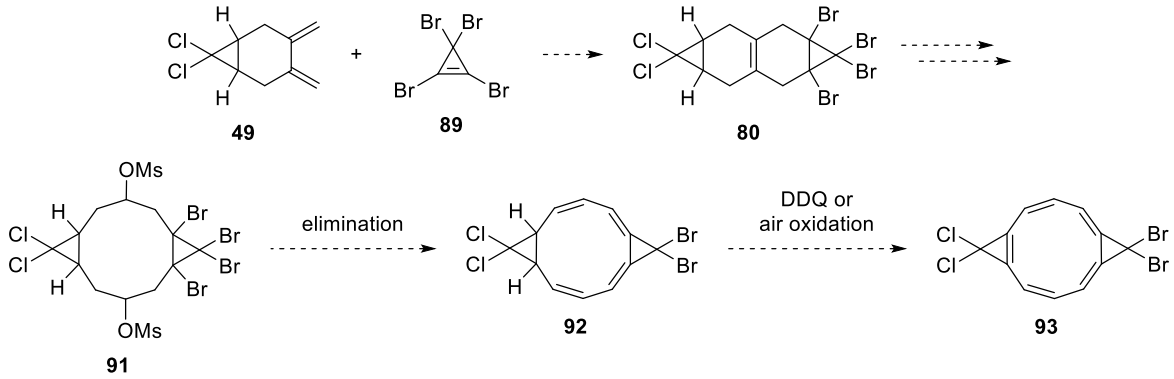

Scheme 2.31 Diels-Alder reaction with a bromine-containing dienophile.

2.5.2 Chloroprene Route

The chloroprene route can be further explored as well. It would be convenient to identify whether the *cis* or *trans* diastereomer of **83** is the major product. A new computational procedure that accurately predicts ^{13}C NMR shifts of halogen-substituted carbon atoms may be useful in determining the configuration of the Diels-Alder adduct obtained.[70] Regardless of the configuration of **83**, longer exposure times of the adduct to ozone or a slightly warmer reaction temperature may allow for the transformation to diol **84** to occur (Scheme 2.32).

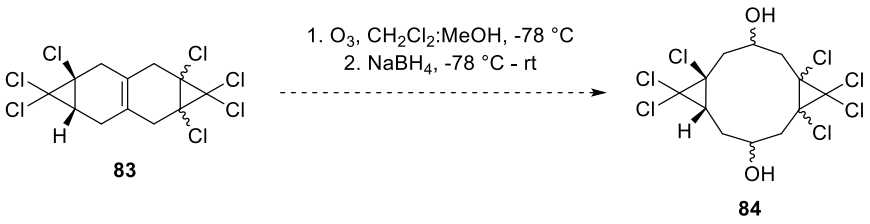

Scheme 2.32 Ozonolysis of Diels-Alder adduct **83**.

Two paths were suggested to reach an all-*cis*, aromatic [10]-annulene from diol **84**, similar to the butadiene route (Scheme 2.33). Route A activates the diol as its corresponding dimesylate or ditosylate. Elimination of the mesylates and chlorine atoms produces aromatic compound **40**. Route B, however, would eliminate the chlorine atoms first to yield triene **96**. The triene would undergo oxidation to form dione **52** so that the dienolate **88** may be formed with triflic anhydride. This ditriflate could then be used for derivatization and optoelectronic applications through transition metal catalyzed cross-couplings.

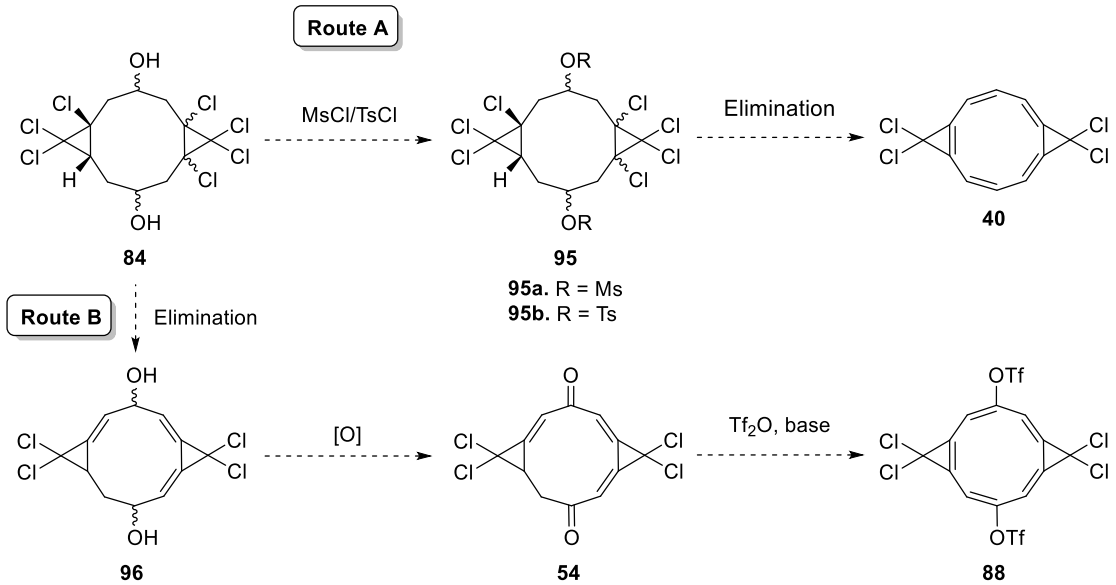

Scheme 2.33 Future work of the chloroprene route.

Once a [10]-annulene is successfully synthesized, its physicochemical properties can be studied. The examination of these properties will aid in assessing the aromaticity of the molecule.

^{1}H NMR will be a valuable tool in this regard as the anisotropic shifts will be observed in the δ = 7-8 ppm region. However, a non-planar, and thus non-aromatic, final product will result in a ^{1}H NMR spectrum that has anisotropic shifts of δ = 5-6 ppm. The study of the physicochemical properties of an aromatic [10]-annulene will determine the usefulness of the molecule in optoelectronic applications.

The reactivity of an aromatic [10]-annulene can be investigated as well. For example, it would be interesting to examine electrophilic aromatic substitution reactions in an attempt to functionalize the annulene. Functionalization will aid in modulating the properties of the ring, and could therefore make it a more efficient molecule for use in optoelectronic applications. Investigations into its reactivity will also give insight into the usefulness of the substrate in synthesis.

CHAPTER 3: EXPERIMENTAL

3.1 General Methods

Anhydrous solvents were dried using a Braun Solvent Purification System and stored under argon with 3 Å molecular sieves. All commercial reagents were used without further purification unless otherwise noted.

Thin layer chromatography (TLC) was performed using glass plates pre-coated (0.25 cm) with Merck Silica Gel 60 F_{254}. Visualization occurred with UV light (254 nm) and/or $KMnO_4$ followed by charring with heat. Column chromatography was performed using Silica gel 60 from Merck.

Nuclear magnetic resonance spectra were recorded on a Bruker instrument in $CDCl_3$ or d_6-DMSO solution at 500 or 600 MHz for ^1H and 125 MHz for ^{13}C. The residual solvent protons (^1H, $CDCl_3$: 7.26 ppm, d_6-DMSO: 2.50 ppm) or the solvent carbons (^{13}C, 77.23 ppm) were used as internal standards for chemical shifts. The ^1H NMR chemical shifts and coupling constants were determined assuming first-order behaviour. High resolution mass spectra (HRMS) were obtained on a double focusing high resolution spectrometer. Any oxygen containing molecule required ESI with a sodium adduct. Compounds **52, 55a, 56a, 63aa**, **71a**, **72aa** and **81** required specific parameters: the declustering potential (DP) was set to 230.0, the focusing potential (FP) was adjusted to 300.0, and the declustering potential 2 (DP2) was set to 20.0. IR spectra were recorded on a Fourier transform interferometer using a diffuse reflectance cell or a Bruker Alpha ATR-FTIR instrument; only diagnostic and/or intense peaks are reported. Samples submitted for IR analysis were prepared as a film on a KBr pellet or a KBr pellet was prepared to incorporate the solid. Solids **51b**, **55a**, **56a** and **72aa** were loaded on a diamond crystal on a Bruker Alpha ATR-FTIR

instrument. Melting points were measured on SRS Digimelt melting point apparatus. XRD was completed on a Bruker APEX II Kappa CCD FR540C diffractometer instrument, using a graphite monochromated Mo Kα radiation (λ = 0.71073 Å).

^{1}H and ^{13}C NMR calculations were performed with the Gaussian 09 or Gaussian 16 software packages according to Hoye's procedure.[71] These calculations were completed at the B3LYP/6-311+G(2d,p)//M062X/6-31+G(d,p) level. ^{1}H NMR MAE exclude protons bonded to oxygen, while ^{13}C NMR MAE calculations excluded carbon atoms bonded to chlorine atoms due to the heavy atom effect.[54]

Energy calculations for **66** and **41** were performed with Spartan '14. SCF energies of **66** and **41** were calculated using the B3LYP functional with the 6-31G* basis set.

3.2 Butadiene Route Experimental Procedures

Materials: Butadiene sulfone (**61**)**,** maleic anhydride (**43**), and tetrachlorocyclopropene (**50**) were received from commercial sources.

3a,4,7,7a-tetrahydroisobenofurane-1,3-dione (**44**)

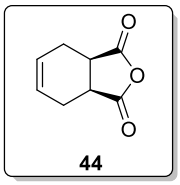

Adapted from reference 44. Butadiene sulfone (51.7 g, 437 mmol, 1 equiv.) and maleic anhydride (42.9 g, 438 mmol, 1 equiv.) were heated in diglyme (48 mL) with a heat gun under atmospheric conditions until bubbling ensued. Intermittent heating was used to keep the solution bubbling. Heating stopped when the solvent was boiling, approximately 1.5 hours after beginning the reaction. Beige solid forms upon cooling the solution. Water was added and the solid was filtered. The solid was washed until the filtrate remained colourless, resulting in **44** as a light beige solid (45.7 g, 67%). **^{1}H NMR** (500 MHz, $CDCl_3$): δ 6.02

– 5.97 (m, 2H), 3.40 – 3.35 (m, 2H), 3.40 – 3.34 (m, 2H), 2.63 (dddd, *J* = 15.5, 3.3, 3.3, 1.6 Hz, 2H), 2.31 (dddd, *J* = 14.8, 5.6, 5.6, 1.3 Hz, 2H)**.**

Diethyl cyclohex-4-ene-1,2-carboxylate (**45**)

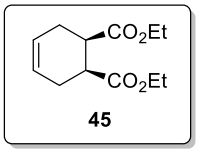

45

Adapted from reference 45. A round bottom flask containing anhydride **44** (45.4 g, 298 mmol, 1 equiv.), *p*-toluenesulfonic acid (4.56 g, 24.0 mmol, 0.08 equiv.) and ethanol (105 mL, 1.80 mol, 6 equiv.) was refluxed under atmospheric conditions for 17.5 hours at 100 °C. Toluene (54 mL) was added and the azeotrope was concentrated under reduced pressure. Ethanol (105 mL, 1.80 mol, 6 equiv.) was added and the solution was again refluxed at 100 °C for 23 hours under atmospheric conditions, after which toluene (54 mL) was added. The solution was concentrated under reduced pressure. The resulting oil was diluted with diethyl ether and extracted twice with 3% $Na_2CO_{3(aq)}$. The collected aqueous layers were washed with diethyl ether three times. The diethyl ether layers were then washed with water and dried over $MgSO_4$, filtered and concentrated. Purification *via* FCC (7:1 Hex:EtOAc) afforded **45** as a yellow oil (64.9 g, 96%). **^{1}H NMR** (600 MHz, $CDCl_3$): δ 5.39 – 5.65 (m, 2H), 4.16 (dq, *J* = 10.8, 7.1 Hz, 2H), 4.13 (dq, *J* = 10.8, 7.1 Hz, 2H), 3.03 – 3.02 (m, 2H), 2.57 – 2.52 (m, 2H), 2.36 – 2.32 (m, 2H), 1.24 (t, *J* = 7.2 Hz, 6H).

Diethyl (1*R*,6*S*)-7,7-dichlorobicyclo[4.1.0]heptane-3,4-dicarboxylate (**46**)

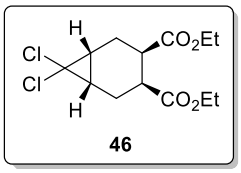

46

Adapted from reference 46. A 50% solution of $NaOH_{(aq)}$ (103 mL) was added to a solution of **45** (20.4 g, 90.4 mmol, 1 equiv.), chloroform (72.0 mL, 899 mmol, 10 equiv.) and triethylbenzyl ammonium chloride (11.1 g, 39.9 mmol, 0.44 equiv.) and stirred at room temperature under atmospheric conditions. The solution was

placed into an ice-water bath for five minutes when it was rapidly refluxing. An additional 30 mL of chloroform was added once the solution was at room temperature. The solution was quenched with water after 4 hours and 1 M HCl was added until the pH = 1. Dichloromethane was used to extract the aqueous layer three times. The organic layer was dried over magnesium sulfate, filtered and concentrated. Several purifications *via* FCC (CH_2Cl_2) resulted in **46** as a yellow oil (23.8 g, 85%). **^{1}H NMR** (500 MHz, $CDCl_3$): δ 4.14 (dq, *J* = 7.2, 3.8 Hz, 2H), 4.13 (dq, *J* = 6.4, 4.5 Hz, 2H), 2.79 - 2.76 (m, 2H), 2.53 – 2.46 (m, 2H), 1.93 – 1.88 (m, 2H), 1.24 (t, *J* = 7.1 Hz, 6H).

((1*R*,6*S*)-7,7-dichlorobicyclo[4.1.0]heptane-3,4-diyl)dimethanol (**47**)

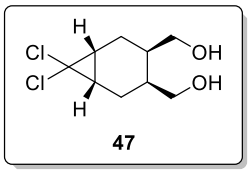

47

Adapted from reference 46. Bicyclo **46** (10.8 g, 34.9 mmol, 1 equiv.) was quantitatively transferred to a cooled round bottom flask containing $LiAlH_4$ (2.28 g, 60.2 mmol, 1.7 equiv.) and THF (174 mL). The flask was warmed to ambient temperature and stirred for 6 hours under inert atmosphere. The solution was cooled in an ice-water bath and quenched with cold water followed by 1 M HCl until the pH = 2. The aqueous layer was extracted five times with dichloromethane and the organic layer was dried over $MgSO_4$, filtered and concentrated resulting in **47** as a yellow oil. Purification was achieved through FCC (EtOAc) affording **47** as a white solid (7.38 g, 94%). **^{1}H NMR** (600 MHz, $CDCl_3$): δ 3.63 (dd, *J* = 10.8, 7.2 Hz, 2H), 3.58 (dd, *J* = 11.4, 4.2 Hz, 2H), 2.43 (br s, OH), 2.09 – 2.04 (m, 2H), 1.81 – 1.77 (m, 2H), 1.73 – 1.70 (m, 4H).

((1*R*,6*S*)-7,7-dichlorobicyclo[4.1.0]heptane-3,4-diyl)bis(methylene)dimethanesulfonate (**48**)

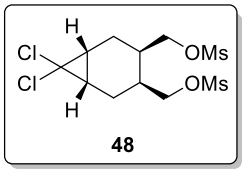

48

Adapted from reference 46. Triethylamine (13.7 mL, 98.2 mmol, 3 equiv.) was slowly added to a cooled flask containing **47** (7.38 g, 32.8 mmol, 1 equiv.), dichloromethane (30 mL) and methanesulfonyl chloride (6.1 mL, 79 mmol, 2.4 equiv.). The solution was stirred at room temperature under inert atmosphere and was quenched with distilled water after 5 hours. The aqueous layer was extracted once with dichloromethane and washed twice with brine. The collected organic layers were dried over $MgSO_4$, filtered and concentrated. Recrystallization (Hex:CH_2Cl_2) yielded **48** as an orange solid (12.0 g, 96%). Dimesylate **48** was also produced when diol **47** (41.8 mmol) was carried forward without purification (15.1 g, 95% over 2 steps). **^{1}H NMR** (500 MHz, $CDCl_3$): δ 4.19 (dd, *J* = 10.0, 7.0 Hz, 2H), 4.11 (dd, *J* = 10.3, 6.8 Hz, 2H), 3.07 (s, 6H), 2.18 – 2.11 (m, 2H), 2.00 – 1.93 (m, 2H), 1.84 – 1.80 (m, 4H).

(1*R*,6*S*)-7,7-dichloro-3,4-bis(iodomethyl)bicyclo[4.1.0]heptane (**98**)

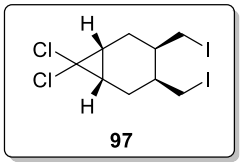

97

Adapted from reference 50. Dimesylate **48** (7.88 g, 20.7 mmol, 1 equiv.) was quantitatively transferred with 2-butanone (103 mL) to a round bottom flask containing sodium iodide (13.7 g, 158 mmol, 7.7 equiv.). The solution was refluxed at 80 °C for 22 hours under inert atmosphere. CH_2Cl_2 was added once the solution had cooled and was extracted with water three times. The organic layer was dried over $MgSO_4$, filtered and concentrated, affording **97** as a yellow-orange oil. The product was carried to the next step without purification. **^{1}H NMR** (500 MHz, $CDCl_3$): δ 3.10 (dd, *J* = 5.3, 9.9 Hz, 2H), 2.97 (dd, *J* = 4.2, 4.2 Hz, 2H), 2.02 – 1.97 (m, 4H), 1.86 – 1.83 (m, 2H), 1.78 – 1.76 (m, 2H).

(1*R*,6*S*)-7,7-dichloro-3,4-dimethylenebicyclo[4.1.0]heptane (**49**)

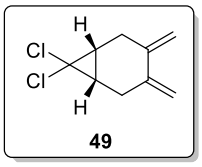

49

Adapted from reference 50. DBU (15.7 mL, 105 mmol, 5.1 equiv.) was slowly added to a cold round bottom flask containing compound **97** (20.7 mmol, 1 equiv.) and THF (207 mL) under inert atmosphere. The round bottom flask was removed from the ice-water bath and stirred at room temperature for 48.5 hours. Water was added to the solution and was subsequently extracted with CH_2Cl_2 three times. The organic layer was dried over $MgSO_4$, filtered and concentrated. Purification *via* flash column chromatography (7:3 Hex:EtOAc) produced **49** as a pungent, yellow oil (3.27 g, 84% over 2 steps) and **62** (209 mg, 5%). **^{1}H NMR** (600 MHz, $CDCl_3$): δ 5.26 – 5.25 (m, 2H), 4.82 – 4.81 (m, 2H), 2.79 – 2.74 (m, 2H), 2.26 (dddd, *J* = 16.1, 4.0, 3.8, 1.9 Hz, 2H), 1.85 – 1.80 (m, 2H).

(3a*R*,4a*R*,5a*S*,6a*S*)-5,5-dichlorooctahydro-1*H*-cyclopropa[*f*]isobenzofuran (**62**)

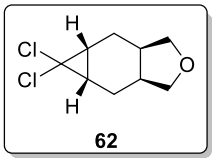

62

Orange, viscous oil. **^{1}H NMR** (500 MHz, $CDCl_3$): δ 3.94 (dd, *J* = 8.6, 7.5 Hz, 2H), 3.42 (dd, *J* = 8.6, 6.8 Hz, 2H), 2.39 – 2.32 (m, 2H), 1.93 (dt, *J* = 5.3, 2.5 Hz, 1H), 1.90 (dt, *J* = 5.3, 2.5 Hz, 1H), 1.74 – 1.68 (m, 2H), 1.44 (dddd, *J* = 15.2, 5.8, 4.3, 2.2 Hz, 2H); **^{13}C NMR** (125 MHz, $CDCl_3$): δ 73.7, 67.7, 34.1, 24.6, 19.0; **HRMS**: (FD) *m/z*: [M] Calcd for $C_9H_{12}Cl_2O$ 206.02652; Found: 206.02693; **FTIR** (KBr film) ν_{max} (cm^{-1}) 3019, 2978, 2944, 2853, 1639, 1477, 1461, 1443, 1250, 1216, 1198, 1127, 1100, 1065, 1044, 937, 819, 776.

(1a*R*,3a*R*,4a*S*,6a*S*)-1,1,1a,4,4,6a-hexachloro-1,1a,2,3,3a,4,4a,5,6,6a-dodecahydrodicyclopropa[*b*,*g*]naphthalene (**51a**) and **(1a*R*,3a*S*,4a*R*,6a*S*)-1,1,1a,4,4,6a-hexachloro1,1a,2,3,3a,4,4a,5,-6,6a-dodecahydrodicyclopro-pa[*b*,*g*]naphthalene** (**51b**)

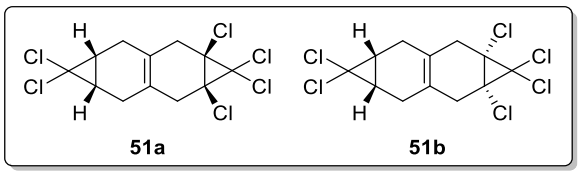

Tetrachlorocyclopropene (**50**) (1.44 mL, 11.7 mmol, 1 equiv.) was added to a solution of **49** (2.22 g, 11.7 mmol, 1 equiv.) in THF (11.8 mL) and stirred at room temperature for 24 hours under inert atmosphere. The solution was concentrated and coevaporated with dichlormethane three times. Recrystallization (Hex:CH_2Cl_2) afforded white crystals containing **51a** and **51b** in a 3:1 ratio (2.62 g, 61%). Major diastereomer **51a**: **^{1}H NMR** (600 MHz, $CDCl_3$): δ 2.91 (d, *J* = 16.8 Hz, 2H), 2.75 (d, *J* = 16.8 Hz, 2H), 2.32 (d, *J* = 20.3 Hz, 2H), 1.97 (d, *J* = 17.0 Hz, 2H), 1.86 – 1.82 (m, 2H); **^{13}C NMR** (125 MHz, $CDCl_3$): δ 121.1, 68.5, 52.8, 37.9, 24.4, 23.6; **HRMS**: (FD) *m/z*: [M] Calcd for $C_{12}H_{10}Cl_6$ 363.8914; Found: 363.8903; **FTIR** (KBr film) ν_{max} (cm^{-1}) 2895, 2828, 1431, 1424, 1075, 1045, 950, 870, 847, 782, 611, 552; **Melting range** = 157.2 - 157.8 °C. Minor diastereomer **51b**: **^{1}H NMR** (500 MHz, $CDCl_3$): δ 2.84 (d, *J* = 16.5 Hz, 2H), 2.78 (d, *J* = 17.1 Hz, 2H), 2.22 (d, *J* = 18.0 Hz, 2H), 2.09 (d, *J* = 17.0 Hz, 2H), 1.87 – 1.82 (m, 2H); **^{13}C NMR** (125 MHz, $CDCl_3$): δ 121.0, 68.6, 64.7, 52.9, 37.6, 24.9, 23.7; **HRMS:** (FD) *m/z*: [M] Calcd for $C_{12}H_{10}Cl_6$ 363.89137; Found: 363.8921; **FTIR** (ATR) ν_{max} (cm^{-1}): 2921, 2896, 2851, 1718, 1426, 1325, 1219, 1157, 1046, 993, 914, 846, 804, 779, 610, 549, 505; **Melting range** = 182.1 – 185.1 °C.

(1*R*,5*R*,7*S*,11*S*)-1,6,6,11,12,12-hexachlorotricyclo[9.1.0.0^{5,7}]dodecane-3,9-dione (**52a**)

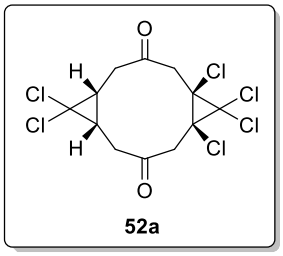

52a

Adapted from reference 48. Ozone was bubbled through a solution of adduct **51** (**51a**/**51b** = 7.4:1) (200 mg, 0.55 mmol, 1 equiv.), 5:1 CH_2Cl_2:MeOH (27.6 mL), and $NaHCO_{3(aq)}$ (5 mg, 0.06 mmol, 0.0013 equiv.) at -78 °C under atmospheric conditions. Oxygen was bubbled through the solution when a blue coloured appeared and was discontinued when the colour disappeared. The solution was transferred *via* cannula to a round bottom flask at 0 °C containing thiourea (61 mg, .80 mmol, 1.2 equiv.), $NaHCO_3$ (37 mg, 0.44 mmol, 0.66 equiv.), and CH_2Cl_2 (10 mL). The solution was stirred at 0 °C for 1 hour and extracted twice with water. The collected aqueous layers were washed twice with CH_2Cl_2 and the organic layers were dried over $MgSO_4$, filtered and concentrated. Recrystallization (petroleum ether:CH_2Cl_2) yielded rectangular, transparent crystals of **52a** (67 mg, 30%). **^{1}H NMR** (500 MHz, $CDCl_3$): δ 3.41 (d, *J* = 14.5 Hz, 2H), 3.24 (d, *J* = 14.5 Hz, 2H), 2.98 (dd, *J* = 14.2, 3.4 Hz, 2H), 2.50 – 2.45 (m, 2H), 2.35 – 2.31 (m, 2H); **^{13}C NMR** (125 MHz, $CDCl_3$): δ 202.8, 71.1, 63.7, 54.0, 48.0, 40.8, 28.7; **HRMS**: (ESI) *m/z*: [M+Na] Calcd for $C_{12}H_{10}Cl_6O_2$ 418.8704; Found: 418.8723; **FTIR** (KBr film) ν_{max} (cm^{-1}) 2973, 2932, 2895, 1732, 1436, 1349, 1313, 1099, 1090, 1041, 924, 794, 745, 608, 569, 516; **Melting range** = 148.1 – 149.0 °C. Larger batches (1–4 g) of this reaction gave larger amounts of aldol side product **63aa**. One experiment, for example, used 4.10 g of **51** and yielded products **52a** and **63aa** as well as recovered starting material **51** (**51a**/**51b** = 1:1.4). Aldol product **63aa** was separated from adducts **51** (**51a**/**51b** = 1:1.4) and dione **50a** through filtration (CH_2Cl_2) to yield **63aa** as a white solid (2.20 g, 49%). Recrystallization (Hex:CH_2Cl_2) of the resulting mother liquors yielded rectangular, transparent crystals of **52a**, **51a** and **51b** (150 mg of a 1:1:1 mixture of **52a**:**51a**:**51b**) and an orange solid of **52a**, **51a** and **51b** (753 mg of a 1:2:1 mixture of **52a**:**51a**:**51b**).

(1a*R*,1b*S*,3a*R*,4a*S*,5a*R*,6a*S*)-1,1,1a,4,4,6a-hexachloro-5a-hydroxydecahydrodicyclopropa[*a*,-*f*]azulen-2(1*H*)-one (**63aa**)

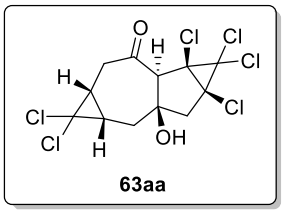

63aa

Transannular aldol product **63aa** was produced in the above ozonolysis reactions as a white solid. **^{1}H NMR** (500 MHz, $CDCl_3$): δ 3.39 (s, 1H), 3.04 (dd, *J* = 12.4, 7.7 Hz, 1H), 2.71 (s, 2H), 2.62 (dd, *J* = 15.2, 8.1 Hz, 1H), 2.52 (dd, *J* = 9.2, 6.2 Hz, 1H), 2.25 (s, OH), 1.96 – 1.86 (m, 2H), 1.67 (dd, *J* = 15.1, 8.4 Hz, 1H); **^{13}C NMR** (125 MHz, DMSO): δ 196.7, 85.1, 77.5, 66.7, 64.4, 60.0, 59.4, 50.6, 41.1, 31.8, 28.6, 26.2; **HRMS**: (ESI) *m/z*: [M+Na] Calcd for $C_{12}H_{10}Cl_6O_2Na$ 418.8704; Found: 418.8720; **FTIR** (KBr Film) ν_{max} (cm^{-1}) 3438, 3039, 2944, 2927, 1711, 1432, 1383, 1286, 1117, 1046, 979, 902, 829, 791, 490; **Melting range** = 164.3 – 164.4 °C.

(1a*R*,1b*R*,3a*R*,4a*S*,5a*R*,6a*S*)-1,1,1a,4,4,6a-hexachlorodecahydrodicyclopropa[*a*,*f*]azulene2,5-a(1*H*)-diol (**71a**)

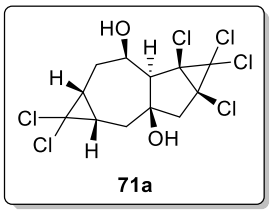

71a

Compound **63aa** (56 mg, 0.14 mmol, 1 equiv.) was added to a cooled round bottom flask containing lithium aluminum hydride (8.2 mg, 0.22 mmol, 1.1 equiv.) and THF (7.0 mL). The solution was stirred at room temperature for 3.5 hours under inert atmosphere and was quenched with cold water at 0 °C. 1 M HCl was added to the solution and the aqueous solution was extracted with CH_2Cl_2 five times. The collected organic layers were dried over $MgSO_4$, filtered and concentrated to give **71a** as a light orange, foamy solid (53 mg, 94%). **^{1}H NMR** (500 MHz, $CDCl_3$): δ 5.14 (s, 1H, OH), 4.69 (ap t, *J* = 5.5 Hz, 1H), 2.96 (m, 1H), 2.78 (ddd, *J* = 14.5, 7.5, 7.0 Hz, 1H), 2.56 (d, *J* = 15.0 Hz, 1H), 2.48 (dd, *J* = 14.5, 7.5 Hz, 1H), 2.44 (dd, *J* = 14.5, 2.0 Hz, 1H), 2.10 (s, 1 H), 2.00 (dddd, *J* = 47.5, 11.5, 10.0, 7.5 Hz, 2H), 1.55 (s, OH), 1.54 (dd, *J* = 15.0, 10.0 Hz, 1H), 1.44 (dd, *J* = 14.5, 10.0 Hz, 1H); **^{13}C**

NMR (125 MHz, $CDCl_3$): δ 88.5, 77.3, 71.2, 66.6, 63.3, 60.4, 59.1, 51.6, 34.1, 31.6, 28.5, 28.3; **HRMS**: (ESI) *m/z*: [M+Na] Calcd for $C_{12}H_{12}O_2Cl_6Na$ 420.8861; Found: 420.8880; **FTIR** (KBr film) ν_{max} (cm^{-1}) 3383, 2924, 2851, 1449, 1430, 1262, 1149, 1115, 879, 822; **Melting range** = 96.2 – 100.3 °C. Compound **71a** was also formed as a side product in the reduction of dione **52a**.

(1*R*,3*R*,5*R*,7*S*,9*S*,11*S*)-1,6,6,11,12,12-hexachlorotricyclo[9.1.0.0^{5,7}]dodecane-3,9-diol (**55a**)

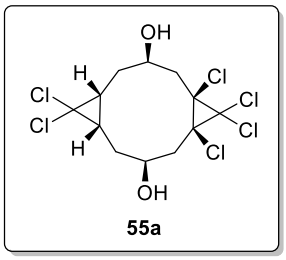

55a

Adapted from reference 58. Ozone was bubbled through a solution of adduct **51** (**51a**/**51b** = 5.8:1) (113 mg, 30.8 mmol, 1 equiv.) and 3:1 CH_2Cl_2:MeOH (14 mL) at -78 °C under atmospheric conditions until the solution turned blue. Oxygen was bubbled through the solution until the colour disappeared and sodium borohydride (71 mg, 1.9 mmol, 5.8 equiv.) was added over five minutes at -78 °C. The solution was warmed to room temperature, quenched with ammonium chloride, and concentrated under reduced pressure. The aqueous layer was extracted with ethyl acetate three times and the collected organic layer was washed once with water and once with brine. The solution was dried over $MgSO_4$, filtered and concentrated. Purification *via* FCC (2:1 Hex:Acetone) yielded **55a** as a white solid (73 mg, 56%). **^{1}H NMR** ($CDCl_3$, 500 MHz): δ 4.39 (ddddd, J = 7.8, 4.4, 4.4, 4.4, 3.3 Hz, 2H), 2.85 (ddd, *J* = 14.8, 4.6, 1.5 Hz, 2H), 2.76 (d, *J* = 7.9 Hz, 2H), 2.37 (dd, *J* = 15.8, 4.5 Hz, 2H), 2.33 – 2.29 (m, 2H), 1.97 (dd, *J* = 16.4, 3.4 Hz), 1.43 (ddt, *J* = 16.0, 7.0, 3.0 Hz, 2H); **^{13}C NMR** (*d*$_6$-DMSO, 125 MHz): δ 73.5, 67.6, 66.4, 56.2, 37.9, 30.3, 26.9; **HRMS**: (ESI) *m/z*: [M+Na] Calcd for $C_{12}H_{14}Cl_6O_2Na$: 422.9023; Found: 422.9017; **FTIR** (ATR) ν_{max} (cm^{-1}) 3391, 2908, 1421, 1311, 1290, 1076, 1036, 993, 939, 925, 859, 817, 788, 753, 708, 635, 575, 540, 485; **Melting range** = 203.3 – 203.7 °C.

(1*R*,3*S*,5*S*,7*R*,9*R*,11*S*)-1,6,6,11,12,12-hexachlorotricyclo[9.1.0.0^{5,7}]dodecane-3,9-diol (**55d**)

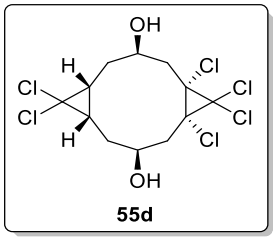

55d

Adapted from reference 58. Ozone was bubbled through a solution of diastereoenriched Diels-Ader adducts 3:1 **51b**:**51a** (45 mg, 0.12 mmol, 1 equiv.) and 3:1 CH_2Cl_2:MeOH (5.7 mL) at -78 °C under atmospheric conditions until the solution turned blue. Oxygen was bubbled through the solution until the colour disappeared and sodium borohydride (29 mg, 0.77 mmol, 5.8 equiv.) was added at -78 °C. The solution was warmed to room temperature, quenched with ammonium chloride, and concentrated under reduced pressure. The aqueous layer was extracted with ethyl acetate three times, and the collected organic layer was washed once with water and once with brine. The resulting solution was dried over magnesium sulfate, filtered and concentrated to yield inseparable diols **55a** and **55d** (6 mg of a 3.5:1 mixture of **55a** and **55d**). **^{1}H NMR** of **55d** (500 MHz, $CDCl_3$): δ 4.14 – 4.10 (m, 2H), 2.74 (dt, *J* = 16.4, 2.3 Hz, 2H), 2.27 (t, *J* = 2.1 Hz, 1H), 2.25 (t, *J* = 2.1 Hz, 1H), 2.10 (d, *J* = 4.4 Hz, 1H), 2.07 (d, *J* = 4.3, 1H), 1.76 – 1.70 (m, 2H), 1.65 – 1.61 (m, 2H), 1.50 (ap d, *J* = 1.5 Hz, 1H), 1.49 (ap d, *J* = 2.6 Hz, 1H).

(1*R*,3*R*,5*R*,7*S*,9*S*,11*S*)-1,6,6,11,12,12-hexachlorotricyclo[9.1.0.0^{5,7}]dodecane-3,9-diyl dimethanesulfonate (**56a**)

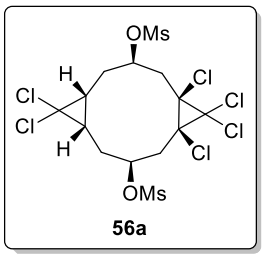

56a

Adapted from reference 59. Diol **55a** (310 mg, 0.76 mmol, 1 equiv.) was quantitatively transferred with pyridine (2.2 mL) to a round bottom flask containing DMAP (30 mg, 0.25 mmol, 0.30 equiv.). The solution was cooled to 0 °C and methansulfonyl chloride (0.15 mL, 1.9 mmol, 2.6 equiv.) was added. The solution was stirred at room temperature for 22 hours under inert atmosphere and quenched with CH_2Cl_2. The organic layer was concentrated and then purified with a silica plug

(CH_2Cl_2) to afford **56a** as a white-orange solid (248 mg, 58%). **^{1}H NMR** ($CDCl_3$, 500 MHz): δ 5.28 (ddd, *J* = 7.9, 5.0, 3.0 Hz, 2H), 3.16 (s, 6H), 3.11 (ddd, *J* = 16.8, 6.3, 1.3 Hz, 2H), 2.57 (dd, *J* = 16.4, 4.8 Hz, 2H), 2.43 (m, 2H), 2.07 (dd, *J* = 16.8, 3.1 Hz, 2H), 1.55 (ddt, *J* = 16.5, 6.5, 3.0 Hz, 2H); **^{13}C NMR** ($CDCl_3$, 125 MHz) δ 74.3, 72.2, 64.5, 54.9, 39.3, 38.1, 30.1, 26.7; **HRMS** (ESI) *m/z*: [M + Na] Calcd for $C_{12}H_{18}Cl_6O_6S_2Na$: 578.85682; Found: 578.8574; **FTIR** (ATR) ν_{max} (cm^{-1}) 3025, 2920, 2850, 1726, 1426, 1346, 1331, 1289, 1259, 1173, 1048, 918, 788, 765, 736, 689, 629, 526, 456; **Melting range** = 183.4 – 183.5 °C.

(1*R*,3*S*,5*S*,7*R*,11*R*,*Z*)-5,6,6,7,12,12-hexachlorotricyclo[9.1.0.0^{5,7}]dodec-8-en-3-yl methanesulfonate (**72aa**)

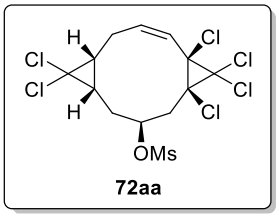

72aa

Adapted from reference 62. A 1.0 M solution of potassium *tert*-butoxide in THF (0.15 mL, 4.1 equiv.) was added to a round bottom flask containing dimesylate **55a** (21 mg, 0.037 mmol, 1 equiv.) and d_6-DMSO (0.93 mL) under inert atmosphere. The vessel was heated to 120 °C for 2 hours. Water was added to the solution and the aqueous layer was extracted with distilled diethyl ether three times. The collected diethyl ether layers were washed with water once, dried over sodium sulfate and concentrated. Purification *via* PTLC (7:3 Hex:EtOAc) afforded **72aa** as a white solid (2.9 mg, 16%). **^{1}H NMR** ($CDCl_3$, 500 MHz): δ 5.98 (ddd, *J* = 12.3, 5.8, 3.3 Hz, 1H), 5.87 (ddd, *J* = 12.3, 2.6, 2.6 Hz, IH), 5.26 – 5.24 (m, 1H), 3.15 (s, 3H), 3.09 (dddd, *J* = 20.5, 5.8, 3.1, 3.1 Hz, 1H), 3.01 (ddd, *J* = 16.3, 4.3, 1.5 Hz, 1H), 2.70 (ddd, *J* = 10.9, 10.9, 5.6 Hz, 1H), 2.52 – 2.50 (m, 1H), 2.48 – 2. 40 (m, 1H), 2.21 (dddd, *J* = 16.7, 11.0, 5.6, 1.8 Hz, 1H), 2.05 (dd, *J* = 16.4, 3.3 Hz, 1H), 1.36 (ddd, *J* = 15.9, 9.5, 2.4 Hz, 1H); **^{13}C NMR** ($CDCl_3$, 125 MHz): δ 136.9, 123.0, 75.2, 73.1, 65.6, 55.7, 53.0, 39.9, 39.3, 29.9, 29.3, 27.1, 26.5; **HRMS** (ESI) *m/z*: [M + Na] Calcd for $C_{12}H_{14}Cl_6O_3SNa$: 482.8687;

Found: 482.8708; **FTIR** (ATR) ν_{max} (cm^{-1}): 2957, 2916, 2848, 1722, 1565, 1462, 1421, 1329, 1076, 1024, 937, 859, 842, 823, 780, 682, 594, 549, 539, 462; **Melting range** = 184.6 – 185.9 °C.

Adapted from reference 61. Potassium *tert*-butoxide (75 µL, 4 equiv.) was added to a Schlenk tube containing dimesylate **56a** (10 mg, 0.018 mmol, 1 equiv.) and THF (0.20 mL) under inert atmosphere. The vessel was heated to 75 °C for 4.5 hours. Water was added to the solution and the aqueous layer was extracted with distilled diethyl ether twice. The collected diethyl ether layers were washed with water once, dried over sodium sulfate and concentrated. Purification *via* PTLC (7:3 Hex:EtOAc) afforded **72aa** as a white oil (3.4 mg, 41%).

3.3 Chloroprene Route Experimental Procedures

Materials: 3,4-Dichlorobut-1-ene (**75**), maleic anhydride (**43**), and tetrachlorocyclopropene (**50**) were received from commercial sources.

2-chlorobuta-1,3-diene (**58**)

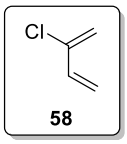

Adapted from reference 49. A 250 mL 3 neck flask was charged with calcium hydroxide (9.81 g, 132 mmol, 0.57 equiv.), ethylene glycol (116 mL), and BHT (0.290 g, 1.31 mmol, 0.0056 equiv.). A thermometer was placed in the solution, a vigreux column was attached to the center neck of the round bottom flask and a dropping funnel was placed in the last neck. Attached to the vigreux column was a distillation head and a receiving flask that was charged with BHT (24.9 mg, 0.113 mmol, 0.00038 equiv.). 3,4-Dichlorobut-1-ene (25.0 mL, 232 mmol, 1 equiv.) was added slowly (~1 drop/3 sec) once the round bottom flask had equilibrated to 105 °C under inert atmosphere. Chloroprene distills from the solution at 55 °C as a pungent, colourless oil

(11.9 g, 58%). The resulting distillate was dried over Na_2SO_4 and stored over BHT in the freezer.[72] **^{1}H NMR** (500 MHz, $CDCl_3$): δ 6.42 (dd, *J* = 16.5, 10.5 Hz, 1H), 5.67 (d, *J* = 16.5 Hz, 1H), 5.42 (s, 1H), 5.38 (s, 1H), 5.31 (d, *J* = 10.5 Hz, 1H).

(3a*S*,7a*S*)-5-chloro-3a,4,7,7a-tetrahydroisobenzofuran-1,3-dione (**59**)

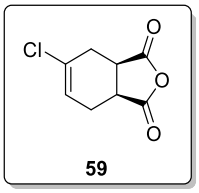

59

Adapted from reference 65. Maleic anhydride (9.57 g, 97.6 mmol, 1 equiv.) and chloroprene (10.4 g, 118 mmol, 1.2 equiv.) were heated to 50 °C in a sealed pressure vessel until the solution became solid. The solid was concentrated and coevaporated with dichloromethane to yield **59** as a white solid (18.2 g, 99%). **^{1}H NMR** (500 MHz, $CDCl_3$): δ 6.00 (ddd, *J* = 6.2, 4.0, 2.3 Hz, 1H), 3.50 (ddd, *J* = 9.7, 8.2, 3.3 Hz, 1H), 3.36 (ddd, *J* = 9.8, 8.0, 3.7 Hz, 1H), 2.85 (dd, *J* = 17.0, 3.3 Hz, 1H), 2.71 (m, 2H), 2.51 – 2.44 (m, 1H); **^{13}C NMR** (125 MHz, $CDCl_3$): δ 173.1, 172.7, 130.7, 122.8, 40.4, 38.3, 30.7, 30.5, 25.0; **HRMS**: (FD) *m/z*: [M] Calcd for $C_8H_7ClO_3$ 186.0084; Found: 186.0090; **FTIR** (KBr film) ν_{max} (cm^{-1}) 2978, 2915, 2858, 1840, 1772, 1200, 1093, 924, 817, 776, 579; **Melting range** = 59.9 – 60.4 °C.

Diethyl (1*S*,2*R*)-4-chlorocyclohex-4-ene-1,2-dicarboxylate (**76**)

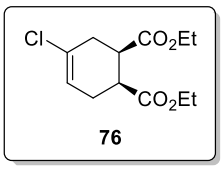

76

Adapted from reference 46. Anhydride **59** (9.03 g, 48.3 mmol, 1 equiv.) was quantitatively transferred to a round bottom flask with ethanol (17.0 mL, 291 mmol, 6 equiv.). *p*-TSA (739 mg, 3.88 mmol, 0.08 equiv.) was added to the flask and the solution was refluxed under atmospheric conditions at 100 °C for 15.5 hours. Toluene (8.8 mL) was added to the solution and the round bottom flask was concentrated under reduced pressure. Ethanol (17.0 mL, 3.88 mmol, 6 equiv.) was again added to the round bottom flask and the solution was refluxed for an additional 6 hours under atmospheric conditions. Toluene (8.8

mL) was added to the solution and concentrated under reduced pressure. The resulting solution was diluted with diethyl ether and then extracted with 3% $Na_2CO_{3(aq)}$ twice and the collected aqueous was washed with diethyl ether three times. The collected organic layers were washed once with water, dried over $MgSO_4$, filtered and concentrated. Purification *via* FCC (7:1 Hex:EtOAc) afforded a pale yellow oil **76** (11.9 g, 95%). **^{1}H NMR** (600 MHz, $CDCl_3$): δ 5.79 – 5.78 (m, 1H), 4.20 – 4.12 (m, 4H), 3.09 (ddd, *J* = 7.8, 7.8, 4.4 Hz, 1H), 3.03 (ddd, *J* = 7.4, 7.4, 4.6 Hz, 1H), 2.85 – 2.80 (m, 1H), 2.66 – 2.59 (m, 2H), 2.45 – 2.39 (m, 1H), 1.25 (ddd, *J* = 8.6, 8.6, 5.0 Hz, 6H); **^{13}C NMR** (150 MHz, $CDCl_3$): δ 172.5, 172.2, 130.2, 122.6, 61.1, 61.1 41.1, 39.0, 33.0, 26.7, 14.3, 14.3; **HRMS**: (FD) *m/z*: [M] Calcd for $C_{12}H_{17}ClO_4$: 260.0815; Found: 260.0815; **FTIR** (KBr thin film) ν_{max} (cm^{-1}) 2982, 2937, 2906, 1735, 1347, 1272, 1198, 1037, 861, 738.

Diethyl (1*S*,3*R*,4*S*,6*S*)-1,7,7-trichlorobicyclo[4.1.0]heptane-3,4-dicarboxylate (**78**)

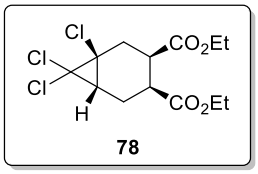

78

Adapted from reference 66. A 22.7 M solution of $NaOH_{(aq)}$ (7.1 mL) was added to a solution of **76** (5.12 g, 19.6 mmol, 1 equiv.), chloroform (8.2 mL, 100 mmol, 5.2 equiv.) and triethylbenzyl ammonium chloride (39.1 mg, 0.3140 mmol, 0.006 equiv.) under atmospheric conditions. The vessel was loosely capped and the solution was quenched with distilled water after 18 hours. The solution was extracted with CH_2Cl_2 three times and the collected organic layer was dried over $MgSO_4$, filtered and concentrated under reduced pressure. Purification *via* FCC (CH_2Cl_2) afforded pure **78** as a yellow oil (1.89 g, 28%). **^{1}H NMR** (500 MHz, $CDCl_3$): δ 4.23 – 4.14 (m, 4H), 2.92 (dt, *J* = 5.8, 3.5 Hz, 1H), 2.84 (dd, *J* = 8.6, 14.9 Hz, 1H), 2.78 – 2.72 (m, 2H), 2.62 (dd, *J* = 14.9, 5.4 Hz, 1H), 2.07 (dd, *J* = 9.8, 2.6 Hz, 1H), 1.88 (ddd, *J* = 15.0, 5.8, 2.7 Hz, 1H), 1.27 (dt, *J* = 7.1, 5.5 Hz, 6H). Alternatively, the crude

product could be quickly purified through a silica plug (CH_2Cl_2) and carried forward with minor amounts of **84** still present.

((1*S*,3*R*,4*S*,6*S*)-1,7,7-trichlorobicyclo[4.1.0]heptane-3,4-diyl)dimethanol (**79**)

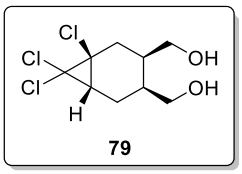

79

Adapted from reference 46. Bicyclic diester **78** (438 mg, 1.27 mmol, 1 equiv.) was quantitatively transferred to a cooled round bottom flask charged with THF (6.5 mL) and $LiAlH_4$ (85 mg, 2.3 mmol, 1.7 equiv.) under inert atmosphere. The solution was stirred at ambient temperature for 10 hours. The solution was acidified with 1 M HCl until the pH = 1 and subsequently extracted with CH_2Cl_2 five times. The organic layer was dried over $MgSO_4$, filtered and concentrated under reduced pressure. Purification *via* FCC (EtOAc) afforded **79** as a white solid (106 mg, 32%). **^{1}H NMR** (600 MHz, $CDCl_3$): δ 3.73 – 3.63 (m, 4H), 2.61 (br s, 1H), 2.46 (dd, *J* = 15.6, 8.0 Hz, 1H), 2.40 (dd, *J* = 15.7, 5.6 Hz, 1H), 2.21 (ddd, *J* = 15.0, 9.6, 7.0 Hz, 1H), 1.94 (dd. *J* = 9.7, 2.5 Hz, 1H), 1.93 – 1.84 (m, 2H), 1.74 (ddd, *J* = 14.9, 5.6, 2.5 Hz, 1H); **^{13}C NMR** (125 MHz, $CDCl_3$): δ 69.2, 63.7, 63.5, 48.7, 37.2, 36.0, 35.4, 32.3, 32.3, 21.4; **HRMS**: (FD) *m/z*: [M+1] Calcd for $C_9H_{13}Cl_3O_2$ 259.0059; Found: 259.0067; **FTIR** (KBr film) ν_{max} (cm^{-1}) 3288, 2934, 2883, 1440, 1340, 1031, 964, 879, 838, 818, 729, 622, 460; **Melting range** = 125.9 – 130.0 °C. When **78** was not separated from **76**, diol **79** was purified *via* triteration with CH_2Cl_2 (7.38 g, 62% over 2 steps). It is postulated that the yield of diol **79** increases as the scale of the reaction increases.

((1*S*,2*R*)-4-chlorocyclohex-4-ene-1,2-diyl)dimethanol (**80**)

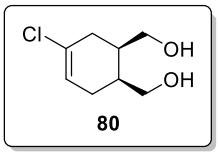

Diol **80** was produced during the reduction of **78** due to **76** being present in the starting material. **^{1}H NMR** (500 MHz, $CDCl_3$): δ 5.71 – 5.70 (m, 1H), 4.36 (br s, OH), 4.11 – 4.06 (m, OH), 3.67 (m, 2H), 3.54 (dtd, *J* = 22.0, 10.9, 4.4 Hz, 2H), 2.40 – 2.35 (m, 1H), 2.30 – 2.26 (m, 1H), 2.19 – 2.15 (m, 2H), 2.11 – 2.02 (m, 2H).

((1*S*,3*R*,4*S*,6*S*)-1,7,7-trichlorobicyclo[4.1.0]heptane-3,4diyl)bis(methylene)dimethanesulfonate (**81**)

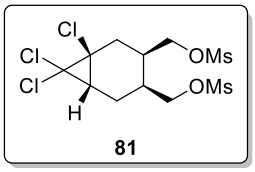

Adapted from reference 46. Triethylamine (6.0 mL, 43 mmol, 3 equiv.) was added to a cooled round bottom flask charged with CH_2Cl_2 (13.0 mL), methanesulfonyl chloride (2.7 mL, 35 mmol, 2.4 equiv.), and diol **79** (3.72 g, 14.3 mmol, 1 equiv.). The solution was stirred at ambient temperature for 6.5 hours under inert atmosphere. Saturated $NaHCO_{3(aq)}$ was added to the solution and was subsequently washed with ethyl acetate three times. The collected organic layers were washed with water once and dried over $MgSO_4$, filtered and concentrated to produce **81** as an orange solid (5.82 g, 98%). **^{1}H NMR** (500 MHz, $CDCl_3$): δ 4.27 (dd, *J* = 10.3, 7.4 Hz, 2H), 4.19 (dd, *J* = 10.2, 6.5 Hz, 2H), 3.07 (d, *J* = 1.4 Hz, 6H), 2.53 (dd, *J* = 15.6, 5.4 Hz, 1H), 2.35 (dd, *J* = 15.6, 7.9 Hz, 1H), 2.30 – 2.20 (m, 2H), 2.16 (m, 1H), 2.04 (dd, *J* = 9.4, 2.4 Hz, 1H), 1.87 (ddd, *J* = 14.4, 5.1, 1.8 Hz, 1H); **^{13}C NMR** (125 MHz, $CDCl_3$): δ 69.0, 68.8, 68.2, 47.4, 37.8, 37.7, 34.8, 34.0, 32.3, 31.9, 20.7; **HRMS**: (ESI) *m/z*: [M+Na] Calcd for $C_{11}H_{17}Cl_3O_6S_2$ 436.9424; Found: 436.9433; **FTIR** (KBr film) ν_{max} (cm^{-1}) 3024, 2944, 1356, 1340, 1184, 953, 926, 847, 596, 534; **Melting range** = 115.0 – 116.1 °C.

(1*S*,3*R*,4*S*,6*S*)-1,7,7-trichloro-3,4-bis(iodomethyl)bicyclo[4.1.0]heptane (**99**)

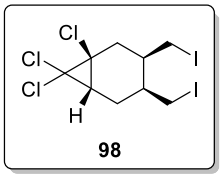

98

Adapted from reference 50. Dimesylate **81** (6.59 g, 15.9 mmol, 1 equiv.) was quantitatively transferred to a round bottom flask containing NaI (22.6 g, 151 mmol, 9.5 equiv.) and 2-butanone (80 mL). The solution was refluxed at 80 °C for 5.5 hours under inert atmosphere. CH_2Cl_2 was added to the round bottom flask and the solution was washed with water three times. The organic solution was dried over $MgSO_4$, filtered and concentrated under reduced pressure. Compound **98** was produced as a yellow oil and was not purified. **^{1}H NMR** (500 MHz, $CDCl_3$): δ 3.18 (dd, *J* = 9.6, 4.7 Hz, 1H), 3.15 (dd, *J* = 10.0, 5.7 Hz, 1H), 3.07 – 2.99 (m, 2H), 2.55 (dd, *J* = 15.7, 5.3 Hz, 1H), 2.34 (dd, *J* = 15.7, 8.0 Hz, 1H), 2.24 (ddd, *J* = 15.3, 9.6, 6.7 Hz, 1H), 2.09 – 2.03 (m, 2H), 1.98 (dd, *J* = 9.6, 2.6 Hz, 1H), 1.84 (ddd, *J* = 15.0, 4.5, 2.7 Hz, 1H).

(1*S*,6*S*)-1,7,7-trichloro-3,4-dimethylenebicyclo[4.1.0]heptane (**82**)

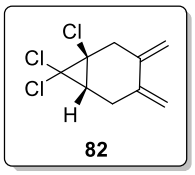

82

Adapted from reference 50. A round bottom flask was charged with THF (160 mL) and diiodide **98** (15.9 mmol, 1 equiv.) under inert atmosphere. DBU (12.1 mL, 80.9 mmol, 5.1 equiv.) was added to the cooled flask and the resulting solution was stirred at ambient temperature. The solution was quenched with water after 42 hours. The aqueous layer was extracted with CH_2Cl_2 three times. The organic layer was dried over $MgSO_4$, filtered and concentrated under reduced pressure. Purification through FCC (7:3 Hex:EtOAc) afforded **82** as a pungent, yellow oil (1.86 g, 53% over 2 steps). The diene was not vacuum dried as polymerization was a concern. **^{1}H NMR** (500 MHz, $CDCl_3$): δ 5.41 (dd, *J* = 11.5, 2.0 Hz, 2 H), 4.93 (d, *J* = 15.2 Hz, 2H), 2.94 – 2.92 (m, 2H), 2.86 (dd, *J* = 16.1, 9.0 Hz, 1H), 2.25 (ddt, *J* = 16.0, 6.4, 2.3 Hz, 1 H), 1.99 (dd, *J* = 9.0, 6.6 Hz, 1H); **^{13}C NMR** (125 MHz, $CDCl_3$): δ

140.0, 139.7, 111.4, 110.9, 69.4, 50.9, 39.4, 36.9, 29.1; **HRMS**: (FD) *m/z*: [M**]** Calcd for $C_9H_9Cl_3$ 221.9769; Found: 221.9772; **FTIR** (KBr thin film) ν_{max} (cm^{-1}) 2960, 2890, 2832, 1425, 1264, 1147, 973, 895, 823, 739.

1,1,1a,3a,4,4,4a-heptachloro-1,1a,2,3,3a,4,4a,5,6,7a decahydrodicyclopropa[*b*,*g*]naphthalene (83)

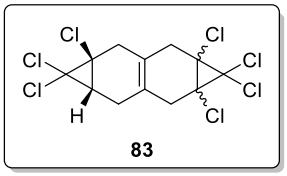

83

Tetrachlorocyclopropene (0.31 mL, 2.5 mmol, 2 equiv.) was added to a solution of **82** (239 mg, 1.26 mmol, 1 equiv.) in THF (1.3 mL) and stirred at room temperature for 24 hours under inert atmosphere. The solution was concentrated and co-evaporated with dichloromethane three times. Recrystallization (Hex:CH_2Cl_2) produced **83** as an off-white solid (287 mg, 61%) and as a single isomer. The relative configuration has not been established. **^{1}H NMR** (500 MHz, $CDCl_3$): δ 2.95 – 2.62 (m, 6 H), 2.50 – 2.42 (m, 1H), 2.18 (d, *J* = 18.8 Hz, 1H), 2.08 (d, *J* = 7.1 Hz, 1H); **^{13}C NMR** (125 MHz, $CDCl_3$): δ 121.6, 120.6, 68.4, 66.4, 52.7, 52.5, 47.8, 37.3, 37.2, 34.8, 34.7, 25.3; **HRMS**: (FD) *m/z*: [M] Calcd for $C_{12}H_9Cl_7$ 397.8523; Found: 397.8518; **FTIR** (KBr film) ν_{max} (cm^{-1}) 2900, 2825, 1426, 1338, 1158, 999, 945, 861, 842, 616, 595, 549, 421; **Melting range** = 229.3 – 230.1 °C.

3.4 Calculated ^{1}H and ^{13}C NMR Chemical Shifts

3.4.1 Butadiene Route

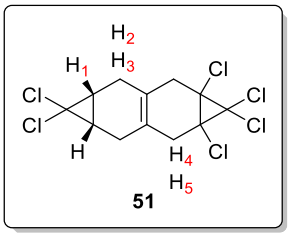

51

(Mixture of isomers)

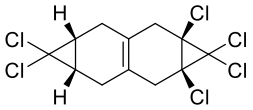

51a

Cis isomer **51a** vs major product*					*Cis* isomer **51a** vs minor product*				
H	Calc (ppm)	Expt (ppm)	Error (ppm)	Abs error (ppm)	H	Calc (ppm)	Expt (ppm)	Error (ppm)	Abs error (ppm)
1	1.85	1.86	-0.01	0.01	1	1.85	1.87	-0.02	0.02
2	2.32	2.33	-0.01	0.01	2	2.32	2.18	0.14	0.14
3	1.97	2.04	-0.07	0.07	3	1.97	2.19	-0.22	0.22
4	2.91	2.89	0.02	0.02	4	2.91	2.83	0.08	0.08
5	2.75	2.79	-0.04	0.04	5	2.75	2.80	-0.05	0.05
			MAE	0.03				MAE	0.10

* Computations performed by Dr. Michel Gravel

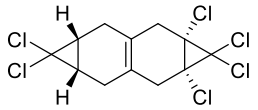

51b

Trans isomer **51b** vs major product*					*Trans* isomer **51b vs** minor product*				
H	Calc (ppm)	Expt (ppm)	Error (ppm)	Abs error (ppm)	H	Calc (ppm)	Expt (ppm)	Error (ppm)	Abs error (ppm)
1	1.84	1.86	-0.02	0.02	1	1.84	1.87	-0.03	0.03
2	2.22	2.33	-0.11	0.11	2	2.22	2.19	0.03	0.03
3	2.09	2.04	0.05	0.05	3	2.09	2.18	-0.09	0.09
4	2.85	2.89	-0.04	0.04	4	2.85	2.83	0.02	0.02
5	2.78	2.79	-0.01	0.01	5	2.78	2.80	-0.02	0.02
			MAE	0.05				MAE	0.04

* Computations performed by Dr. Michel Gravel

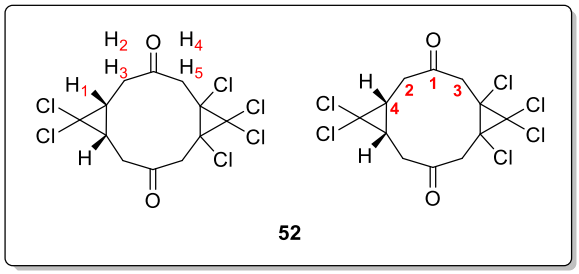

52

(Single isomer)

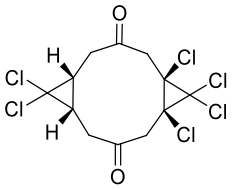

52a

52a ^{1}H NMR Chemical Shift Comparison*					**52a** ^{13}C NMR Chemical Shift Comparison*				
H	Calc (ppm)	Expt (ppm)	Error (ppm)	Abs Error (ppm)	C	Calc (ppm)	Expt (ppm)	Error (ppm)	Abs Error (ppm)
1	2.40	2.31	0.09	0.09	1	206.21	202.76	3.45	3.45
2	2.99	2.97	0.02	0.02	2	39.81	40.86	-1.05	1.05
3	2.70	2.48	0.22	0.22	3	48.72	48.05	0.67	0.67
4	3.24	3.25	-0.01	0.01	4	32.01	28.73	3.28	3.28
5	3.27	3.34	-0.07	0.07	5[a]	62.72	54.09	8.63	8.63
					6[a]	85.90	71.15	14.75	14.75
					7[a]	80.64	63.75	16.89	16.89
			MAE	0.08				MAE	2.1

[a] These values were not included in the MAE calculation due to the heavy atom effect.[54]

* Computations performed by Dr. Michel Gravel

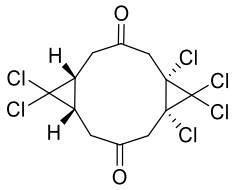

52b

52b ^{1}H NMR Chemical Shift Comparison*					**52b** ^{13}C NMR Chemical Shift Comparison*				
H	Calc (ppm)	Expt (ppm)	Error (ppm)	Abs Error (ppm)	C	Calc (ppm)	Expt (ppm)	Error (ppm)	Abs Error (ppm)
1	2.19	2.31	-0.12	0.12	1	207.21	202.76	4.45	4.45
2	3.03	2.97	0.06	0.06	2	38.96	40.86	-1.90	1.90
3	2.86	2.48	0.38	0.38	3	48.92	48.05	0.87	0.87
4	3.18	3.25	-0.07	0.07	4	32.05	28.73	3.32	3.32
5	3.39	3.34	0.05	0.05	5[a]	63.42	54.09	9.33	9.33
					6[a]	85.19	71.15	14.04	14.04
					7[a]	81.31	63.75	17.56	17.56
			MAE	0.14				MAE	2.6

[a] These values were not included in the MAE calculation due to the heavy atom effect.[54]

* Computations performed by Dr. Michel Gravel

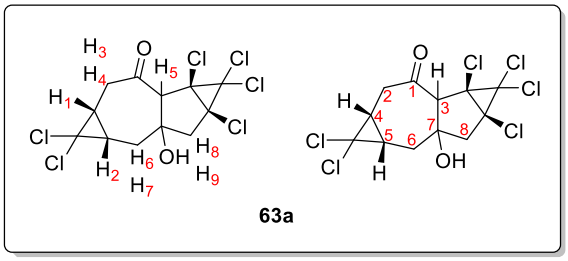

63a

(Isolated major isomer)

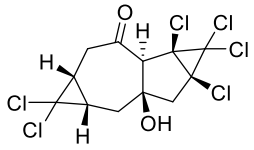

63aa

63aa ^{1}H NMR Chemical Shift Comparison[a]					**63aa** ^{13}C NMR Chemical Shift Comparison[b]				
H	Calc (ppm)	Expt (ppm)	Error (ppm)	Abs error (ppm)	C	Calc (ppm)	Expt (ppm)	Error (ppm)	Abs error (ppm)
1	1.85	1.91	0.06	0.06	1	201.13	196.72	-4.41	4.41
2	1.96	1.91	-0.05	0.05	2	41.57	41.09	-0.48	0.48
3	2.82	2.71	-0.11	0.11	3	64.44	59.38	-5.06	5.06
4	2.53	2.62	0.09	0.09	4	29.60	26.18	-3.42	3.42
5	3.66	3.39	-0.27	0.27	5	31.92	31.76	-0.16	0.16
6	2.51	2.52	0.01	0.01	6	31.73	28.64	-3.09	3.09
7	1.76	1.67	-0.09	0.09	7	86.87	77.51	-9.36	9.36
8	2.58	2.71	0.13	0.13	8	51.80	50.63	-1.17	1.17
9	2.85	3.04	0.19	0.19	9[d]	66.47	59.99	-6.48	6.48
10[c]	2.15	2.25	0.10	0.10	10[d]	68.02	64.36	-3.66	3.66
					11[d]	83.47	66.73	-16.74	16.74
					12[d]	92.03	85.11	-6.92	6.92
			MAE	0.11				MAE	3.4

[a] Calculations performed using $CHCl_3$ solvent parameters; [b] Calculations performed using DMSO solvent parameters; [c] This value was not included as the proton is bonded to a heteroatom; [d] These values were not included in the MAE calculation due to the heavy atom effect.[54]

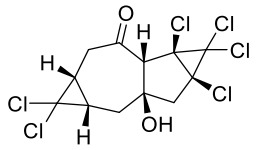

63ab

63ab ^{1}H NMR Chemical Shift Comparison[a]					**63ab** ^{13}C NMR Chemical Shift Comparison[b]				
H	Calc (ppm)	Expt (ppm)	Error (ppm)	Abs error (ppm)	C	Calc (ppm)	Expt (ppm)	Error (ppm)	Abs error (ppm)
1	1.84	1.91	-0.07	0.07	1	205.6	196.72	8.88	8.88
2	2.29	2.52	-0.23	0.23	2	40.33	41.09	-0.76	0.76
3	3.00	2.71	0.29	0.29	3	76.88	64.35	12.53	12.53
4	2.63	2.62	0.01	0.01	4	29.30	26.18	3.12	3.12
5	4.01	3.39	0.62	0.62	5	31.40	28.64	2.76	2.76
6	2.20	1.91	0.29	0.29	6	33.96	31.76	2.20	2.20
7	1.76	1.67	0.09	0.09	7	83.69	77.51	6.18	6.18
8	2.63	2.71	-0.08	0.08	8	54.66	59.38	-4.72	4.72
9	3.08	3.04	0.04	0.04	9[d]	71.18	60.00	11.18	11.18
10[c]	1.70	2.25	-0.55	0.55	10[d]	65.97	50.63	15.34	15.34
					11[d]	82.38	66.73	15.65	15.65
					12[d]	89.19	85.11	4.08	4.08
			MAE	0.19				MAE	5.1

[a] Calculations performed using $CHCl_3$ solvent parameters; [b] Calculations performed using DMSO solvent parameters; [c] This value was not included as the proton is bonded to a heteroatom; [d] These values were not included in the MAE calculation due to the heavy atom effect.[54]

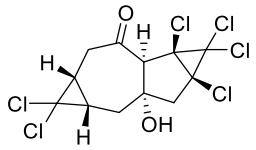

63ac

63ac ^{1}H NMR Chemical Shift Comparison[a]					**63ac** ^{13}C NMR Chemical Shift Comparison[b]				
H	Calc (ppm)	Expt (ppm)	Error (ppm)	Abs error (ppm)	C	Calc (ppm)	Expt (ppm)	Error (ppm)	Abs error (ppm)
1	2.40	2.52	0.12	0.12	1	207.76	196.72	-11.04	11.04
2	2.28	1.91	-0.37	0.37	2	40.19	41.09	0.90	0.90
3	3.32	3.04	-0.28	0.28	3	73.32	64.35	-8.97	8.97
4	2.79	2.62	-0.17	0.17	4	28.53	26.18	-2.35	2.35
5	3.52	3.39	-0.13	0.13	5	31.16	28.64	-2.52	2.52
6	2.22	1.91	-0.31	0.31	6	36.58	31.76	-4.82	4.82
7	1.53	1.67	0.14	0.14	7	85.23	77.51	-7.72	7.72
8	2.95	2.71	-0.24	0.24	8	52.70	50.63	-2.07	2.07
9	2.88	2.71	-0.17	0.17	9[d]	65.19	59.38	-5.81	5.81
10[c]	1.83	2.25	0.42	0.42	10[d]	67.55	60.00	-7.55	7.55
					11[d]	82.75	66.73	-16.02	16.02
					12[d]	89.78	85.11	-4.67	4.67
			MAE	0.21				MAE	5.0

[a] Calculations performed using $CHCl_3$ solvent parameters; [b] Calculations performed using DMSO solvent parameters; [c] This value was not included as the proton is bonded to a heteroatom; [d] These values were not included in the MAE calculation due to the heavy atom effect.[54]

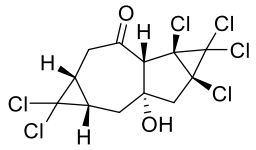

63ad

63ad ^{1}H NMR Chemical Shift Comparison[a]					**63ad** ^{13}C NMR Chemical Shift Comparison[b]				
H	Calc (ppm)	Expt (ppm)	Error (ppm)	Abs error (ppm)	C	Calc (ppm)	Expt (ppm)	Error (ppm)	Abs error (ppm)
1	2.12	1.91	0.21	0.21	1	208.00	196.72	11.28	11.28
2	2.07	1.67	0.40	0.40	2	39.57	41.09	-1.52	1.52
3	2.92	2.71	0.21	0.21	3	71.47	64.35	7.12	7.12
4	3.06	3.04	0.02	0.02	4	33.31	28.64	4.67	4.67
5	4.57	3.39	1.18	1.18	5	32.97	26.18	6.79	6.79
6	2.43	1.91	0.52	0.52	6	39.10	31.76	7.34	7.34
7	2.46	2.52	-0.06	0.06	7	77.31	66.73	10.58	10.58
8	2.92	2.71	0.21	0.21	8	55.78	50.63	5.15	5.15
9	2.87	2.62	0.25	0.25	9[d]	68.20	60.00	8.20	8.2
10[c]	1.49	2.25	-0.76	0.76	10[d]	67.10	59.38	7.72	7.72
					11[d]	82.56	77.51	5.05	5.05
					12[d]	86.49	85.11	1.38	1.38
			MAE	0.34				MAE	6.9

[a] Calculations performed using $CHCl_3$ solvent parameters; [b] Calculations performed using DMSO solvent parameters; [c] This value was not included as the proton is bonded to a heteroatom; [d] These values were not included in the MAE calculation due to the heavy atom effect.[54]

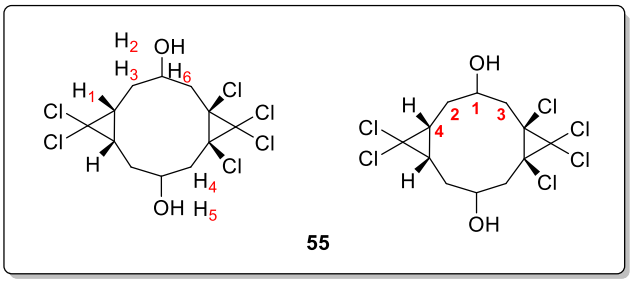

55

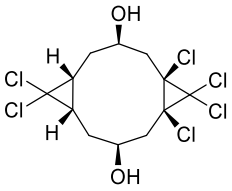

55a

55a ^{1}H NMR Comparison[a]					**55a** ^{13}C NMR Comparison[c]				
H	Calc (ppm)	Expt (ppm)	Error (ppm)	Abs error (ppm)	C	Calc (ppm)	Expt (ppm)	Error (ppm)	Abs error (ppm)
1	2.55	2.37	-0.18	0.18	1	69.69	66.48	3.21	3.21
2	2.24	2.31	0.07	0.07	2	31.28	30.31	0.97	0.97
3	1.52	1.44	-0.08	0.08	3	39.13	37.90	1.23	1.23
4	1.91	1.96	0.05	0.05	4	30.28	26.96	3.32	3.32
5	2.75	2.85	0.10	0.10	5[d]	65.90	56.22	9.68	9.68
6	4.20	4.39	0.19	0.19	6[d]	87.87	73.51	14.36	14.36
7[b]	1.95	2.77	0.82	0.82	7[d]	84.06	67.63	16.43	16.43
			MAE	0.11				MAE	2.2

[a] Calculations performed using $CHCl_3$ solvent parameters; [b] This value was not included as the proton is bonded to a heteroatom; [c] Calculations performed using DMSO solvent parameters; [d] These values were not included in the MAE calculation due to the heavy atom effect.[54]

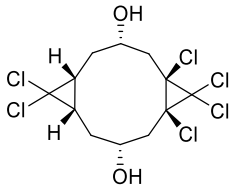

55b

55b ^{1}H NMR Chemical Shift Comparison [a]					**55b** ^{13}C NMR Chemical Shift Comparison [c]				
H	Calc (ppm)	Expt (ppm)	Error (ppm)	Abs error (ppm)	C	Calc (ppm)	Expt (ppm)	Error (ppm)	Abs error (ppm)
1	2.10	2.31	0.21	0.21	1	70.47	66.48	3.99	3.99
2	2.15	2.37	0.22	0.22	2	33.39	30.31	3.08	3.08
3	1.33	1.44	0.11	0.11	3	40.83	37.90	2.93	2.93
4	1.88	1.96	0.08	0.08	4	31.53	26.96	4.58	4.58
5	2.54	2.85	0.31	0.31	5[d]	64.92	56.22	8.70	8.70
6	4.37	4.39	0.02	0.02	6[d]	86.60	73.51	13.09	13.09
7[b]	1.32	2.77	1.45	1.45	7[d]	82.00	67.63	14.37	14.37
			MAE	0.16				MAE	3.6

[a] Calculations performed using $CHCl_3$ solvent parameters; [b] This value was not included as the proton is bonded to a heteroatom; [c] Calculations performed in DMSO solvent parameters; [d] These values were not included in the MAE calculation due to the heavy atom effect.[54]

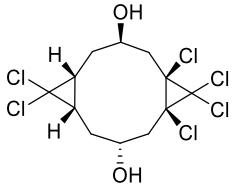

55c

Isomer **55c** was not considered as the reduction product due to its lack of symmetry. The experimental ^{1}H NMR spectrum showed 7 proton signals only, while isomer **55c** is expected to have 14 proton signals because it is unsymmetrical.

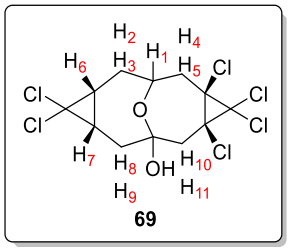

69

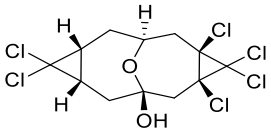

69a

69a ^{1}H NMR Chemical Shift Comparison				
H	Calc (ppm)	Expt (ppm)	Error (ppm)	Abs error (ppm)
1	2.79	4.66	-1.87	1.87
2	2.00	1.91	0.09	0.09
3	2.02	1.46	0.56	0.56
4	2.54	2.04	0.50	0.50
5	2.78	2.50	0.28	0.28
6	1.93	1.46	0.47	0.47
7	2.06	2.03	0.03	0.03
8	2.55	2.38	0.17	0.17
9	1.92	2.42	-0.50	0.50
10	2.94	2.86	0.08	0.08
11	2.88	2.58	0.30	0.30
12[a]	2.71	3.44	-0.73	0.73
			MAE	0.44

[a] This value was not included as the proton is bonded to a heteroatom.

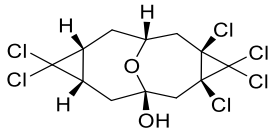

69b

69b ^{1}H NMR Chemical Shift Comparison				
H	Calc (ppm)	Expt (ppm)	Error (ppm)	Abs error (ppm)
1	4.64	4.66	0.02	0.02
2	2.29	2.04	-0.25	0.25
3	1.92	1.46	-0.46	0.46
4	2.74	2.42	-0.32	0.32
5	2.81	2.50	-0.31	0.31
6	1.99	1.91	-0.08	0.08
7	1.90	1.46	-0.44	0.44
8	2.44	2.38	-0.06	0.06
9	2.08	2.03	-0.05	0.05
10	2.91	2.58	-0.33	0.33
11	2.96	2.86	-0.10	0.10
12[a]	2.87	3.44	0.57	0.57
			MAE	0.22

[a] This value was not included as the proton is bonded to a heteroatom.

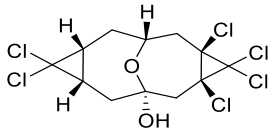

69c

69c ^{1}H NMR Chemical Shift Comparison				
H	Calc (ppm)	Expt (ppm)	Error (ppm)	Abs error (ppm)
1	4.06	4.66	-0.60	0.60
2	2.16	1.91	0.25	0.25
3	2.16	2.03	0.13	0.13
4	2.53	2.38	0.15	0.15
5	2.49	2.04	0.45	0.45
6	2.12	1.46	0.66	0.66
7	1.94	1.46	0.48	0.48
8	3.58	2.86	0.72	0.72
9	2.74	2.42	0.32	0.32
10	2.91	2.58	0.33	0.33
11	2.76	2.50	0.26	0.26
12[a]	3.17	3.44	-0.27	0.27
			MAE	0.40

[a] This value was not included as the proton is bonded to a heteroatom.

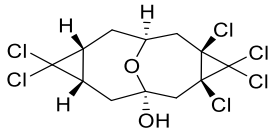

69d

69d ^{1}H NMR Chemical Shift Comparison				
H	Calc (ppm)	Expt (ppm)	Error (ppm)	Abs error (ppm)
1	4.08	4.66	-0.58	0.58
2	2.11	1.91	0.20	0.20
3	2.48	2.03	0.45	0.45
4	2.79	2.42	0.37	0.37
5	3.15	2.50	0.65	0.65
6	2.06	1.46	0.60	0.60
7	2.04	1.46	0.58	0.58
8	2.60	2.38	0.22	0.22
9	2.58	2.04	0.54	0.54
10	3.17	2.86	0.31	0.31
11	3.15	2.58	0.57	0.57
12[a]	3.28	3.44	-0.16	0.16
			MAE	0.46

[a] This value was not included as the proton is bonded to a heteroatom.

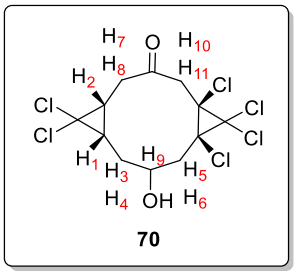

70

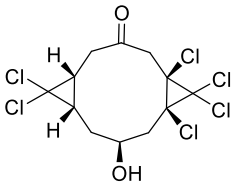

70a

70a ^{1}H NMR Chemical Shift Comparison				
H	Calc (ppm)	Expt (ppm)	Error (ppm)	Abs error (ppm)
1	2.38	1.91	0.47	0.47
2	2.62	2.38	0.24	0.24
3	2.39	2.03	0.36	0.36
4	2.85	2.50	0.35	0.35
5	3.06	2.86	0.20	0.20
6	2.94	2.58	0.36	0.36
7	2.41	2.04	0.37	0.37
8	1.63	1.46	0.17	0.17
9	4.36	4.66	-0.30	0.30
10	2.21	1.46	0.75	0.75
11	2.78	2.42	0.36	0.36
12[a]	1.50	3.44	-1.94	1.94
			MAE	0.36

[a] These values were not included as the protons are bonded to a heteroatom.

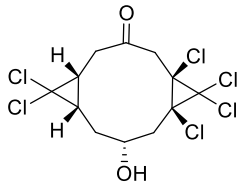

70b

70b ^{1}H NMR Chemical Shift Comparison				
H	Calc (ppm)	Expt (ppm)	Error (ppm)	Abs error (ppm)
1	2.28	2.04	-0.24	0.24
2	2.20	2.03	-0.17	0.17
3	2.49	2.38	-0.11	0.11
4	2.90	2.50	-0.40	0.40
5	3.12	2.58	-0.54	0.54
6	3.15	2.86	-0.29	0.29
7	2.21	1.91	-0.30	0.30
8	1.54	1.46	-0.08	0.08
9	4.25	4.66	0.41	0.41
10	1.98	1.46	-0.52	0.52
11	2.66	2.42	-0.24	0.24
12[a]	1.63	3.44	1.81	1.81
			MAE	0.30

[a] These values were not included as the protons are bonded to a heteroatom.

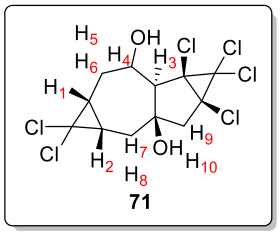

71

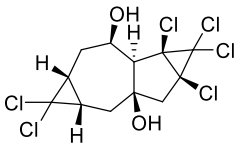

71a

71a ^{1}H NMR Chemical Shift Comparison				
H	Calc (ppm)	Expt (ppm)	Error (ppm)	Abs error (ppm)
1	2.10	2.04	0.06	0.06
2	2.00	1.95	0.05	0.05
3	2.29	2.10	0.19	0.19
4	4.57	4.69	-0.12	0.12
5	2.69	2.78	-0.09	0.09
6	1.60	1.54	0.06	0.06
7	2.35	2.44	-0.09	0.09
8	1.55	1.44	0.11	0.11
9	2.42	2.48	-0.06	0.06
10	2.51	2.56	-0.05	0.05
11[a]	2.52	1.55	0.97	0.97
12[a]	4.61	5.14	-0.53	0.53
			MAE	0.09

[a] These values were not included as the protons are bonded to a heteroatom.

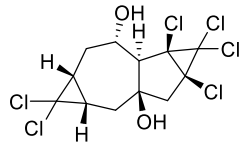

71b

71b ^{1}H NMR Chemical Shift Comparison				
H	Calc (ppm)	Expt (ppm)	Error (ppm)	Abs error (ppm)
1	1.83	1.95	-0.12	0.12
2	1.84	2.04	-0.20	0.20
3	2.33	2.48	-0.15	0.15
4	4.26	4.69	-0.43	0.43
5	2.32	2.44	-0.12	0.12
6	1.66	1.54	0.12	0.12
7	2.24	2.10	0.14	0.14
8	1.61	1.44	0.17	0.17
9	2.36	2.56	-0.20	0.20
10	2.70	2.78	-0.08	0.08
11[a]	2.11	5.14	-3.03	3.03
12[a]	1.41	1.55	-0.14	0.14
			MAE	0.17

[a] These values were not included as the protons are bonded to a heteroatom.

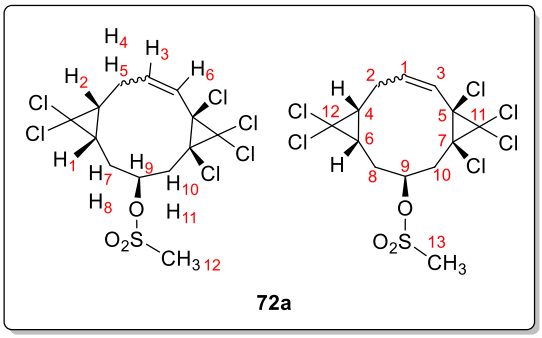

72a

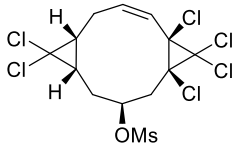

72aa

72aa ^{1}H NMR Chemical Shift Comparison					**72aa** ^{13}C NMR Chemical Shift Comparison				
H	Calc (ppm)	Expt (ppm)	Error (ppm)	Abs error (ppm)	C	Calc (ppm)	Expt (ppm)	Error (ppm)	Abs error (ppm)
1	2.63	2.52	0.11	0.11	1	140.20	136.9	3.3	3.3
2	2.88	2.70	0.18	0.18	2	28.51	26.5	2.0	2.0
3	6.01	5.98	0.03	0.03	3	122.53	123.0	-0.5	0.5
4	3.07	3.01	0.06	0.06	4	32.09	29.9	2.2	2.2
5	2.32	2.21	0.11	0.11	5[a]	61.47	53.0	8.5	8.5
6	5.91	5.87	0.04	0.04	6	29.23	27.1	2.1	2.1
7	1.41	1.36	0.05	0.05	7[a]	65.37	55.7	9.7	9.7
8	2.33	2.43	-0.10	0.10	8	30.46	29.3	1.2	1.2
9	5.10	5.25	-0.15	0.15	9	70.86	65.6	5.3	5.3
10	3.37	3.15	0.22	0.22	10	39.60	39.3	0.3	0.3
11	1.92	2.05	-0.13	0.13	11[a]	88.61	75.2	13.4	13.4
12	3.11	3.09	0.02	0.02	12[a]	82.98	73.1	9.9	9.9
					13	40.26	39.9	0.4	0.4
			MAE	0.10				MAE	1.9

[a] These values were not included in the MAE calculation due to the heavy atom effect.[54]

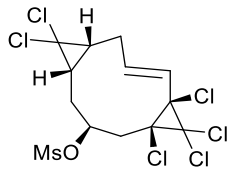

72ab

72ab ^{1}H NMR Chemical Shift Comparison					**72ab** ^{13}C NMR Chemical Shift Comparison				
H	Calc (ppm)	Expt (ppm)	Error (ppm)	Abs error (ppm)	C	Calc (ppm)	Expt (ppm)	Error (ppm)	Abs error (ppm)
1	2.27	2.43	-0.16	0.16	1	141.91	136.9	5.0	5.0
2	2.04	2.05	-0.01	0.01	2	29.64	26.5	3.1	3.1
3	6.59	5.98	0.61	0.61	3	126.58	123.0	3.6	3.6
4	2.96	3.01	-0.05	0.05	4	31.98	27.1	4.9	4.9
5	2.35	2.70	-0.35	0.35	5[a]	64.62	53.0	11.6	11.6
6	5.87	5.87	0.00	0.00	6	32.14	29.3	2.8	2.8
7	1.59	1.36	0.23	0.23	7[a]	70.09	65.6	4.5	4.5
8	2.35	2.52	-0.17	0.17	8	33.32	29.9	3.4	3.4
9	5.12	5.25	-0.13	0.13	9	69.48	55.7	13.8	13.8
10	2.98	3.09	-0.11	0.11	10	41.89	39.3	2.6	2.6
11	2.16	2.21	-0.05	0.05	11[a]	88.51	75.2	13.3	13.3
12	3.31	3.15	0.16	0.16	12[a]	81.31	73.1	8.2	8.2
					13	42.55	39.9	2.7	2.7
			MAE	0.17				MAE	4.7

[a] These values were not included in the MAE calculation due to the heavy atom effect.[54]

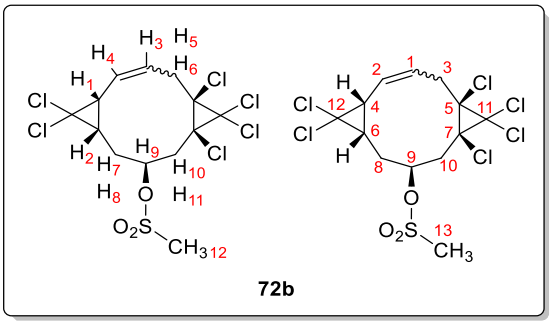

72b

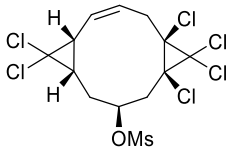

72ba

72ba ^{1}H NMR Chemical Shift Comparison					**72ba** ^{13}C NMR Chemical Shift Comparison				
H	Calc (ppm)	Expt (ppm)	Error (ppm)	Abs error (ppm)	C	Calc (ppm)	Expt (ppm)	Error (ppm)	Abs error (ppm)
1	2.99	2.70	0.29	0.29	1	130.64	136.9	-6.3	6.3
2	2.64	2.43	0.21	0.21	2	122.81	123.0	-0.2	0.2
3	5.79	5.98	-0.19	0.19	3	37.10	29.9	7.2	7.2
4	5.66	5.87	-0.21	0.21	4	35.25	29.3	6.0	6.0
5	3.08	3.01	0.07	0.07	5[a]	65.80	55.7	10.1	10.1
6	2.65	2.52	0.13	0.13	6	31.26	27.1	4.2	4.2
7	2.35	2.21	0.14	0.14	7[a]	64.37	53.0	11.4	11
8	1.50	1.36	0.14	0.14	8	30.16	26.5	3.7	3.7
9	5.14	5.25	-0.11	0.11	9	70.54	65.6	4.9	4.9
10	2.11	2.05	0.06	0.06	10	38.84	39.3	-0.5	0.5
11	3.45	3.09	0.36	0.36	11[a]	86.94	75.2	11.7	11.7
12	3.12	3.15	-0.03	0.03	12[a]	81.58	73.1	8.5	8.5
					13	40.32	39.9	0.4	0.4
			MAE	0.16				MAE	3.7

[a] These values were not included in the MAE calculation due to the heavy atom effect.[54]

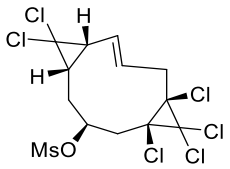

72bb

72bb ^{1}H NMR Chemical Shift Comparison					**72bb** ^{13}C NMR Chemical Shift Comparison				
H	Calc (ppm)	Expt (ppm)	Error (ppm)	Abs error (ppm)	C	Calc (ppm)	Expt (ppm)	Error (ppm)	Abs error (ppm)
1	2.74	2.70	0.04	0.04	1	131.41	123.0	8.4	8.4
2	2.72	2.52	0.20	0.20	2	133.90	136.9	-3.0	3.0
3	6.28	5.98	0.30	0.30	3	42.12	39.3	2.8	2.8
4	5.78	5.87	-0.09	0.09	4	37.50	27.1	10.4	10.4
5	3.29	3.15	0.14	0.14	5[a]	64.98	55.7	9.3	9.3
6	3.09	3.01	0.08	0.08	6	40.76	29.9	10.9	10.9
7	2.66	2.43	0.23	0.23	7[a]	64.72	53.0	11.7	11.7
8	1.63	1.36	0.27	0.27	8	31.02	26.5	4.5	4.5
9	4.92	5.25	-0.33	0.33	9	72.44	65.6	6.8	6.8
10	2.38	2.05	0.33	0.33	10	39.49	29.3	10.2	10.2
11	2.59	2.21	0.38	0.38	11[a]	83.62	73.1	10.5	10.5
12	3.23	3.09	0.14	0.14	12[a]	85.47	75.2	10.3	10.3
					13	42.75	39.9	2.9	2.9
			MAE	0.21				MAE	6.7

[a] These values were not included in the MAE calculation due to the heavy atom effect.[54]

3.4.2 Chloroprene Route

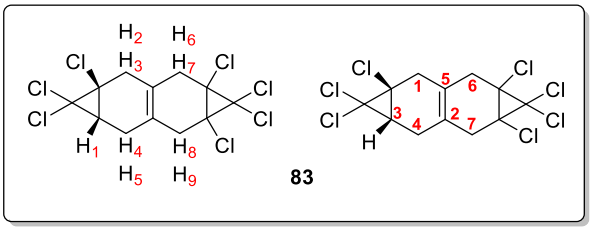

83

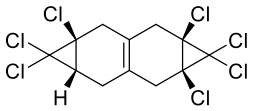

83a

83a ^{1}H NMR Chemical Shift Comparison					**83a** ^{13}C NMR Chemical Shift Comparison				
H	Calc (ppm)	Expt (ppm)	Error (ppm)	Abs error (ppm)	C	Calc (ppm)	Expt (ppm)	Error (ppm)	Abs error (ppm)
1	2.12	2.08	0.04	0.04	1	35.25	34.7	0.55	0.55
2	2.71	2.67	0.04	0.04	2	122.00	120.6	1.40	1.40
3	2.68	2.67	0.01	0.01	3	36.93	34.8	2.13	2.13
4	2.57	2.46	0.11	0.11	4	25.29	25.3	-0.01	0.01
5	2.13	2.18	-0.05	0.05	5	122.84	121.6	1.24	1.24
6	2.89	2.84	0.05	0.05	6	38.13	37.3	0.83	0.83
7	2.78	2.81	-0.03	0.03	7	38.05	37.2	0.85	0.85
8	2.90	2.84	0.06	0.06	8[a]	56.62	47.8	8.82	8.82
9	2.81	2.81	0.00	0.00	9[a]	61.05	52.5	8.55	8.55
					10[a]	61.42	52.7	8.72	8.72
					11[a]	83.12	66.4	16.72	16.72
					12[a]	84.00	68.4	15.6	15.6
			MAE	0.04				MAE	1.0

[a] These values were not included in the MAE calculation due to the heavy atom effect.[54]

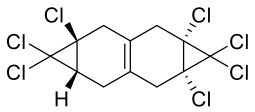

83b

83b ^{1}H NMR Chemical Shift Comparison					**83b** ^{13}C NMR Chemical Shift Comparison				
H	Calc (ppm)	Expt (ppm)	Error (ppm)	Abs error (ppm)	C	Calc (ppm)	Expt (ppm)	Error (ppm)	Abs error (ppm)
1	2.14	2.08	0.06	0.06	1	35.27	34.7	0.57	0.57
2	2.76	2.67	0.09	0.09	2	122.75	120.6	2.15	2.15
3	2.62	2.67	-0.05	0.05	3	37.92	37.3	0.62	0.62
4	2.27	2.18	0.09	0.09	4	25.59	25.3	0.29	0.29
5	2.44	2.46	-0.02	0.02	5	124.07	121.6	2.47	2.47
6	2.79	2.81	-0.02	0.02	6	37.90	34.8	3.10	3.10
7	2.85	2.84	0.01	0.01	7	37.91	37.2	0.71	0.71
8	2.81	2.81	0.00	0.00	8[a]	57.53	47.8	9.73	9.73
9	2.86	2.84	0.02	0.02	9[a]	61.76	52.5	9.26	9.26
					10[a]	61.89	52.7	9.19	9.19
					11[a]	82.91	66.4	16.51	16.51
					12[a]	84.29	68.4	15.89	15.89
			MAE	0.04				MAE	1.4

[a] These values were not included in the MAE calculation due to the heavy atom effect.[54]

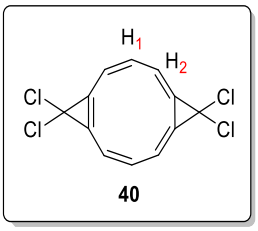

40

^{1}H NMR Chemical Shifts Predictions for **40**		
H	Integration	δ (ppm)
1	2	8.68
2	4	8.95

3.5 B3LYP/6-31* Energy Calculations of Triene **66** and Aromatic Diol **41**

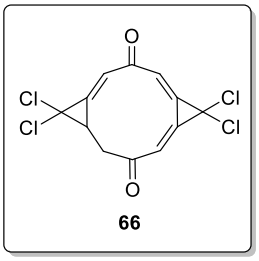

66

24

E = -613.5677 hartrees, rel. E = 0 kcal/mol

C	2.510312	-0.074217	-0.366556
C	2.064221	1.271344	0.055716
C	1.492416	-1.168396	-0.644501
C	0.608640	-1.504119	0.567663
C	0.818370	1.741625	0.212597
C	-0.602390	1.745742	0.185894
C	-0.830843	-1.718271	0.376947
C	-1.869220	1.334473	0.039655
C	-2.042878	-1.314821	0.006829
C	-2.549779	0.044379	-0.284199
O	-3.684231	0.144021	-0.750678
O	3.707811	-0.284833	-0.501944
C	0.112654	3.023641	0.502101
C	-0.014905	-2.904781	0.664372
H	0.931200	-1.073790	1.515406
H	2.889963	1.959680	0.224863
H	0.865985	-0.862560	-1.492035
H	2.066731	-2.047215	-0.951719
H	-2.620605	2.118780	0.121873
H	-2.826640	-2.061758	-0.110082
H	0.181549	-3.612257	-0.140947
H	-0.085376	-3.361008	1.651092
H	0.154368	3.817724	-0.246862
H	0.080612	3.388043	1.531487

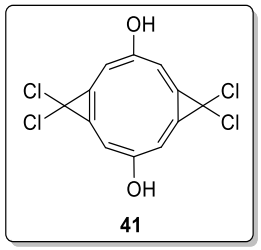

41

24

E = -613.5466 hartrees, rel. E = 13.2 kcal/mol

C	-0.000013	0.004989	2.556257
C	0.000181	1.287485	1.982275
C	0.000095	-1.270266	1.983540
C	-0.000312	-1.717860	0.678437
C	-0.000068	1.730483	0.683811
C	-0.000068	1.730483	-0.683811
C	-0.000312	-1.717860	-0.678437
C	0.000181	1.287485	-1.982275
C	0.000095	-1.270266	-1.983540
C	-0.000013	0.004989	-2.556257
O	0.000215	0.074085	3.931919
O	0.000215	0.074085	-3.931919
C	0.001006	-3.056618	0.000000
C	-0.000826	3.065427	0.000000
H	0.000998	2.077758	2.730340
H	0.000842	-2.085987	2.709654
H	0.000998	2.077758	-2.730340
H	0.000842	-2.085987	-2.709654
H	-0.001397	-0.824731	4.294634
H	-0.001397	-0.824731	-4.294634
H	-0.917084	3.664358	0.000000
H	0.913857	3.666526	0.000000
H	-0.913792	-3.658912	0.000000
H	0.916996	-3.656802	0.000000

3.6 X-Ray Crystallography Data

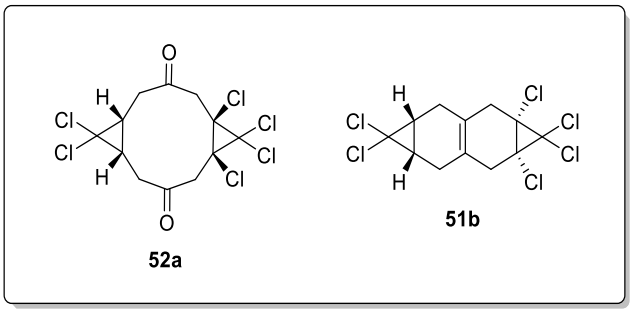

Crystal Structure Report and Refinement Data for Compound **52a** and **51b**

Table 3.1 Crystal data and structure refinement for dione **52a** and Diels-Alder adduct **51b**.

Identification code	1570_0m, CB-4-040A	
Empirical formula	C24 H20 Cl12 O2	
Formula weight	765.80	
Temperature	173(2) K	
Wavelength	0.71073 Å	
Crystal system	Triclinic	
Space group	P-1	
Unit cell dimensions	a = 9.9862(2) Å	α = 117.3680(10)°.
	b = 12.7443(3) Å	β = 94.9270(10)°.
	c = 13.1277(3) Å	γ = 93.2760(10)°.
Volume	1469.40(6) $Å^3$	
Z	2	
Density (calculated)	1.731 Mg/m^3	
Absorption coefficient	1.156 mm^{-1}	
F(000)	768	
Crystal size	0.310 x 0.180 x 0.130 mm^3	
Theta range for data collection	2.589 to 27.600°.	
Index ranges	-12<=h<=12, -16<=k<=16, -16<=l<=17	
Reflections collected	32732	
Independent reflections	6756 [R(int) = 0.0261]	
Completeness to theta = 25.242°	99.8 %	
Absorption correction	Multi-scan	

Refinement method	Full-matrix least-squares on F^2
Data / restraints / parameters	6756 / 0 / 343
Goodness-of-fit on F^2	1.042
Final R indices [I>2sigma(I)]	R1 = 0.0274, wR2 = 0.0597
R indices (all data)	R1 = 0.0363, wR2 = 0.0634
Extinction coefficient	n/a
Largest diff. peak and hole	0.375 and -0.310 e.$Å^{-3}$

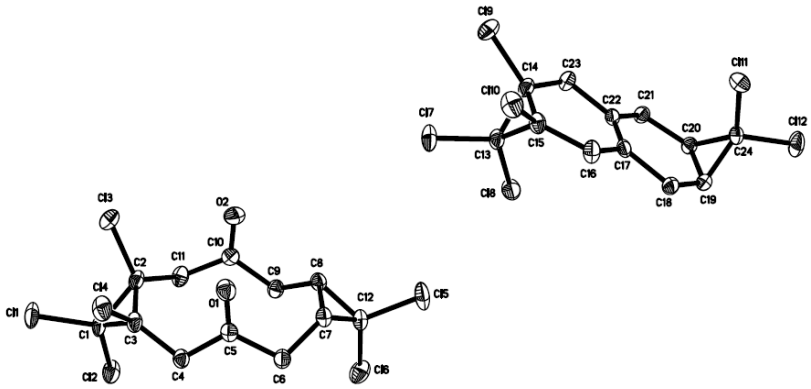

Figure 3.1 Structures generated from a co-crystal of *cis* dione **52a** and *trans* Diels-Alder adduct **51b** obtained through X-ray diffraction.

Table 3.2 Xyz coordinates of the structures generated from a co-crystal of *cis* dione **52a** and *trans* Diels-Alder adduct **51b** obtained from X-ray diffraction.

58

Cis dione, *trans* Diels-Alder adduct, CB-4-040A

Cl	2.296004	11.494363	-4.599509
Cl	1.481925	12.217715	-1.937895
Cl	1.342214	8.503558	-4.160629
Cl	4.341973	9.397250	-3.423611
Cl	1.942846	5.712802	3.745804

Cl	1.605688	8.595014	3.665429
O	3.720416	7.600379	-1.007747
O	0.771942	6.870124	-1.397824
C	2.069703	10.924894	-2.969003
C	1.584376	9.495346	-2.738866
C	3.023743	9.904557	-2.379320
C	3.434216	9.962965	-0.921937
H	2.738019	10.444844	-0.408928
H	4.277540	10.475627	-0.843795
C	3.632885	8.587489	-0.316063
C	3.666433	8.483230	1.199721
H	4.604519	8.493878	1.515865
H	3.195764	9.257051	1.599501
C	2.995119	7.196980	1.629465
H	3.557092	6.375237	1.534877
C	1.508751	7.001121	1.327280
H	1.251256	6.070866	1.066010
C	0.727618	8.087875	0.647276
H	1.118762	8.965049	0.887347
H	-0.204852	8.071232	0.979483
C	0.716903	7.947934	-0.864345
C	0.541089	9.230955	-1.666356
H	-0.349315	9.207360	-2.098483
H	0.543811	9.994109	-1.035734
C	1.986657	7.149762	2.736206
Cl	2.098936	1.932735	1.418063
Cl	1.336388	2.139282	4.188500
Cl	1.093859	-1.027667	1.305885
Cl	4.174281	-0.370921	2.125822
Cl	1.860762	-3.515850	7.277776
Cl	0.906201	-2.879242	9.943669

C	1.917156	1.070621	2.928874
C	1.446855	-0.372241	2.898806
C	2.879109	-0.049685	3.275468
C	3.331040	-0.270079	4.705211
H	3.975436	-1.021666	4.714000
H	3.816493	0.538902	5.004933
C	2.249303	-0.566775	5.705441
C	2.737954	-0.494340	7.129286
H	3.516459	-1.099018	7.220751
H	3.057605	0.426888	7.300536
C	1.736070	-0.851296	8.195897
H	1.829567	-0.350777	9.056553
C	0.313277	-1.202736	7.798766
H	-0.386334	-0.901334	8.446666
C	-0.100236	-1.134466	6.353757
H	-0.523556	-1.995730	6.110471
H	-0.788767	-0.429277	6.260349
C	0.999835	-0.853865	5.368099
C	0.505710	-0.914605	3.946682
H	-0.344994	-0.411318	3.891195
H	0.306129	-1.858992	3.726664
C	1.231416	-2.252462	8.321490

LIST OF REFERENCES

(1) Faraday, M. *Philos. Trans. R. Soc. Lond.* **1825**, *115*, 440–466.

(2) Astruc, D. In *Modern Arene Chemistry*; Wiley-VCH Verlag GmbH & Co. KGaA, 2002; pp 1–19.

(3) Balaban, A. T. *Pure Appl. Chem.* **1980**, *52*, 1409–1429.

(4) Loschmidt, J. *Chemische Studien, A. Konstitution-Formeln der organischen Chemie in geographischer Darstellung, B. Das Mariotte'sche Gesetz*; Vienna, 1861.

(5) Kekulé, A. *Bull. Soc. Chim. Fr.* **1865**, *3*, 100.

(6) Dewar, J. *Proc. R. Soc. Edinburgh* **1869**, *6*, 82–86.

(7) Ladenburg, A. *Ber. Dtsch. Chem. Ges.* **1869**, *2*, 140–142.

(8) Armit, J. W.; Robinson, R. *J. Chem. Soc., Trans.* **1925**, *127*, 1604–1618.

(9) Hückel, E. *Z. Physik* **1931**, *70*, 204–286.

(10) Sondheimer, F.; Wolovsky, R.; Amiel, Y. *J. Am. Chem. Soc.* **1962**, *84*, 274–284.

(11) Jackman, L. M.; Sondheimer, F.; Amiel, Y.; Ben-Efraim, D. A.; Gaoni, Y.; Wolovsky, R.; Bothner-By, A. A. *J. Am. Chem. Soc.* **1962**, *84*, 4307–4312.

(12) Sondheimer, F.; Gaoni, Y. *J. Am. Chem. Soc.* **1960**, *82*, 5765–5766.

(13) Vogel, E.; Sombroek, J.; Wagemann, W. *Angew. Chem.* **1975**, *87*, 591–592.

(14) Miyoshi, H.; Nobusue, S.; Shimizu, A.; Tobe, Y. *Chem. Soc. Rev.* **2015**, *44*, 6560–6577.

(15) Bleeke, J. R. *Chem. Rev.* **2001**, *101*, 1205–1228.

(16) Lee, V. Y.; Sekiguchi, A. *Angew. Chem., Int. Ed.* **2007**, *46*, 6596–6620.

(17) McMurry, J. *Organic Chemistry with Biological Applications*, 2nd ed.; Brooks/Cole: Belmont, 2011.

(18) Albert, A. *Heterocyclic Chemistry*; Athlone Press: London, 1959.

(19) Gershoni-Poranne, R.; Stanger, A. *Chem. Soc. Rev.* **2015**, *44*, 6597–6615.

(20) Schleyer, P. v. R.; Maerker, C.; Dransfeld, A.; Jiao, H.; van Eikema Hommes, N. J. R. *J. Am. Chem. Soc.* **1996**, *118*, 6317–6318.

(21) Chen, Z.; Wannere, C. S.; Corminboeuf, C.; Puchta, R.; Schleyer, P. v. R. *Chem. Rev.* **2005**, *105*, 3842–3888.

(22) Fleischer, U.; Kutzelnigg, W.; Lazzeretti, P.; Muehlenkamp, V. *J. Am. Chem. Soc.* **1994**, *116*, 5298–5306.

(23) Schleyer, P. v. R.; Manoharan, M.; Wang, Z.; Kiran, B.; Jiao, H.; Puchta, R.; van Eikema Hommes, N. J. R. *Org. Lett.* **2001**, *3*, 2465–2468.

(24) Schleyer, P. v. R.; Jiao, H.; van Eikema Hommes, N. J. R.; Malkin, V. G.; Malkina, O. L. *J. Am. Chem. Soc.* **1997**, *119*, 12669–12670.

(25) Krygowski, T. M.; Ejsmont, K.; Stepień, B. T.; Cyrański, M. K.; Poater, J.; Solà, M. *J. Org. Chem.* **2004**, *69*, 6634–6640.

(26) Corminboeuf, C.; Heine, T.; Seifert, G.; Schleyer, P. v. R.; Weber, J. *Phys. Chem. Chem. Phys.* **2004**, *6*, 273–276.

(27) Mislow, K. *J. Chem. Phys.* **1952**, *20*, 1489–1490.

(28) Smith, M. B.; March, J. *March's Advanced Organic Chemistry: Reactions, Mechanisms, and Structures*, 6th ed.; John Wiley & Sons, Inc.: Hoboken, 2007.

(29) Vogel, E.; Roth, H. D. *Agnew. Chem., Int. Ed.* **1964**, *3*, 228–229.

(30) Vogel, E.; Böll, W. A. *Angew. Chem., Int. Ed. Engl.* **1964**, *3*, 642–642.

(31) Vogel, E.; Pretzer, W.; Böll, W. A. *Tetrahedron Lett.* **1965**, *6*, 3613–3617.

(32) Wei, J.; Zhang, Y.; Chi, Y.; Liu, L.; Zhang, W.-X.; Xi, Z. *J. Am. Chem. Soc.* **2016**, *138*, 60–63.

(33) van Tamelen, E. E.; Burkoth, T. L. *J. Am. Chem. Soc.* **1967**, *89*, 151–152.

(34) Masamune, S.; Seidner, R. T. *J. Chem. Soc. D* **1969**, *11*, 542–544.

(35) Masamune, S.; Hojo, K.; Hojo, K.; Bigam, G.; Rabenstein, D. L. *J. Am. Chem. Soc.* **1971**, *93*, 4966–4968.

(36) Masamune, S.; Hojo, K.; Seidner, R. T. *J. Am. Chem. Soc.* **1970**, *92*, 6641–6642.

(37) Katz, T. J.; Garratt, P. J. *J. Am. Chem. Soc.* **1964**, *86*, 5194–5202.

(38) Loos, D.; Leška, J. *Collect. Czech. Chem. Commun.* **1980**, *45*, 187–200.

(39) Baird, N. C. *J. Am. Chem. Soc.* **1972**, *94*, 4941–4948.

(40) Farnell, L.; Kao, J.; Radom, L.; Schaefer, H. F. *J. Am. Chem. Soc.* **1981**, *103*, 2147–2151.

(41) Xie, Y.; Schaefer, H. F.; Liang, G.; Bowen, J. P. *J. Am. Chem. Soc.* **1994**, *116*, 1442–1449.

(42) Sulzbach, H. M.; Schleyer, P. v. R.; Jiao, H.; Xie, Y.; Schaefer, H. F. *J. Am. Chem. Soc.* **1995**, *117*, 1369–1373.

(43) Schleyer, P. v. R.; Jiao, H.; Uni, V. *J. Am. Chem. Soc.* **1996**, *118*, 2093–2094.

(44) Harwood, L. M.; Moody, C. *Experimental Organic Chemistry: Principles and Practice*; Wiley-Blackwell, 1989.

(45) Cope, A.; Herrick, E. C. *Org. Synth.* **1950**, *30*, 29–30.

(46) Müller, P.; Miao, Z. *Helv. Chim. Acta* **1994**, *77*, 2051–2059.

(47) Billups, W. E.; Haley, M. M.; Claussen, R. C.; Rodin, W. A. *J. Am. Chem. Soc.* **1991**, *113*, 4331–4332.

(48) Payne, A. D.; Skelton, B. W.; Wege, D.; White, A. H. *Eur. J. Org. Chem.* **2007**, *2007*, 1184–1195.

(49) Tassara, J.-P.; Baudoin, M. Process for Preparing Chloroprene. EP0646561 (A1), 1995.

(50) Tsue, H.; Imahori, H.; Kaneda, T.; Tanaka, Y.; Okada, T.; Tamaki, K.; Sakata, Y. *J. Am. Chem. Soc.* **2000**, *122*, 2279–2288.

(51) Kato, M.; Yamamoto, S.; Nomura, S.; Miwa, T. *Bull. Chem. Soc. Jpn.* **1990**, *63*, 64–73.

(52) Halton, B.; Boese, R.; Blaser, D.; Lu, Q. *Aust. J. Chem.* **1991**, *44*, 265–276.

(53) Byrne, L. T.; Payne, A. D.; Roemkens, C. A.; Wege, D. *Aust. J. Chem.* **1999**, *52*, 395–401.

(54) Lodewyk, M. W.; Siebert, M. R.; Tantillo, D. J. *Chem. Rev.* **2012**, *112*, 1839–1862.

(55) Pierens, G. K. *J. Comput. Chem.* **2014**, *35*, 1388–1394.

(56) Stewart, C.; McDonald, R.; West, F. G. *Org. Lett.* **2011**, *13*, 720–723.

(57) Johnstone, R. A. W. In *Comprehensive Organic Synthesis*; Trost, B. M., Fleming, I., Eds.;

Elsevier Ltd: Oxford, 1991; pp 259–281.

(58) Xu, Z.; Bao, X.; Wang, Q.; Zhu, J. *Angew. Chem., Int. Ed.* **2015**, *54*, 14937–14940.

(59) Govindaraju, T.; Kumar, V. A.; Ganesh, K. N. *J. Org. Chem.* **2004**, *69*, 1858–1865.

(60) Shani, A. *Isr. J. Chem.* **1975**, *13*, 35–51.

(61) Cakmak, O.; Erenler, R.; Tutar, A.; Celik, N. *J. Org. Chem.* **2006**, *71*, 1795–1801.

(62) Klärner, F.; Polkowska, J.; Panitzky, J.; Seelbach, U. P.; Burkert, U.; Kamieth, M.; Baumann, M.; Wigger, A. E.; Boese, R.; Bläser, D. *Eur. J. Org. Chem.* **2004**, *2004*, 1405–1423.

(63) Bonfantini, E.; Vogel, P.; Pinkerton, A. A. *Helv. Chim. Acta* **1989**, *72*, 906–916.

(64) Araki, S.; Vogel, P.; Blanc, E.; Chapuis, G.; Schenk, K. *Helv. Chim. Acta* **1991**, *74*, 878–886.

(65) Carothers, W. H.; Williams, I.; Collins, A. M.; Kirby, J. E. *J. Am. Chem. Soc.* **1931**, *53*, 4203–4225.

(66) Baird, M. S.; Nethercott, W.; Slowey, P. D. *J. Chem. Res., Miniprint* **1985**, 3815–3829.

(67) Nefedov, O. M.; Shafran, R. N. *Bull. Acad. Sci. USSR, Div. Chem. Sci.* **1965**, *14*, 515–518.

(68) Hashem, M. A.; Marschall-Weyerstahl, H.; Weyerstahl, P. *Chem. Ber.* **1986**, *119*, 464–471.

(69) Cheshev, P.; Marra, A.; Dondoni, A. *Carbohydr. Res.* **2006**, *341*, 2714–2716.

(70) Kutateladze, A. G.; Reddy, D. S. *J. Org. Chem.* **2017**, *82*, 3368–3381.

(71) Willoughby, P. H.; Jansma, M. J.; Hoye, T. R. *Nat. Protoc.* **2014**, *9*, 643–660.

(72) Sherburn, M.; Personal Communication.